

FIELD DETERMINATION OF THE
LONGITUDINAL DISPERSION CHARACTERISTICS
OF LOWER SPENCER CREEK

FIELD DETERMINATION OF THE
LONGITUDINAL DISPERSION CHARACTERISTICS
OF LOWER SPENCER CREEK

by

Donald C. Ambler, B.Sc. (Eng.)

A Project

Submitted to the School of Graduate Studies
in Partial Fulfilment of the Requirements
for the Degree
Master of Engineering

McMaster University

April 1973

Master of Engineering (1973)
(Civil Engineering)

McMaster University
Hamilton, Ontario

TITLE: Field Determination of the Longitudinal Dispersion
Characteristics of Lower Spencer Creek

AUTHOR: Donald C. Ambler, B.Sc. (Eng.)

SUPERVISOR: Dr. Wm. James

NUMBER OF PAGES: 139

SCOPE AND CONTENTS: Five tests were conducted to study the longitudinal dispersion patterns of a fluorescent tracer in a natural stream. The Rhodamine WT dye was injected as a slug. Analysis of the relation between time and concentration of the tracer at several sections in the reach provided a longitudinal dispersion coefficient for each sub-reach.

The history, importance, and physical characteristics of the study area were investigated and documented. The views and findings of past and current workers in the field of fluorometrics and dispersion are presented in a literature review. Consideration was given to the various chemicals and dyes employed as tracer materials. Sampling procedures, analysis, and preliminary correlations are presented for all of the tests.

ACKNOWLEDGEMENTS

The writer is profoundly indebted to Dr. Wm. James who, as project advisor, suggested the problem and provided continual stimulation throughout the work.

The writer is also grateful for field assistance provided by Augusto Vieira Ribeiro and for field equipment provided by the Department of Physical Education of McMaster University.

A note of thanks is due to the Royal Botanical Gardens and the Hamilton Region Conservation Authority who encouraged the field experiments within their areas, and also to the Department of Chemical Engineering, McMaster University, who provided laboratory equipment and space.

Financial support for this work was provided by a grant to Dr. Wm. James from the Research Board of the Division of Science and Engineering at McMaster University.

Figure 2 was originally drawn by Mr. John Lamoureux, Chief Conservationist of the Royal Botanical Gardens.

TABLE OF CONTENTS

Chapter	<u>Page</u>
A INTRODUCTION	1
A.1 DISPERSION TESTS IN CONSERVATION AREAS	1
A.2 THE STUDY AREA: LOWER SPENCER CREEK AND COOTES PARADISE	2
A.2.1 Significance of the Area	2
A.2.2 Hydrography and Hydrology	3
A.2.3 Current Problems	4
B MECHANICS OF DISPERSION IN RIVERS	8
B.1 LITERATURE REVIEW	8
B.1.1 Effects of Lateral Velocity	8
B.1.2 Effects of Cross-Sectional Geometry	13
B.1.3 Effects of Dead Zones	18
B.1.4 Effects of Bends	20
B.2 DISCUSSION OF DISPERSION IN THE STUDY AREA	21
C FIELD PROCEDURES AND RESULTS	24
C.1 SELECTION OF TRACER	24
C.1.1 Desirable Properties	24
C.1.2 Sodium Chloride	24
C.1.3 Radioisotopes	25
C.1.4 Chemicals	26
C.1.5 Dyes	27
C.1.6 Organic Dyes	31
C.1.7 Comparison of Tracers Considered	32

TABLE OF CONTENTS

Chapter		<u>Page</u>
C.2	INJECTION AND SAMPLING	33
	C.2.1 Injection	33
	C.2.2 Sampling	34
C.3	ANALYSIS	35
C.4	RESULTS	36
	C.4.1 Calculation of Dispersion Coefficient from Observed Concentration Distribution.	36
	C.4.2 Preliminary Dispersion Coefficient Correlations	45
D	NUMERICAL MODEL	59
E	DISCUSSION	64
F	APPENDICES	69
	A. FLUOROMETER CALIBRATION AND CALIBRATION CURVES	70
	B. FIELD EXPERIMENT COUNTDOWN AND FLOWCHART	75
	C. FLUORESCENCE	81
	C.1 Precautions.	83
	C.2 Factors Affecting.	84
	D. FLUVIOLOGY OF LOWER SPENCER CREEK.	86
	E. CONCENTRATION OBSERVATIONS	105
	F. NOTATION	134
	G. BIBLIOGRAPHY	137

LIST OF FIGURES

<u>Figure</u>	<u>Title</u>	<u>Page</u>
1	Lower Spencer Creek	5
2	Royal Botanical Gardens Cootes Paradise Trails	6
3	Triangular Cross Section	14
4	Circular Cross Section	16
5	Lower Spencer Creek Photo Locations	23
6	Temperature Difference	37
7	Longitudinal Dispersion Test #1	40
8	Longitudinal Dispersion Test #2	41
9	Longitudinal Dispersion Test #3	42
10	Longitudinal Dispersion Test #4	43
11	Longitudinal Dispersion Test #5	44
12	Dispersion Coefficient vs Flow Velocity Test #1	46
13	Dispersion Coefficient vs Flow Velocity Test #3	47
14	Dispersion Coefficient vs Flow Velocity Test #4	48
15	Dispersion Coefficient vs Flow Velocity Test #5	49
16	Dispersion Coefficient vs Discharge Station 6	50
17	Dispersion Coefficient vs Discharge Station 8	51
18	Dispersion Coefficient vs Discharge Station 9	52

LIST OF FIGURES

<u>Figure</u>	<u>Title</u>	<u>Page</u>
19	Dispersion Coefficient vs Discharge	53
20	Dispersion Coefficient vs Flow Velocity	54
21	Sampling Station Number 8	55
22	Isothermal Lines Test #1 :	57
23	Isothermal Lines Test #5	58

LIST OF TABLES

<u>Table</u>	<u>Title</u>	<u>Page</u>
1	Characteristics of Organic Dyes Used as Tracers ..	31
2	Comparison of Tracers Considered	32
3	Recovery Ratios	39
4	Calibration Constants - Follows Page ..	74
5	Calibration of Fluorometer 10X Scale - " "	.. 74

PHOTOGRAPHS

A number of photographs are presented in Appendix D of this report. The location at which each of the photographs were taken along the study reach is illustrated in Fig. 5 on page 23.

A

INTRODUCTION

A. INTRODUCTION

A.1. DISPERSION TESTS IN CONSERVATION AREAS

Longitudinal dispersion is the action by which a flowing stream spreads out and dilutes a mass of pollutant. Rather than flowing downstream as a slug, the pollutant will be distributed along the length of the stream.

The primary mechanism for dispersion is the variation in the convective velocity within the cross section; parts of the stream travel faster and slower than the mean stream velocity. This velocity differential, or gradient, causes the pollutant to mix as it moves along with the bulk motion. The rate at which the cloud spreads out, the decrease in peak concentration, and the resulting concentration pattern along the stream are of importance in pollution control. The usual objective of dispersion theory is to allow the engineer, knowing the distribution of a pollutant at some upstream station, to predict the pattern at a downstream station, in particular the expected duration of cloud passage and the peak concentration.

A dispersion coefficient obtained by any method is of little or no value unless it correctly predicts these quantities. If the capacity of the stream to transport, disperse, or assimilate a contaminant is overestimated, serious pollution may result. Underestimation, on the other hand, may mean that a valuable resource is not optimally utilized, resulting in greater expenditure in treatment facilities. Virtually no water quality management study, aimed at achieving optimum usage of a river system, can

bypass the need for a reliable means of predicting the dispersion characteristics of the water body.

The dispersion process is extremely complex and not yet adequately understood. As a result a considerable discrepancy exists between analytically predicted and actual dispersion rates in natural streams, despite scientific effort exerted on this problem in recent years. In particular, dispersion characteristics have been observed to vary greatly from stream to stream. Hence, development of a rational pollution control program for a particular stream, such as the Spencer Creek, is aided by reliable estimation of the stream dispersive capacity. This can be obtained by direct tracer studies or detailed velocity distribution measurements.

A tracer study using Rhodamine WT as the tracer material in the lower reach of a local catchment is outlined in this report. The general method can be applied to relatively short reaches (less than, say, 10 miles) of small streams (discharge, say, less than 300 cfs). The field tests can usually be successfully carried out by one person, although two or three may be needed in extreme conditions. Laboratory procedures are straight forward and inexpensive except perhaps in the case where a fluorometer is not available and must be purchased.

A.2. THE STUDY AREA: LOWER SPENCER CREEK AND COOTES PARADISE

A.2.1. Significance of the Area

The study area has a long history of local importance. Archeologists have discovered primitive tools in the area which date back to 1500 B.C. The first European in the Dundas Valley was Captain Thomas Coote, after whom Cootes Paradise was named. More recently, the histor-

ical events associated with the lower Spencer Creek and Cootes Paradise have played an important role in the development of West Hamilton and the Town of Dundas. Spencer Creek and the marsh were used as early as 1790 as a means of transporting crops to the mills at Grimsby. The first steps toward cutting a proper channel through the marsh came later in 1804 when a Dundas entrepreneur cleared and deepened the creek so that larger boats could reach his warehouses. Durham boats 80 feet long with a 10-foot beam and capable of carrying some 30 tons appeared on the waterway by 1816. The tortuous Spencer's Creek made navigation difficult and a straight canal costing £27,000 was opened on August 16, 1837. The canal owners had many difficulties with the railway companies who finally closed off the old entrance and constructed a new cut through Burlington Heights. As a result of poor construction, two bridges collapsed in this cut, the second causing 81 deaths. The combined effects of the railroad and the automobile, along with silting in the canal, caused it to fall into disuse by the year 1900. By 1927, Cootes Paradise and adjoining lands were declared a Crown Game Preserve. The Royal Botanical Gardens was set up in 1941 to administer and control the new parklands on the western edge of the city.

At present, Cootes Paradise Sanctuary covers 1200 acres, half of which is marsh or open waters. Such relatively undisturbed habitat, particularly near large industrial cities, is now extremely rare. It is of great value to the citizen, firstly as a site for study and research, and secondly as a place for personal recreation.

A.2.2. Hydrography and Hydrology

The lower Spencer Creek enters the Town of Dundas immediately

below the Webster's Falls on the Niagara Escarpment. In this reach the flow is rapid (velocities to 3 or 4 fps) but the depth of water is generally less than one foot. Over the four mile reach to Cootes Paradise the creek passes through the town largely unnoticed, along and behind many industrial buildings. Evidently, the stream was at one time a sink for industrial wastes, since numerous drain pipes end over the banks of the stream from neighbouring buildings. However, probably all or most effluent discharges into the stream have now stopped. At the end of the reach the creek becomes deeper, wider, and slower (typically, depth to 8 feet, width to 50 feet, and velocities less than 1 fps).

The flow records used in this study were obtained from the recording gauge "Spencer Creek at Dundas Crossing" (Station No. 02HB010). This is a regulated control site with a drainage area of 64 sq. miles. The records of 1970 indicate a mean monthly flow of 60.4 cfs and 23.7 cfs for the months of May and September, respectively.

Figure 1 illustrates the study section of Spencer Creek. Of the ten sampling stations originally proposed, data collection at stations #7 and #10 proved difficult or impossible.

Figure 2 illustrates the Cootes Paradise area and the associated nature trails. It is included in this dissertation for completeness, and to indicate the conservation interests in this particular study (see also acknowledgements).

For further details of hydrography, see Appendix D.

A.2.3. Current Problems

Some measure of flood control and low flow augmentation for the

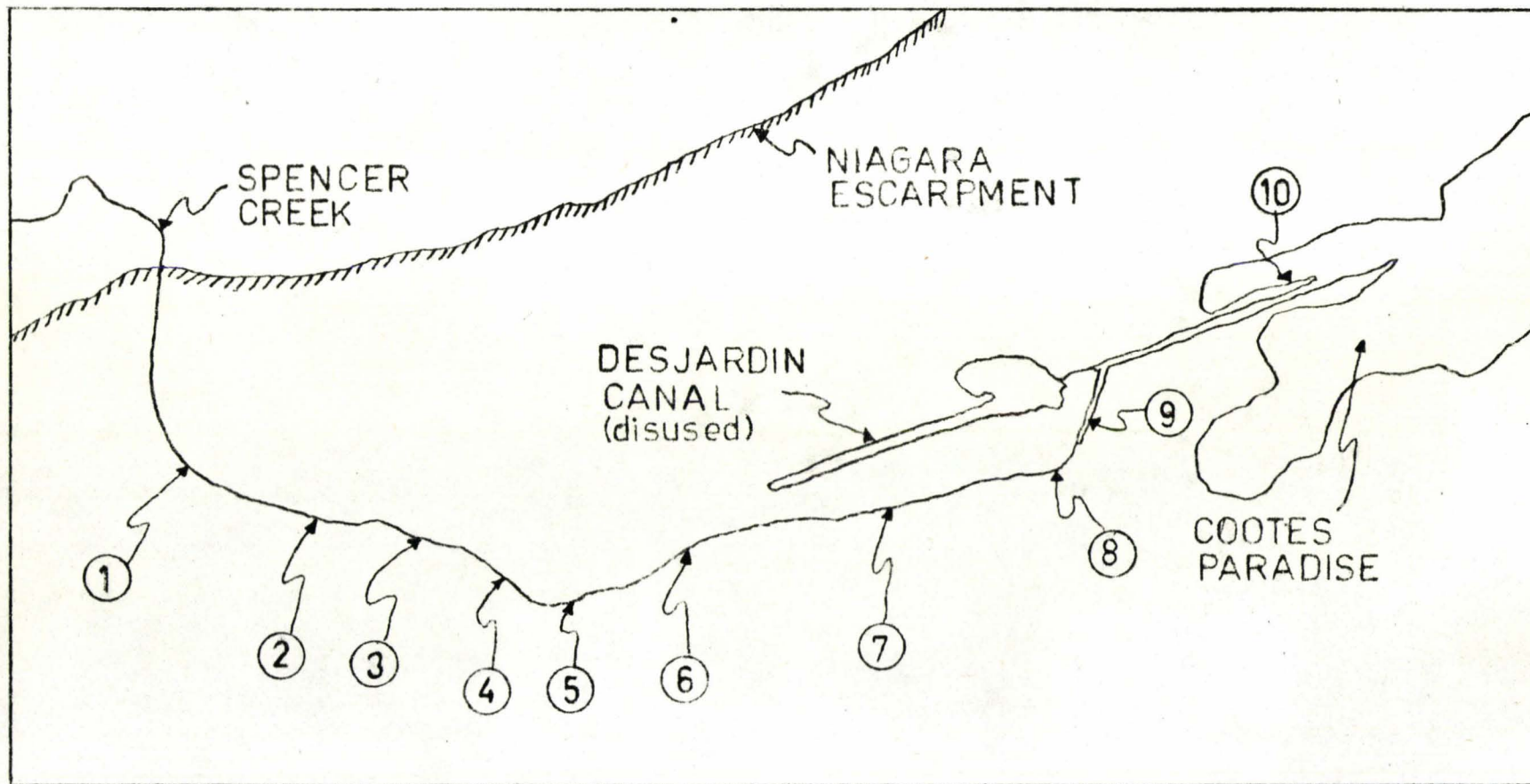


FIG.1

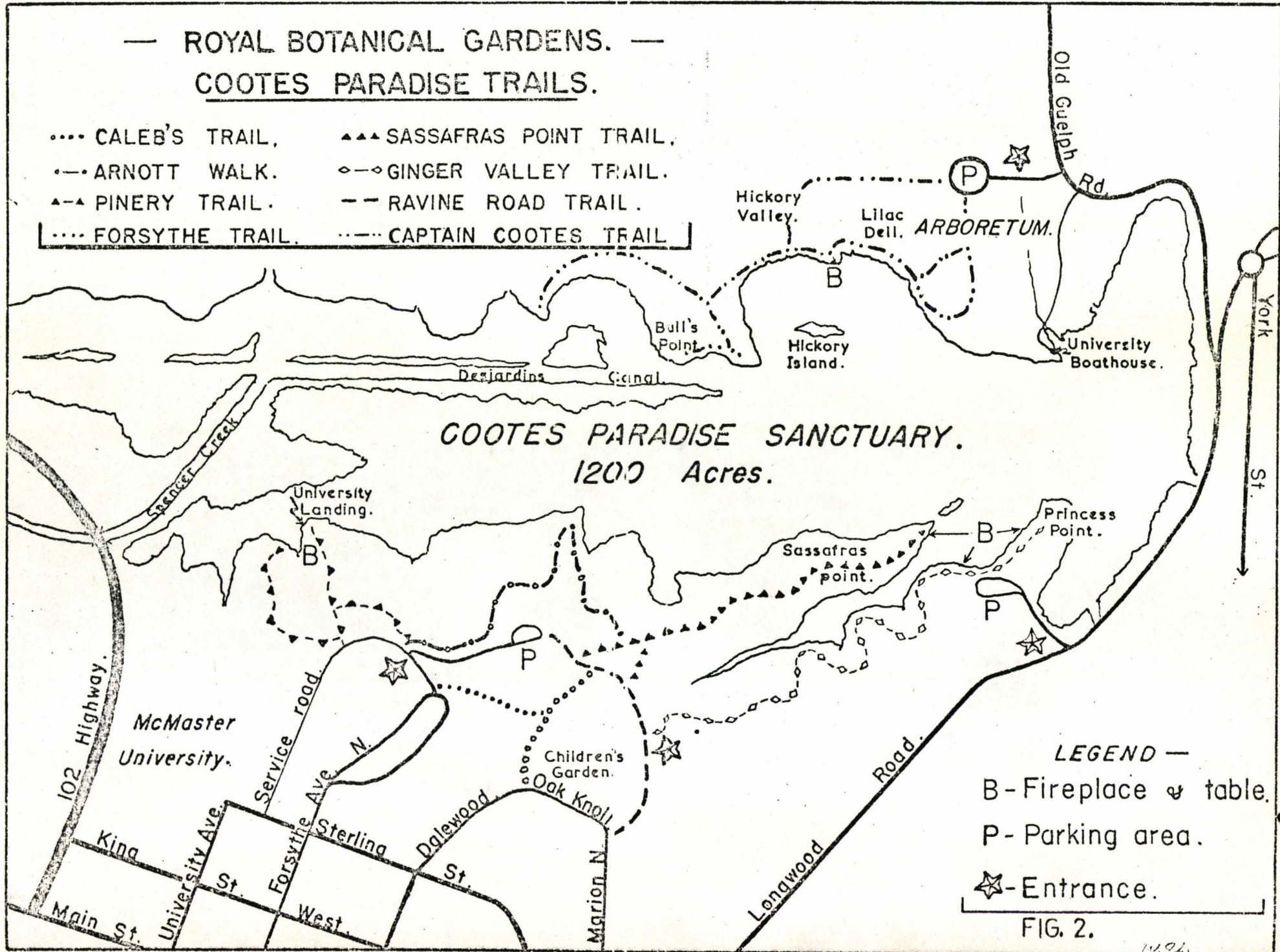
LOWER SPENCER CREEK

scale: 1" = .5 mile

○ sampling station

— ROYAL BOTANICAL GARDENS. —
COOTES PARADISE TRAILS.

- | | |
|-----------------------|----------------------------|
| CALEB'S TRAIL, | ▲▲▲ SASSAFRAS POINT TRAIL, |
| —•— ARNOTT WALK. | ◇—◇ GINGER VALLEY TRAIL. |
| ▲—▲ PINERY TRAIL. | — — RAVINE ROAD TRAIL. |
| FORSYTHE TRAIL. | —•— CAPTAIN COOTES TRAIL |



LEGEND —
 B - Fireplace & table.
 P - Parking area.
 ☆ - Entrance.

FIG. 2.

1991

lower Spencer Creek has been accomplished by the newly constructed Christie Dam on the escarpment above Dundas. The Cootes Paradise conservation area is in constant danger of deterioration and ultimate destruction because of its location between a highly industrialized center to the east and a rapidly developing town to the west. Pollution control must be maintained on the Spencer Creek and the canal if the downstream area is to be preserved.

Solid waste (chunks of concrete, wood, steel, plastic) occurs throughout the reach in the town of Dundas and along the canal. This waste greatly reduces the aesthetic value of the areas and an increased effort should be made to prevent further use of the stream for waste disposal.

From time to time it may be necessary, however, to discharge pollutants into the creek, e.g. salt off the roads in winter. It is a major aim of this study to facilitate a rational management of such waste discharges.

B

MECHANICS OF DISPERSION IN RIVERS

B. MECHANICS OF DISPERSION IN RIVERS

B.1. LITERATURE REVIEW

B.1.1. Effects of Lateral Velocity

Thackston and Krenkel (6) postulate that the basic mechanism of dispersion results from differences in velocity in different parts of the stream cross-section. A complete mathematical model of the mixing process must therefore describe the variation of velocity and turbulent eddy diffusion coefficients at any point in the stream, in order to predict the concentration at any point. The form of the general transport equation for uniform flow in the x-direction is

$$\frac{\partial c}{\partial t} = \frac{\partial}{\partial x} \left(K_x \frac{\partial c}{\partial x} \right) + \frac{\partial}{\partial y} \left(K_y \frac{\partial c}{\partial y} \right) + \frac{\partial}{\partial z} \left(K_z \frac{\partial c}{\partial z} \right) - U \frac{\partial c}{\partial x} \quad (1)$$

where c is the concentration, t is time, x , y , and z are the distances in the direction of flow, the lateral direction, and the vertical direction respectively; K_x , K_y , and K_z are the eddy diffusion coefficients in the x , y and z directions respectively. These authors found that the longitudinal mixing coefficients in two dimensional flow could be accurately predicted using the following equation relating the dispersion coefficient as a function of shear velocity:

$$D_L = 7.25 h u^* \left(\frac{\bar{u}}{u^*} \right)^{\frac{1}{4}} \quad (2)$$

where D_L is the dispersion coefficient, \bar{u} is the mean velocity, h is the depth of flow, and the friction velocity u^* is defined by $(\tau_0/\rho)^{\frac{1}{2}}$ in which τ_0 is the stress at the boundary and ρ is the fluid density. Equation (1) was found to be valid regardless of the scale. Thackston

and Krenkel (6) further concluded that two-dimensional equations have been used inappropriately by many workers in this field. If a significant lateral velocity profile exists in the stream, the mixing coefficient will be much greater than predicted by two-dimensional equations, since these include the effect of vertical velocity gradients only. For non-uniform flow conditions (caused by varying depth, slope, or width, or the presence of bends, islands, control structures or other discontinuities), the two-dimensional equations are inappropriate (6).

Field experiments must be carried out for accurate determinations of mixing coefficients. Thackston (6) used selected reaches in the TVA system. The reaches were straight and uniform, and approximated two-dimensional flow as closely as any in the TVA system. From the available plans, profiles, and cross sections, average depths and cross-sectional areas could be readily determined. Also, the hydraulic variables of discharge, velocity, and depth were controlled, and held steady during the measurement period. The reaches chosen ranged from slow and deep to shallow and fast. Rhodamine B dye was used as a tracer and was injected from a boat moving rapidly across the stream. Time-concentration curves were made by taking grab samples for later analysis or by direct measuring instruments in a sampling boat.

Fischer (1) applied analytical methods for predicting dispersion coefficients in natural streams and for determining the time scale for dispersion. The solution by which Taylor obtained the dispersion coefficient for a long, straight pipe may also be applied to natural streams. Only one modification is required: whereas in a pipe (Taylor's solution) dispersion is caused by differences in velocity in the radial direction, or in infinitely-wide, two-dimensional flow (Elder's solution) the cause

is velocity variations from surface of the flow to bottom, in a natural stream the primary cause of dispersion is differences in velocity in the lateral (transverse) direction (1). Using the Taylor solution and the above assumption, Fischer developed the following equation for predicting the dispersion coefficient in a channel of large width to depth ratio (preferably 6 or greater) and in which there are significant lateral variations in downstream velocity:

$$D = \frac{1}{A} \iint_A u' f dA$$

$$= \frac{1}{A} \int_0^b q'(z) d(z) \int_0^z \frac{1}{\epsilon z d(z)} d(z) \int_0^z q'(z) d(z) \quad (3)$$

where A is the cross-sectional area, u' is the deviation of the velocity from the cross-sectional mean, $q'(z)$ is the depth integrated velocity at any point z , ϵz is the lateral turbulent mixing coefficient. Use of this equation requires knowledge of the channel geometry, (width, b , and depth $d(z)$ as a function of lateral position z), cross-sectional distribution of downstream relative velocity, u' , and shear velocity, u^* . (1) Since the mixing time between zones of different velocities varies as the square of the separation, greater differences in concentration can occur between the surface and bed (1). In natural streams, the important length is the distance over which mixing must take place to establish a uniform distribution; for symmetric channels this is the half-width. This characteristic distance is between the thread of maximum velocity and the furthest distant point within the cross section, i.e. approximately the distance from the point of maximum surface velocity to the most distant bank (1). Fisher designed his laboratory experiments such that velocity distributions were similar to those often found in natural streams. His experiments confirmed his basic hypothesis, viz.

that the primary dispersion mechanism is lateral rather than vertical variations in velocity. This agreed with Thackston and Krenkel. Fischer's experiments showed that variations in lateral velocity induced by secondary currents caused values of coefficient (D) to vary. With all other variables held constant, the mean velocity was varied by using smooth or rough banks. Rough banks produced mean velocities of 45.1 cm/sec and a dispersion coefficient of 4150 cm²/sec. While smooth banks produced mean velocities of 48.3 cm/sec and a dispersion coefficient of only 282 cm²/sec. These secondary currents produce alternating zones of high and low velocity across the channel, which alter the dispersion in the same way as lateral variations induced by side roughnesses. Fischer applied the three dimensional equation (3) and found it to predict the dispersion coefficient D accurately.

Lateral velocity variations were found to increase the dispersion coefficient, i.e. the value given by two-dimensional theory is too small. In fact, these lateral velocity differences increased the actual dispersion coefficient by up to a factor of 14. However, Fischer's method of predicting the dispersion coefficient, based on the time scale, produced less accurate results than the Taylor approach. This was caused by the fact that the time-scale method considers only bulk parameters (the characteristic length) of the channel and the mean squared velocity variation, whereas the Taylor approach included the effect of the distribution of velocity differences within the channel; known to be the important dispersion mechanism (1).

Fischer separated the dispersion of a cloud of tracer particles into two periods, (a) the convective period, and (b) the diffusive, or "Taylor", period. The convective period has been defined as the initial

period when the movement of tracer particles is influenced primarily by their initial convective velocity and in which the movement of the tracer cloud does not obey the Taylor one-dimensional diffusion theory. During the Taylor period the one-dimensional diffusion equation is valid:

$$\frac{\partial \bar{c}}{\partial t} + \bar{u} \frac{\partial \bar{c}}{\partial x} = D \frac{\partial^2 \bar{c}}{\partial x^2}$$

Fischer concluded that assuming similar cross-sectional distribution of velocity, the dispersion coefficient is proportional to the square of the channel width, and inversely to the depth.

In a later paper Fischer (3) reports applications of the theories to field tests and to previously published data obtained from natural streams. Here Fischer also presented a routing method. In this procedure the upstream observed concentration-time curve is used as the initial tracer distribution, and a concentration-time curve for the downstream station is predicted by the one-dimensional dispersion model. The predicted and the observed downstream station curves are compared; if the comparison is not adequate, a new dispersion coefficient is selected, and the calculation is repeated until the best possible comparison is obtained. The coefficient obtained by this procedure is by definition the best possible coefficient. Any dispersion coefficient calculated for a natural stream by whatever method should be checked by the routing procedure; if an adequate routing is not obtained, the coefficient must be adjusted. (3) Fischer feels that the routing procedure is the definitive test whereby a coefficient derived by another method should be judged.

B.1.2. Effects of Cross-Sectional Geometry

Sooky (5) demonstrated that there are three significant factors in determining the dimensionless dispersion coefficient in an open channel where there is an appreciable lateral velocity variation and the width-to-depth ratio is large. These are the width-to-hydraulic radius ratio, the cross-sectional shape, and the Reynold Number. Sooky expressed the dispersion coefficient, K , as follows:

$$K = C_{L,t} R u^*$$

where $C_{L,t}$ is a dimensionless coefficient, R is the hydraulic radius, and u^* is the friction velocity. It was found that the value of $K/(Ru^*)$ for an open channel of finite width varies directly and quite significantly with the width-to-hydraulic radius ratio. This variation actually reflects a hidden scale effect because larger streams, in general, tend to have larger width-to-hydraulic radius ratios. (5) This partly explains why previous theoretical equations failed to predict values for the dispersion coefficient for natural streams. (5)

The second observation relates to the cross-sectional shape, represented by the ratio W_L/W , and thus the cross-sectional velocity distribution. A simplified triangular cross-section is shown in Figure 3. A highly asymmetrical cross section ($W_L/W=0$) results in a nearly four-fold increase in $K/(Ru^*)$ with respect to the symmetrical arrangement. The symmetrical arrangement ($W_L/W=0.5$) is in close agreement with Fischer's time scale formulation which predicts an increase of a factor of four. (5) This partly explains the rapid increase of the dispersion coefficient when there is a bend in the direction of flow, as was first noted by Taylor for pipe flow. In order to gain more information regarding

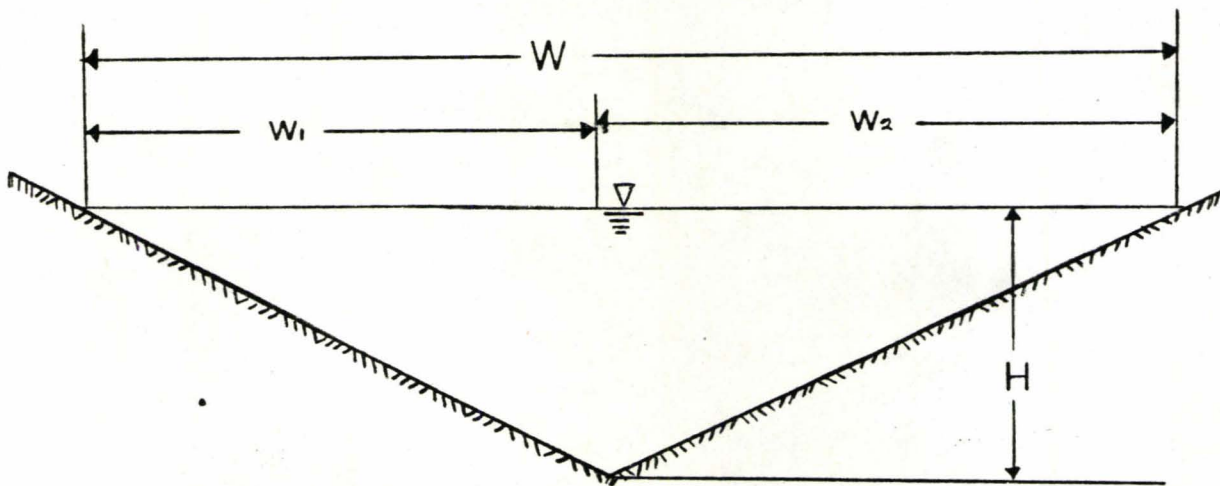


FIG. 3.

TRIANGULAR CROSS
SECTION

the cross-sectional shape and its influence on the dispersion process, Sooky used the same approach for a circular cross section, as shown in Figure 4. A comparison between the circular arc and the triangular cross-sections indicates that, keeping the same W/R ratio, the dimensionless dispersion coefficient for the latter shape is more than twice the value for the former. (5) For streams with an irregular cross section containing protruding sand banks and deep areas, the dispersion coefficient will be larger than for those with a smoothly shaped cross section. (5)

Sooky found that previous researchers had accurately predicted the dispersion coefficient for the conditions under which they were derived. Most of the actual dimensional dispersion coefficients are in excess of the theoretical values indicated by the models, both for the symmetrical triangular or the circular arc cross sections. The larger part of this excess is probably due to nonuniformities along the flow, mainly bends and meandering, which are not accounted for in the analysis, and a smaller part is probably due to deviation in the cross-sectional shape. (5) Accumulating evidence indicates that the failure of the theoretical models is due to assumptions made in their derivation. Results from laboratory experiments confirmed such theories because they were conducted under the very conditions assumed in the derivation. Sooky (5) further points out that there are three assumptions implied in these theories which are never satisfied in natural streams: (1) a natural stream can be considered uniform for stretches only, in conflict with the theoretical assumption of uniformity throughout the entire length. In the presence of these non-uniformities the dispersion coefficient must be measured in the field. (2) The velocity is assumed to

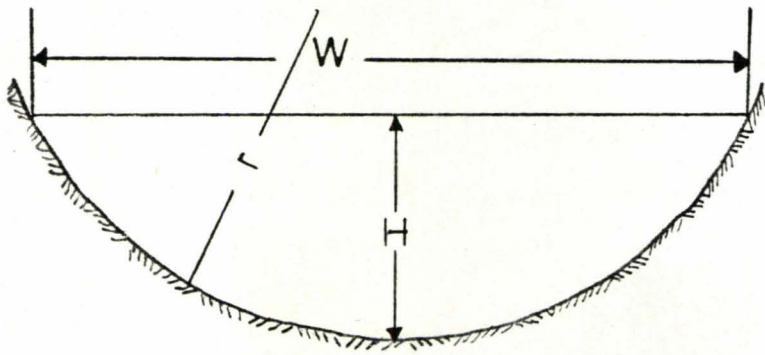


FIG. 4.

CIRCULAR CROSS
SECTION

vary in only one direction, such as radially in a tube or vertically in an infinitely wide open-channel. In reality, however, velocity varies in two directions in any cross section. Thus, the effects of lateral variations in downstream velocity are not included in existing theories for open channels. However, it was experimentally verified by Fischer that side effects are important in the dispersion process. (3) All existing theories assume that the flow is two-dimensional. In flow of streams and rivers there are always small but non-zero transverse components due to secondary currents. This secondary circular flow superimposed on the forward component may produce a spiral motion. These secondary currents play an important part in dispersion.

Sooky applied a logarithmic velocity profile assumed by Elder ($K=C_{L,t} R u_*$) and a power law profile assumed by Thomas ($K=C_p, c R u_*$). He found that although these methods were not as accurate as direct tracer measurements or Fischer's method of using measured velocity distribution, this method predicts realistic values of the dispersion coefficient for natural streams and only requires knowledge of the cross-sectional geometry and the mean channel shear velocity (and mean flow velocity if the power laws velocity profile is assumed.) (5) In Sooky's method, $K=K_L+K'+K''$, where K is the virtual coefficient of diffusion or dispersion coefficient, K_L is the convective diffusion coefficient, K' is the mean coefficient of turbulent diffusion in the cross section due to the radial velocity gradient, and K'' is the mean coefficient of turbulent diffusion in the cross section due to the lateral velocity gradient.

$$K_L = -\frac{1}{A} \int_0^w \left[\int_0^h (u-U) dz \right] \int_0^y \frac{\int_0^h (u-U) dz dy}{\int_0^h E_y dz} dy dy$$

$$K' = \frac{1}{A} \int_A E_y dA$$

$$K'' = \frac{1}{A} \int_A E_z dA$$

where W is the top width of the stream, and E_y and E_z are the turbulent mixing coefficients in the y and z directions, respectively.

Godfrey and Frederick (8) carried out field studies to obtain data for an evaluation of the one-dimensional approach to describing dispersion in large open channels. To verify part of the one-dimensional theory, that is, constant dispersion coefficient, Godfrey and Frederick hoped to and did find that dispersion increased directly with time, for long times after release of the tracer. However, the magnitude of the discrepancies between observed and theoretical dispersion coefficients suggests that one-dimensional models are too limited to describe dispersion in natural streams.

B.1.3. Effects of Dead Zones

Thackston and Krenkel (6) investigated the effects of "dead zones" and found these flow discontinuities resulted in significantly higher values of the apparent mixing coefficients. Thackston and Krenkel applied the Hays (9) "dead zone" model in separating the effects of "dead zones" from those where there were velocity gradients. Hays previously developed equations which describe the effects of temporary storage in such dead zones in addition to mixing caused by turbulence and velocity gradients. The equations are, for the main stream:

$$\frac{\partial C_a}{\partial t} = D_L \frac{\partial^2 C_a}{\partial x^2} - \bar{u} \frac{\partial C_a}{\partial x} + K_a (C_d - C_a)$$

and for the dead zone:

$$\frac{\partial C_d}{\partial x} = K_d(C_a - C_d)$$

where C_a and C_d are the concentrations in the main stream and the dead zone, respectively, and K_a and K_d are the eddy diffusion coefficients in the main stream and the dead zone, respectively.

Thackston and Schnelle (14) found that measured time-concentration curves and visual observation of tracers used for dispersion studies in natural streams have shown two significant characteristics. First, the time-concentration curves exhibit a considerable deviation from the results that would be predicted by the one-dimensional dispersion model of Taylor. A typical example of this is seen where the leading edge of the measured curve rises faster and the tail extends much longer than would be predicted by Taylor's model. Second, visual observation confirms that parts of a tracer used in a natural stream study will become entrapped in pockets of little or no flow along the sides of the stream. These pockets, caused by the meandering nature of streams and the debris usually found lodged along the sides of the streams, hold onto a portion of the tracer as the main bulk passes by. There is then a slow, continual release of tracer into the main stream until the pocket along the side is completely clear of tracer. Thus, a sensor in the stream at first sees a large bulk of material pass by fast, and then continues to see a diminishing amount of tracer over an extended period of time. Thackston and Krenkel (6) postulate that the influence of a dead zone is proportional to its volume and to the rate at which material is transferred into and out of it. If the transfer rate is high it will have little effect and will act as a part of the main stream. If the transfer rate is low, it

will also have little effect, and will be negligible as far as flow in the main stream is concerned.

The stream is divided into a main stream and a dead zone where it is assumed the tracer will be held. Hays (9) has written a model for this process in which the main stream is assumed to follow the Taylor one-dimensional dispersion equation, with a term being added to account for the mass transfer to and from the dead zone. A second, coupled equation is used to describe the concentration distribution in the dead zone. Two types of mechanisms are proposed for the mass transport mechanism to and from the dead zone: one in which the dead zone is assumed to be completely mixed; and the other in which there is lateral dispersion dependent upon the geometry of the dead zone. Hays' work indicates that each of these models fits the experimental data quite well and that there is no significant difference between the ability of the various dead zone models to predict the time-concentration curves. (14)

B.1.4. Effect of Bends

A bend brings about considerable changes in the transverse distribution of the longitudinal velocity component; the maximum velocity region moves close to the outer bank where the maximum depth is located, resulting in a velocity distribution similar to the one assumed in the analysis for an asymmetrical triangular cross section. In the case of an actual bend, the effect of this velocity redistribution on the dispersion process will be opposed by the bend-induced secondary current which transports the dispersing material in the transverse direction. (5)

The net effect of these two factors in a particular situation is not established analytically at the present time. (5)

Fischer (19) states that bends in streams induce secondary currents that alter the rates of both transverse mixing and longitudinal dispersion. Within a bend the transverse mixing coefficient depends on the square of the mean velocity, cube of the depth, and inversely on the shear velocity and square of the radius of curvature, as verified by a laboratory experiment. The longitudinal coefficient depends on the channel geometry, velocity distribution, rate of transverse mixing, and a dimensionless parameter that includes the mean velocity and length of an average bend. Fischer (19) shows that in narrow streams, such as those he studied, it makes little difference whether the bends alternate in direction or are continuous and uniform in one direction only. Fischer concludes that stream meanders influence longitudinal dispersion in two ways: first, by concentrating the zone of high velocity towards the outside of the curve they greatly increase the rate of dispersion, and second, by inducing secondary currents they increase the transverse mixing, which tends to reduce the dispersion.

B.2. DISCUSSION OF DISPERSION IN THE STUDY AREA

The section of Spencer's Creek used in the study has many of the physical characteristics noted for producing inaccurate estimates of dispersion coefficients, i.e. varying depth, slope, and width; bends, small islands, bridge piers, pools, falls, and other discontinuities. Many of these irregularities are illustrated in the photos in Appendix D. Along the study reach there are seven falls varying from eight feet to two feet in height. Immediately downstream from two of the above mentioned falls are pools, or "dead zones". The study reach has four relatively straight sections which are divided by bends varying in degree from

nearly 90° to slight turns. The section has many constructions as a result of bridges, resulting in geometry changes from section to section. Figure 5 indicates the position along the reach at which each photo was taken.

Dispersion coefficient values would be larger than theoretical values, as found by Thackston and Krenkel (6). Bottom roughness and bank conditions vary along the study section, but a distinction can be made between the steep and flat sections. The width to depth ratio varies from 30 to 1 in the upstream sections and from 6 to 1 in the downstream sections. Several small dead zones, mentioned previously, exist along the reach which cause temporary storage of a pollutant or tracer material. Some dead zones result from obstructions of trapped debris, and are thus temporary or flood dependent.

In particular, two sharp bends and several lesser curves along the study reach will affect dispersion.

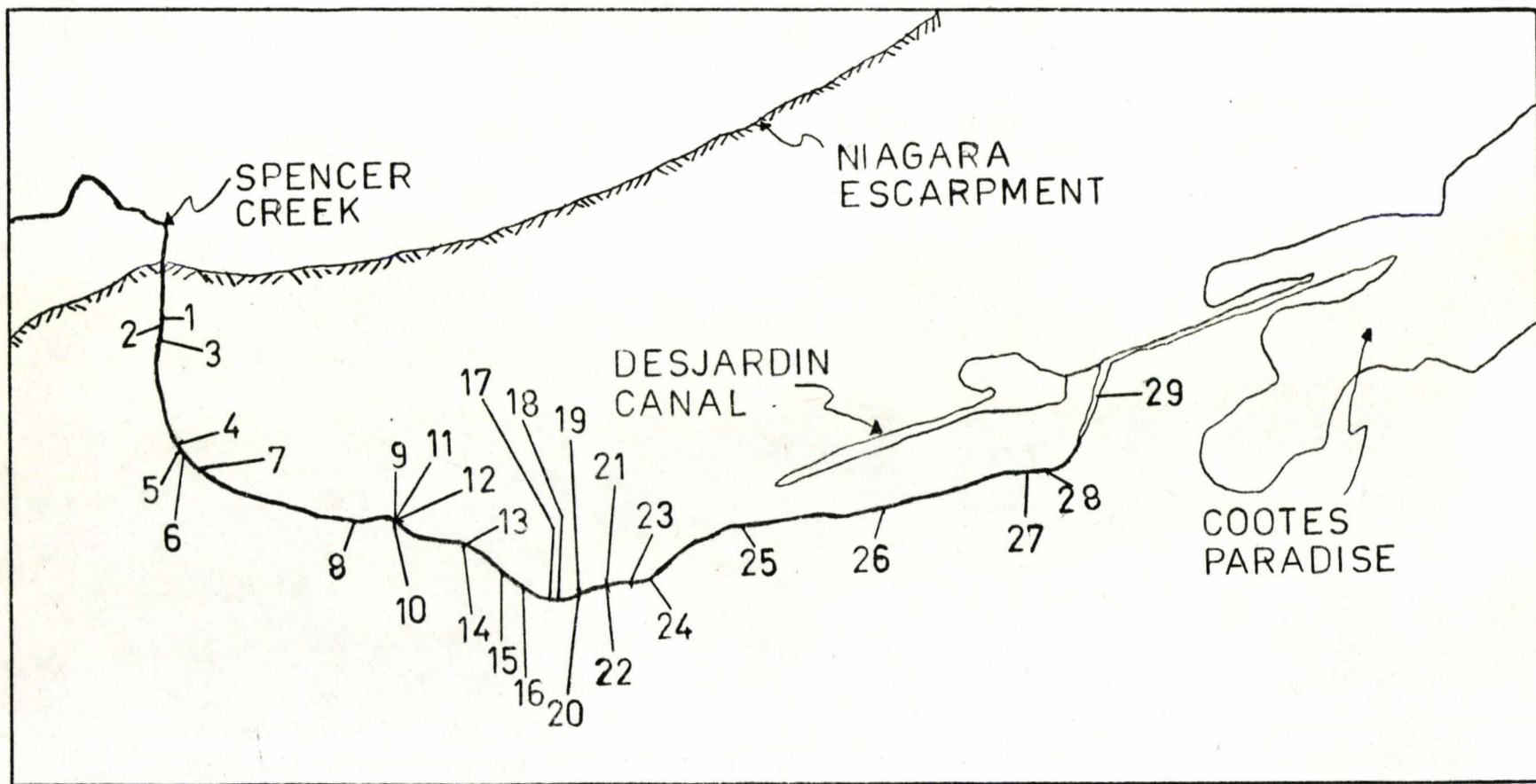


FIG. 5.
 LOWER SPENCER CREEK
 scale: 1"=.5 mile
 PHOTO LOCATIONS

C

FIELD PROCEDURES AND RESULTS

C. FIELD PROCEDURES AND RESULTS

C.1. SELECTION OF TRACER

C.1.1. Desirable Properties

Ideally, the tracer used in this investigation should possess the following characteristics: (18)

- (a) be stable in a natural environment, i.e. not affected by light, bacteria, pH, temperature, algae, absorption, or by chemicals such as chlorine that might be present in the system;
- (b) be non-toxic at levels employed;
- (c) be easily measured in situ, detectable at low concentrations, measured accurately over the whole range without requiring large quantities or expensive equipment;
- (d) large or variable background amounts should not exist;
- (e) be inexpensive, easily handled and water soluble; and
- (f) be physically undetectable over prolonged periods of time.

A search of the literature was undertaken to find a tracer that would satisfy all or most of the above criteria.

Generally, there are three types of tracers: various salts, fluorescent dyes, and radioactive tracers. Each type is discussed and compared briefly herein.

C.1.2. Sodium Chloride

Sodium chloride (common salt) has been widely used as a tracer, but its use has been limited because it cannot readily or accurately be

detected at concentrations lower than 1.0 ppm. (16) Furthermore, it cannot be readily separated from naturally occurring substances such as chlorides, which are found quite commonly at various concentrations in many water supplies. (16) The greatest advantage of salt is its low cost. Fischer (1) employed salt as a tracer in early laboratory studies using a conductivity probe. Using a strip recorder (SANBORN SERIES 150) he was able to obtain a sampling accuracy as low as 0.5 ppm. Glover (13) found that salt was an adequate tracer in laboratory studies since background quantities could be accurately estimated. Field studies by C.P. Straub using sodium chloride as a tracer to determine time of travel indicated that large amounts of salt were required, long times were required to determine chloride concentrations, and incomplete mixing in the water occurred. (12) Hudspeth (18) also found that large quantities were required, background counts were large and possibly variable, and density effects may be involved. Fischer (1) found that the density could be adjusted to that of the receiving water by addition of methanol.

C.1.3. Radioisotopes

Radioisotopes are being employed as tracers but their use has been limited because of their high cost and their threat to public health. Extreme safety precautions have to be taken (16), including approval and licensing by various governmental agencies. Although the cost of most radioisotopes is high, however, the expense is offset to a large degree by the extremely small quantity that can be detected. The necessary detecting instruments, such as scintillation counters, are quite expensive, however. (16) In field studies Fischer (3) used gold-198 because of its higher permissible concentration, shorter half-life, and lower

cost. The amount of activity required was proportional to the discharge. Fischer (3) used 2 curies per 1000 cfs. Fischer found that the resulting concentrations of activity dropped rapidly to a level below that specified as the maximum permissible concentration in unrestricted areas, but were sufficiently high to be easily detected at all cross sections within the reach. Godfrey and Frederick (8) found that grab sampling is adequate only if time of travel of the labelled water is accurately known for proper timing of sample collection at several measuring sites. Godfrey and Frederick further point out that unless there are no finite boundaries within 3 to 4 feet of any side of the crystal used in radiation detection, the sensing apparatus must be calibrated in situ; this limits their use to large bodies of water unless relative readings are satisfactory.

C.1.4. Chemicals

Glover (10) chose potassium carbonate as a tracer material. This material was chosen because it is non-poisonous and highly soluble in water and because potassium yields a brilliant flame colour. This latter consideration was important since a flame photometer was used to analyze the samples. Background counts of approximately 9 ppm of potassium ion were found to exist in the natural stream used. The potassium carbonate used was of technical grade having a purity of 98 to 100 per cent. It is of the dry anhydrous form and visually is a white, free-running powder.

C.1.5. Dyes

Fluorometric techniques now seem to be more generally favourable than radioactive techniques. (18) This may not be the case where there is a need for very accurate measurements and where calibration can be done in situ, or where large bodies of water are being studied. Fluorescent dyes possess unique properties which allow their detection at extremely low concentrations with the naked eye. Furthermore, they provide the least expensive method of tracing and with the development of modern fluorometric techniques, they can be detected at levels of less than one part per billion (ppb). The measurements can be made very quickly without the use of any elaborate preparation of the samples. (21)

Fluorescent dyes are available in a wide range of colours. The selection of a dye for a particular application depends upon its inherent properties and conditions of use.

Four dyes, each a variation of the same basic organic structure (xanthene), have been used extensively as tracers: Rhodamine B, Rhodamine WT, Pontacyl Pink, and Fluorescein.

C.P. Straub used fluorescein with colourmetric analysis, but the spectrophotometer can only detect comparatively large quantities of dye, and it cannot be used directly in the field. (17) Fluorescein is also known as sodium fluorescein, uranine, and acid yellow dye. Though highly fluorescent and readily detectable at extremely low concentrations, it is not recommended for use in surface water tracing because of its rapid rate of decay in sunlight. It is also difficult to distinguish trace quantities with the "black" light of a fluorometer in samples with high background interferences. Acid pH may cause a loss of sensitivity while alkaline pH tends to intensify its fluorescence. It has a low adsorptive

See Appendix C on the principles of Fluorescence; Factors Affecting and Precautions.

tendency and therefore it is suggested as a good under-ground tracer in permeable soils that are relatively free from organic matter. (21)

Rhodamine B has been favoured in recent water tracing studies. It is related to the more familiar disodium fluorescein dye. It is non-toxic to human beings, and is used as a pigment in lipstick and pink birthday candles. The dye may be obtained commercially in solution concentrations of 40% by weight in acetic acid. Because of its high solubility in methanol, concentrated dye solution may be adjusted to the same density as that of the water. Rhodamine B dye is less affected by light and the action of bacteria than fluorescein. Prichard and Carpenter found that the dye in glass bottles, when exposed to "daylight" fluorescent lighting for 8 months, decreased in fluorescence only 5 per cent, while when exposed to direct sunlight for 2 months, it decreased 40 per cent in fluorescence. Pritchard and Carpenter suggest that, in natural streams, the decomposition by light would be negligible for periods up to 2 weeks. Fluorescence makes Rhodamine B readily detectable. The long wavelength of the exciting light reduces the absorption and scattering by the water, thereby aiding in the reduction of background. The fluorescence of Rhodamine B is not affected by acidity within a pH range of 4.0-10.5. Tests have indicated that part of the dye used in tracer studies in stream channels will be lost by adsorption on the stream boundaries. A chemical property of Rhodamine B that must not be overlooked is the phenol component of its molecule. If the surface waters to be tested are used as municipal water supplies, precautions must be taken to keep the dye concentration low enough to prevent formation of chlorphenol tastes; especially where chlorination is the only chemical treatment. The cost of Rhodamine B in 1964 was approximately

\$2.00 per pound of solution. (17)

The fluorescence of Rhodamine B decreases with increasing temperature. Pritchard and Carpenter found that the range of decrease is 2.3% per degree centigrade within a temperature range of 12°C to 28°C.

(17) For accurate determination of concentrations, the temperature of samples should be taken. Thackston and Krenkel (5) used Rhodamine B for field studies. Grab samples were taken every 15 seconds to 60 seconds and measurement of fluorescence was made using a Beckman Model 772 Ratio Fluorometer. Continuous sampling was recorded using a Photomultiplier Fluoro-Microphotometer (model 10-213) on paper charts.

Fischer (11) used Rhodamine B as a tracer for a grab sampling method. Sample bottles (16 oz.) were filled by gravity, stored in a dark place, and returned to the laboratory for analysis.

Its minimum visual concentration in clean water is about 10-15 ppb and it becomes visible in a glass of water at 30 ppb. Rhodamine B is not recommended for tracing ground waters because it tends to be absorbed by the soil particles.

Preparation and handling the powdered form of the dye should be done with utmost care because it will stain hands, clothing, and any other porous materials such as wood and concrete. (21)

Pontacyl Brilliant Pink is an expensive dye costing about four times as much as Rhodamine B. The intensity of fluorescence is much lower than that of Rhodamine B but is independent of pH over a wider range (pH 3 to 10). It has very low absorption tendency. Two other commercial dyes, namely Kiton Rhodamine B and Sulfo Rhodamine B, have similar properties. (21)

Another fluorescent dye very similar to Rhodamine B is increa-

singly favoured for tracer studies. This is Rhodamine WT. Hudspith (18) found this dye very suitable. Hudspith lists the properties of Rhodamine WT in the same order as those for an ideal tracer:

(a) The dye is slightly less adsorbed, on most materials, than Pontacyl Brilliant Pink and far less than Rhodamine B. It can be considered negligible in short reaches of a few miles. The concentration is affected by sunlight but the decay rate is small enough to be ignored for usual periods of exposure. The concentration has been found to be independent of pH between the values of 5-10 but is very sensitive to temperature. The dependence on temperature has been measured and can be easily corrected for.

(b) The tolerance level for human consumption has been set at 0.75mg/day which is equivalent to $2\frac{1}{2}$ quarts at 370 ppb. At this concentration the dye is brilliant red.

(c) The concentration of the dye can be easily and continuously measured using a flow-through fluorometer. It can be detected at concentrations as low as 2 ppb and the fluorescent intensity is linear with concentration within the range 0-800 ppb.

(d) The background from natural sources was found to be small and easily corrected for. The indirect form of background or interference due to turbidity is appreciable at high concentrations of suspended solids but can be ignored at low concentrations.

(e) The dye is available as a 20% solution and is relatively inexpensive.

A summary of organic dyes used as tracers is presented in Table 1, and Table 2 lists a summary of the advantages and disadvantages of the various tracers considered for this study.

CHARACTERISTICS OF ORGANIC
DYES USED AS TRACERS

C.1.6
TABLE. 1.

DYE	COLOUR (10PPM)	DETERIORATION BY			MINIMUM VISIBLE CONCENTRATION	
		ACIDS	ALKALIS	SUNLIGHT	NAKED EYE	ULTRAVIOLET
SODIUM FLUORESCEIN	BRILLIANT FLUORESCENT	YES	NO	YES	25 (PPM)	15-25 (PPM)
RHODAMINE B EXTRA	DEEP DARK RED	NO	NO	NO	15	10
CRYSTAL VIOLET	OPAQUE PURPLE	NO	SLIGHT	NO	25-50	—
KITON GREEN UV EXTRA	GREENISH BLACK	TURN BLUE	YES	YES	15-20	25
RHODAMINE 6GDN	RED- GREEN	NO	SLIGHT	NO	10-25	10
KITON RHODAMINE B	DEEP RED	NO	NO	NO	100-150	125
PONTACYL BRILLIANT PINK	DEEP RED	NO	NO	NO	50	25
PYLA TEL BLACK	DARK GREEN	YES	YES	YES	75	25
PYLA TEL GREEN	BRILLIANT GREEN	YES	NO	YES	50	75
RHODAMINE WT	DEEP DARK RED	NO	NO	NO	10-15	10

COMPARISON OF TRACERS
CONSIDERED

C-17

TABLE 2.

ADVANTAGE ✓
DISADVANTAGE X

	EFFECT OF SUNLIGHT	PH EFFECT	TEMPERATURE EFFECT	EFFECT OF AQUATIC LIFE	ADSORPTION	CHEMICALLY AFFECTED	TOXICITY	QUANTITY REQUIRED	COST	DETECTABLE	BACKGROUND EFFECT	HANDLING	DENSITY EFFECT
SODIUM CHLORIDE	✓							X	✓	X	X		X
RHODAMINE B	✓	✓	X	✓	✓		✓	✓	✓	✓	✓	✓	X
PONTACYL BRILLIANT PINK	✓	✓			X		✓		X		✓		
FLUORESCEIN	X	X			✓					✓	X		
POTASSIUM CARBONATE			✓				✓						
RADIOACTIVE MATERIALS	✓	✓	✓	X	X	✓	X	✓	X	✓		X	
RHODAMINE WT	✓	✓	X	✓	✓		✓	✓	✓	✓	✓	✓	

C.2. INJECTION AND SAMPLING

C.2.1. Injection

The amount of Rhodamine WT dye required is a function of the discharge, the length, and the dispersion characteristics of the reach. The theoretical method of computing the dosage would be to use the basic dispersion equation, but because of the difficulty of predicting dispersion coefficients, this method appears to be unsatisfactory.

A "rule-of-thumb" formula was used (1) to compute a dosage equivalent to 1 ppb of Rhodamine WT solution for the volume of water in the reach. A calculation using values of reach length, average discharge, and mean velocity indicates very small quantities of the dye are required:

EXAMPLE: Length of reach 3 miles
 Average discharge 10 cfs
 Mean velocity 0.5 fps

Volume of water in the reach: $\text{Volume} = \frac{Q \times L}{V}$

where Q is the discharge in cfs measured or from gaging-station rating

L is the length of the reach in feet measured from maps

V is the mean velocity in fps estimated or measured from spot tests

$$\text{Volume} = \frac{1 \times 10^1 \times 3 \times 5.28 \times 10^3}{5 \times 10^{-1}}$$

$$= 3.16 \times 10^3 \text{ cu. ft.}$$

$$\text{Dosage required} = 3.16 \times 10^3 \times 1 \times 10^{-9} \times 2.832 \times 10^4$$

$$= 8.95 \times 10^{-2}$$

$$= 0.0895 \text{ ml. (100\% solution)}$$

$$= 0.4475 \text{ ml. (20\% solution)}$$

$$= \frac{1}{2} \text{ millilitre}$$

NOTE: Because the dye does not disperse throughout the entire length of the reach, the peak concentration will greatly exceed 1 ppb.

To the calculated amount of dye an amount of methanol could be added to adjust the density of the resulting solution to the density of the water. However, this was not necessary in the tests because of rapid mixing of the dye after injection. The injection sites were highly turbulent producing complete mixing in the vertical direction. The computed amount of dye for each test was taken from the stock solution of Rhodamine WT (20% solution) and taken to the injection site in a sealed glass container. All injections were made by "instantaneously" pouring the dye from a wide mouth container while standing on a bridge. The first sampling stations from both injection points were sufficiently well downstream to ensure complete mixing in both the lateral and the vertical directions.

C.2.2. Sampling

Samples were taken at predetermined points along the reach. The sampling sites were usually bridges because of the convenience of working from these structures, either from the deck or immediately beneath the deck where the flow was contained in a restricted area. Other samples were obtained from a boat or by wading. As could be expected the dye cloud comes through a cross section in the form of a wedge, first along the maximum velocity thread and then near the banks. For this reason, samples were taken as close to the center of the section as possible. Most samples were taken near the water surface; in the upper reaches because of shallow depth and at a depth of 2 to 3 feet in the lower reaches.

Grab samples were taken at all cross sections. Sampling intervals varied depending upon the flow speed at the station. For the rapid sections grab samples were taken at intervals of 30 seconds, while for the slow sections sampling intervals ranged from one to five minutes. All samples were contained in styrofoam cups and sealed with a plastic lid and then returned to the laboratory for analysis.

C.3. ANALYSIS

The samples were stored in the laboratory overnight before analysis for two reasons: first, to allow floating material to settle out, and second, to allow all samples to reach a common temperature, since Rhodamine WT fluorescence is temperature dependent. This aids in correcting for temperature differences between sampling and analysis.

A Turner model 111 Fluorometer was used to analyse all samples. The calibration procedure and calibration curves are given in Appendix A. Each sample was pumped through the fluorometer, yielding a dial reading on the scale between zero and one hundred. From this dial reading the background count was subtracted giving the net reading. A temperature correction factor (27) was applied to the net reading, then this was converted to a value in ppb by multiplying by the appropriate scale calibration constant. An example calculation is given below:

Dial Reading	32	
Sample Temperature	82.5°F	
Base Temperature	77°F	
Temperature Difference	5.5°F	
Correction Factor	0.92	
Corrected Dial Reading	29.4	
Concentration	23.5 ppb	(calibration constant 0.8)

Samples from tests #1 and #2 were analysed at 20°C with a correc-

tion factor of 0.92, while samples from tests #3, #4, and #5 were analysed at 21°C with a correction factor of 1.1. Figure 6 shows the temperature-correction curves for Rhodamine B, Rhodamine WT, and Pontacyl Pink dyes. (27)

C.4. RESULTS

C.4.1. Calculation of Dispersion Coefficient From Observed Concentration Distribution

Methods based on the properties of the Gaussian distribution will give incorrect results if applied to skewed concentration distributions, as almost always encountered in tests in natural streams. (5) Thus, none of these methods should be used with natural stream data, unless sufficient dimensionless time has passed for the time-concentration curves to become nearly Gaussian. (5)

A theoretically exact method for calculating a dispersion coefficient from concentration versus time curves obtained at two stations is:

$$D_L = \left(\frac{1}{2}\right)(\bar{u})^2 \frac{\sigma_{t_2}^2 - \sigma_{t_1}^2}{\bar{t}_2 - \bar{t}_1}$$

in which $\sigma_{t_1}^2$ and $\sigma_{t_2}^2$ are the variances of the concentration-time curves at the upstream and downstream stations, respectively, and \bar{t}_1 and \bar{t}_2 are the mean time of passage of the tracer cloud past each station (based on the peak-to-peak time between stations), and \bar{u} is the mean velocity of flow.

This equation was used to calculate the dispersion coefficients.

The variance of each concentration-time curve was calculated using the standard deviation value for each curve. For each curve values of mean, skewness, kurtosis, correlation coefficients, regression coeffi-

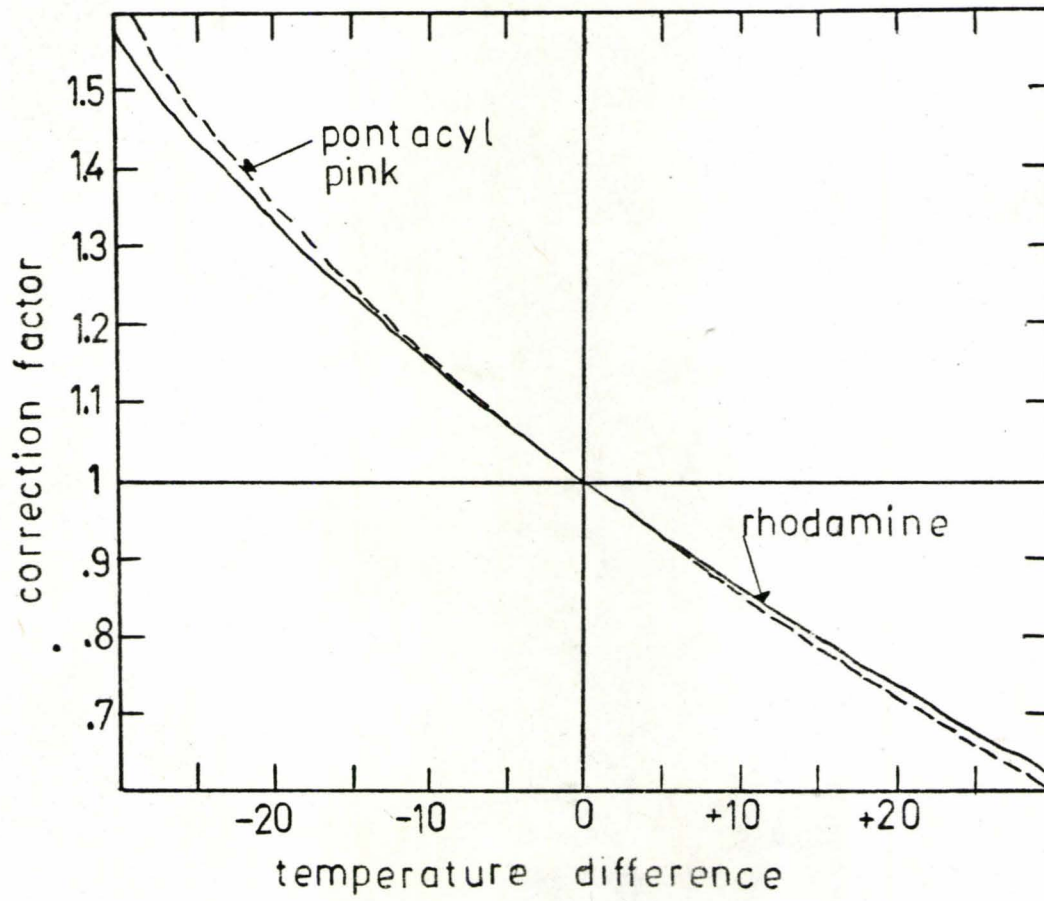


FIG. 6.

coefficients were also calculated using the SUBROUTINE MISR available at the McMaster University Computing Centre.

The dispersion coefficients for each test are summarized below:

<u>Test Number</u>	<u>Sampling Station Number</u>	<u>Dispersion Coefficient (ft²/sec)</u>
#1	#6	3.02×10^2
	#8	1.52×10^{-4}
	#9	9.45×10^{-7}
	#10	2.34×10^{-7}
#2	#6	3.93×10^1
	#8	2.54×10^{-1}
#3	#6	6.68×10^1
	#8	1.86×10^{-2}
	#9	1.83×10^{-3}
#4	#1	3.16×10^2
	#2	1.09×10^2
	#3	2.80×10^1
	#5	5.58×10^1
	#6	7.42×10^{-1}
	#8	8.32×10^{-3}
	#9	8.55×10^{-4}
#5	#1	6.75
	#2	1.70
	#5	6.90×10^{-1}
	#6	7.78×10^{-2}
	#8	9.56×10^{-5}
	#9	2.38×10^{-6}

The observed concentration was plotted for each station and each test, and these are presented in Appendix E. The recovery ratio was calculated in each case and these are summarized in Table 3.

The concentration distributions for each station are presented in this part of the report.

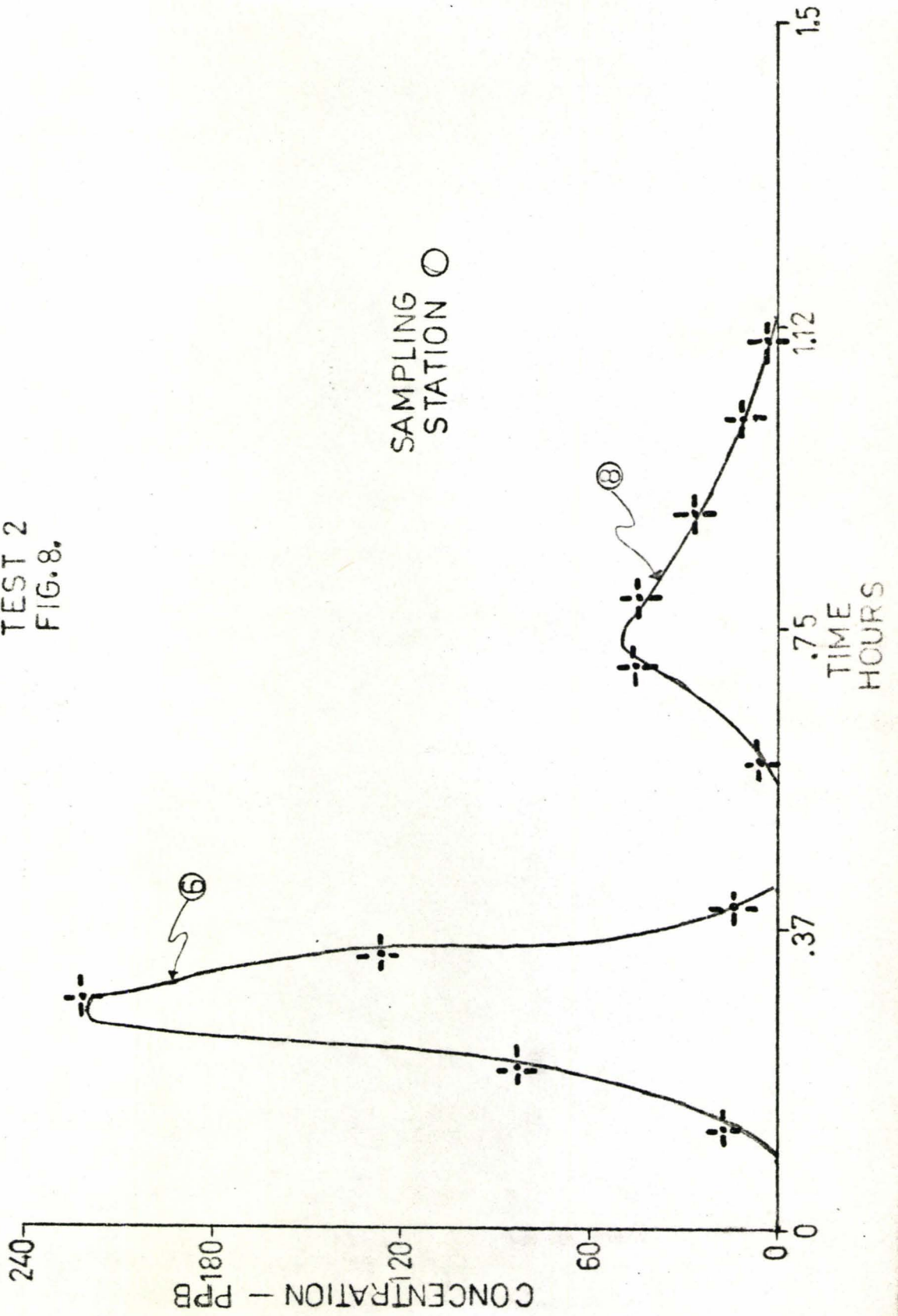
Recalculated concentration distribution curves for two values of dispersion coefficient are presented in Appendix E.

Table 3

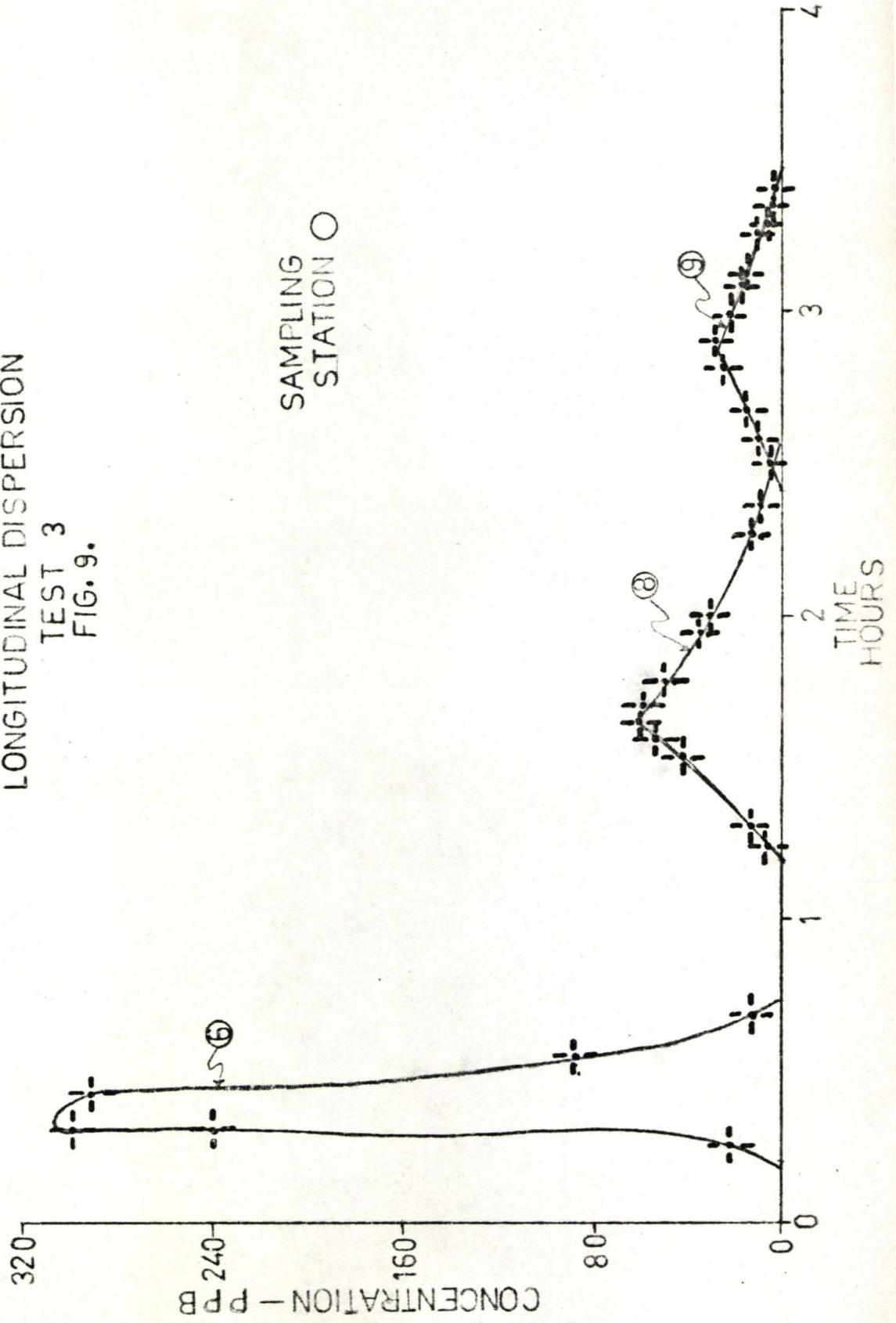
RECOVERY RATIOS

Test #	Sampling Station #	Recovery Ratio
#1	#6	0.93
	#8	0.98
	#9	0.24
	#10	0.32
#2	#6	1.34
	#8	1.20
#3	#6	3.4
	#8	1.8
	#9	0.81
#4	#1	0.85
	#2	0.78
	#3	0.75
	#5	0.75
	#6	0.69
	#8	0.75
	#9	0.49
#5	#1	0.07
	#2	0.88
	#5	0.65
	#6	0.55
	#8	0.71
	#9	0.32

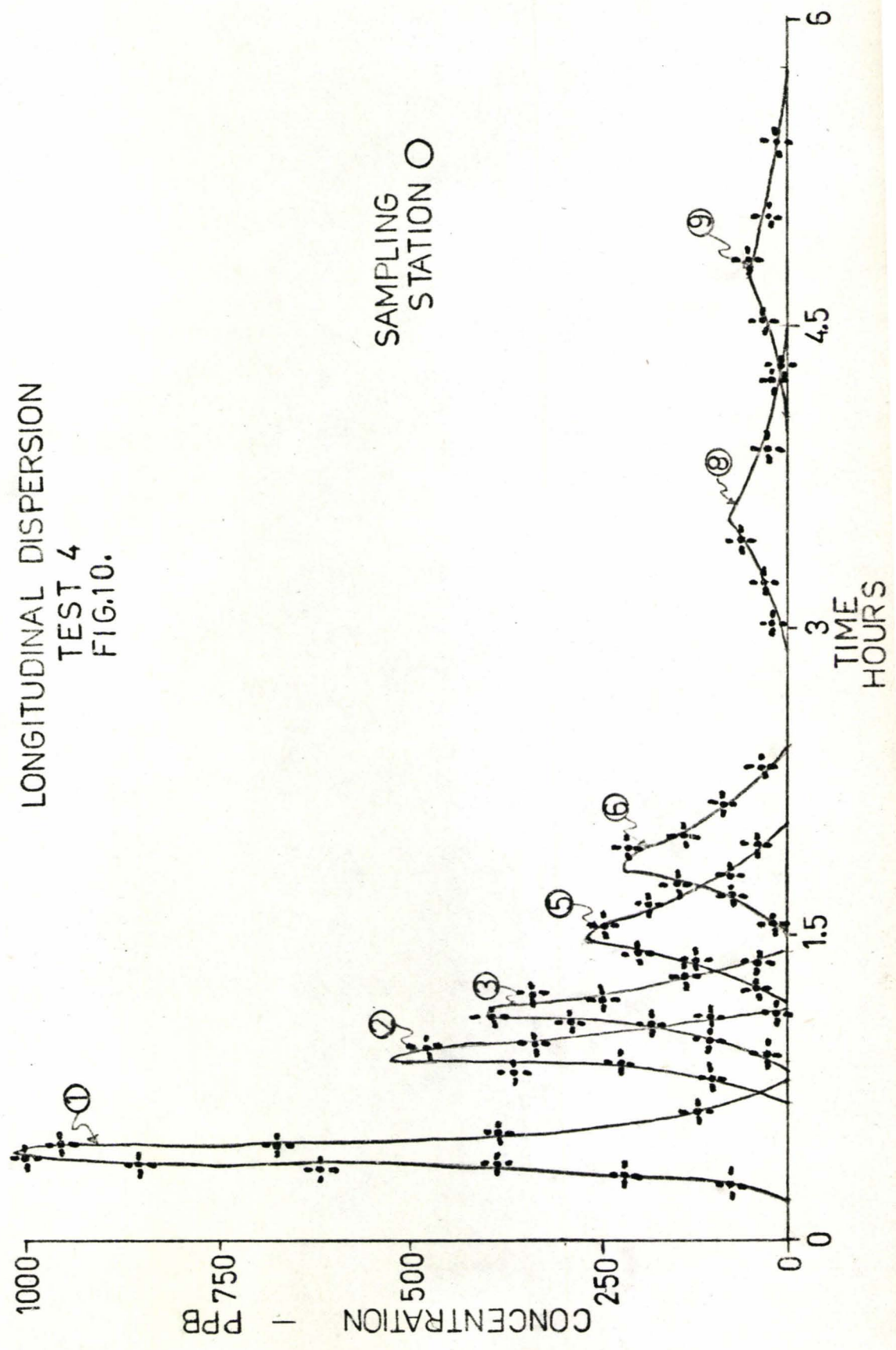
LONGITUDINAL DISPERSION
TEST 2
FIG. 8.

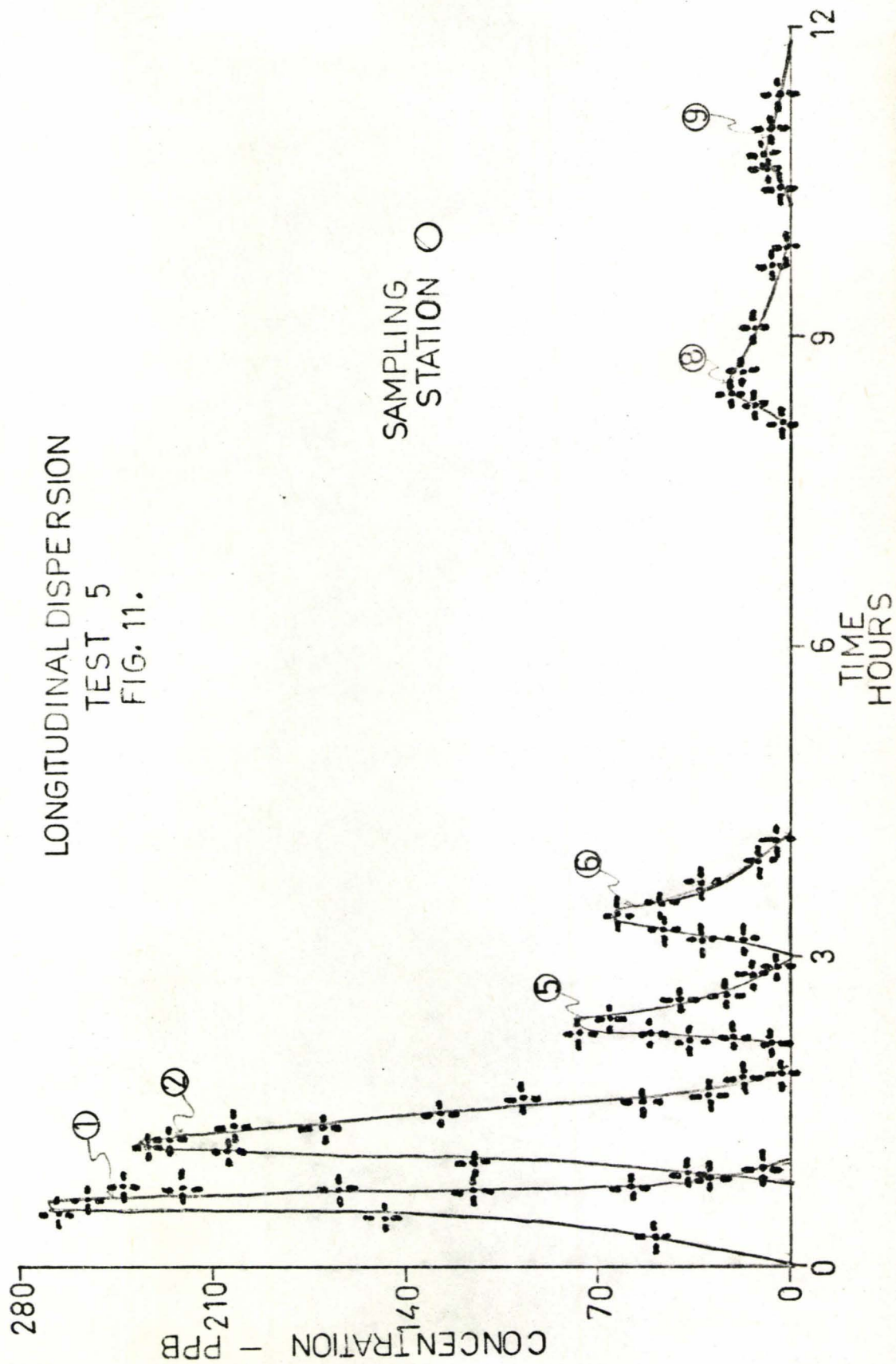


LONGITUDINAL DISPERSION
TEST 3
FIG. 9.



LONGITUDINAL DISPERSION
TEST 4
FIG.10.





C.4.2. Preliminary Dispersion Coefficient Correlations

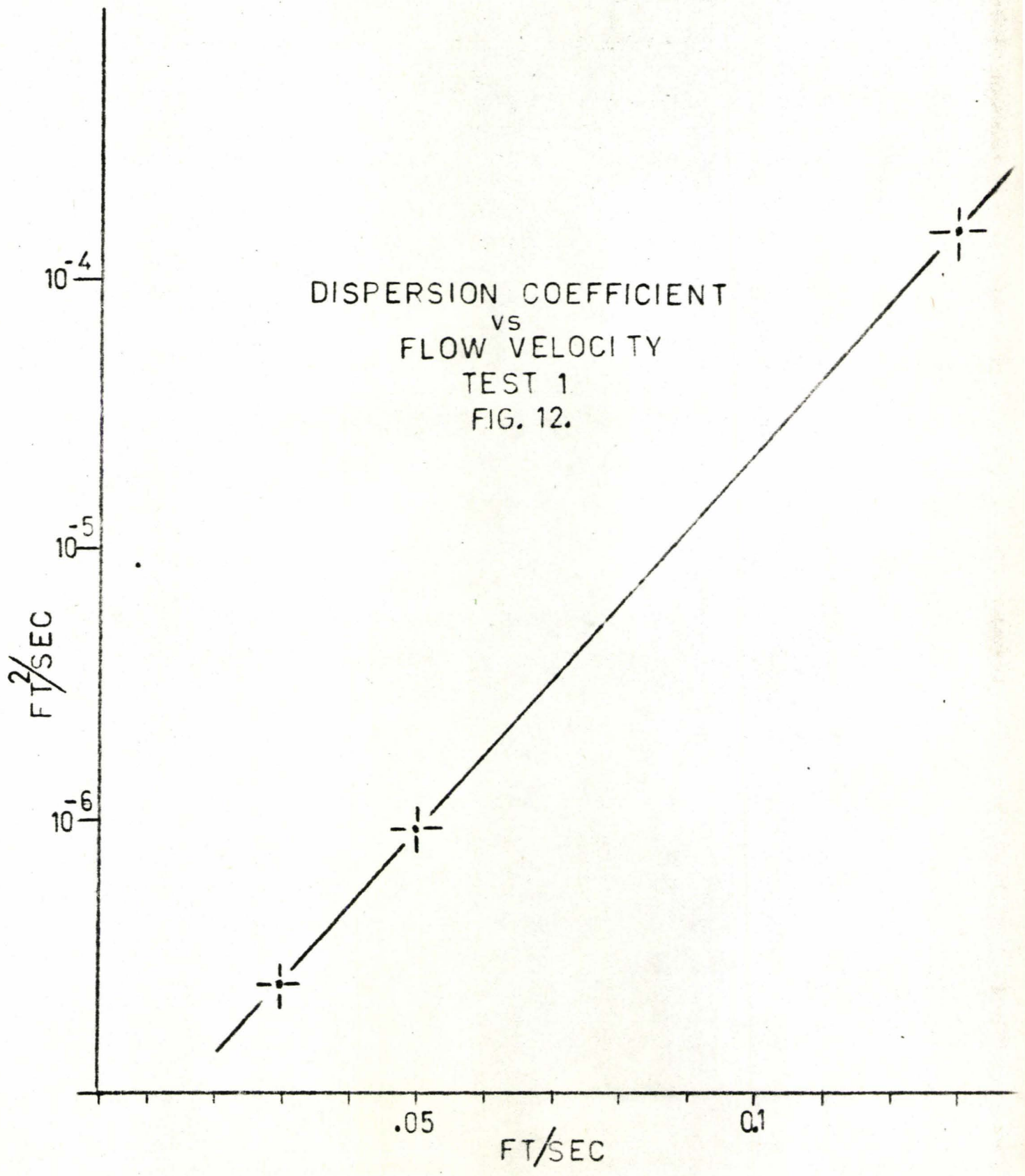
Semi-log plots of dispersion coefficient vs. flow velocity for tests #1, #3, #4, and #5 are presented in Figures 12, 13, 14 and 15 respectively. The results of test #2 were omitted since only two sampling points were analyzed. All plots illustrate that the dispersion coefficient increases as the flow velocity increases.

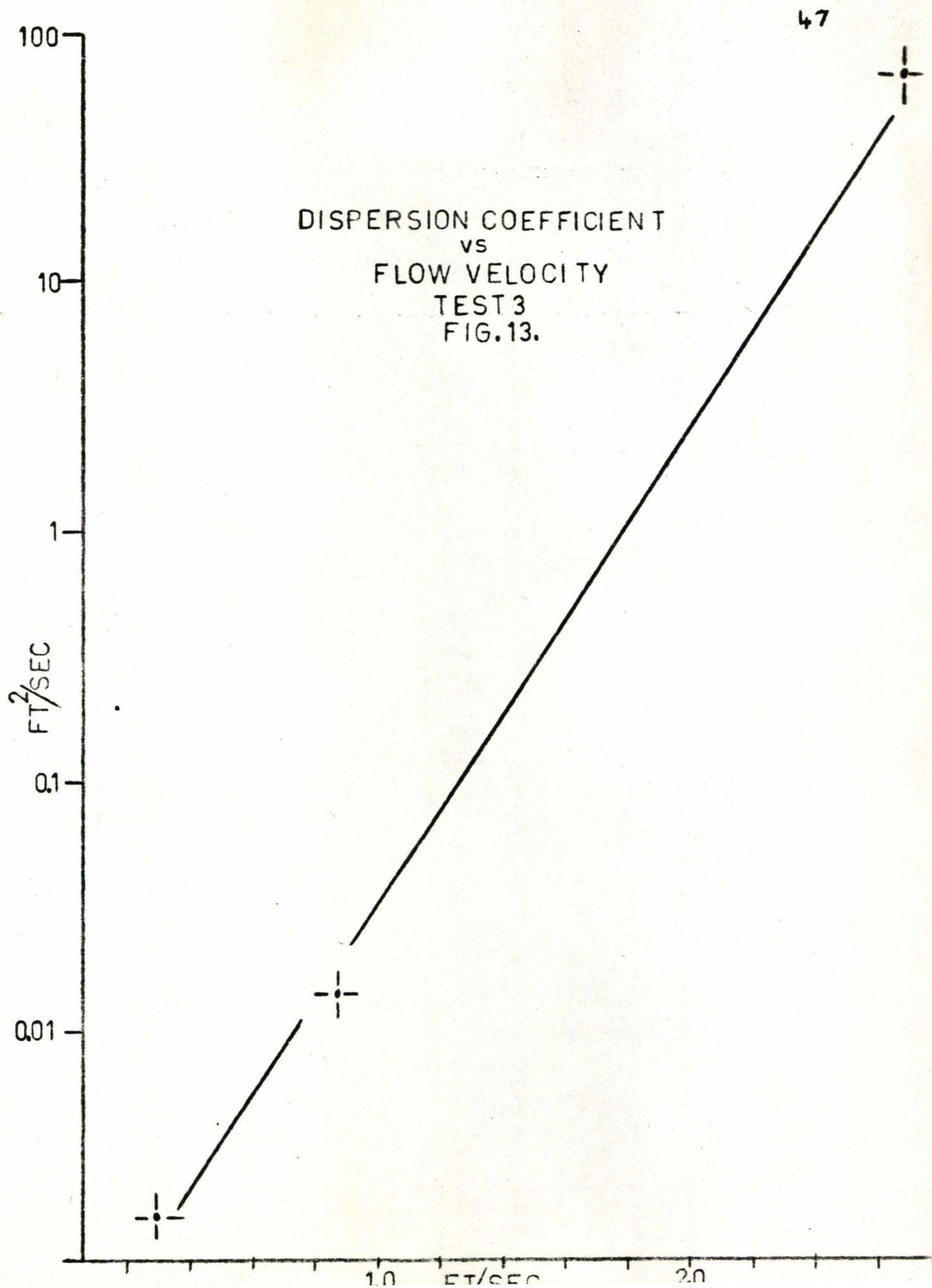
Dispersion coefficient is plotted against discharge at sampling stations #6, #8, and #9 in Figures 16, 17, and 18, respectively, and these also demonstrate D increases with discharge.

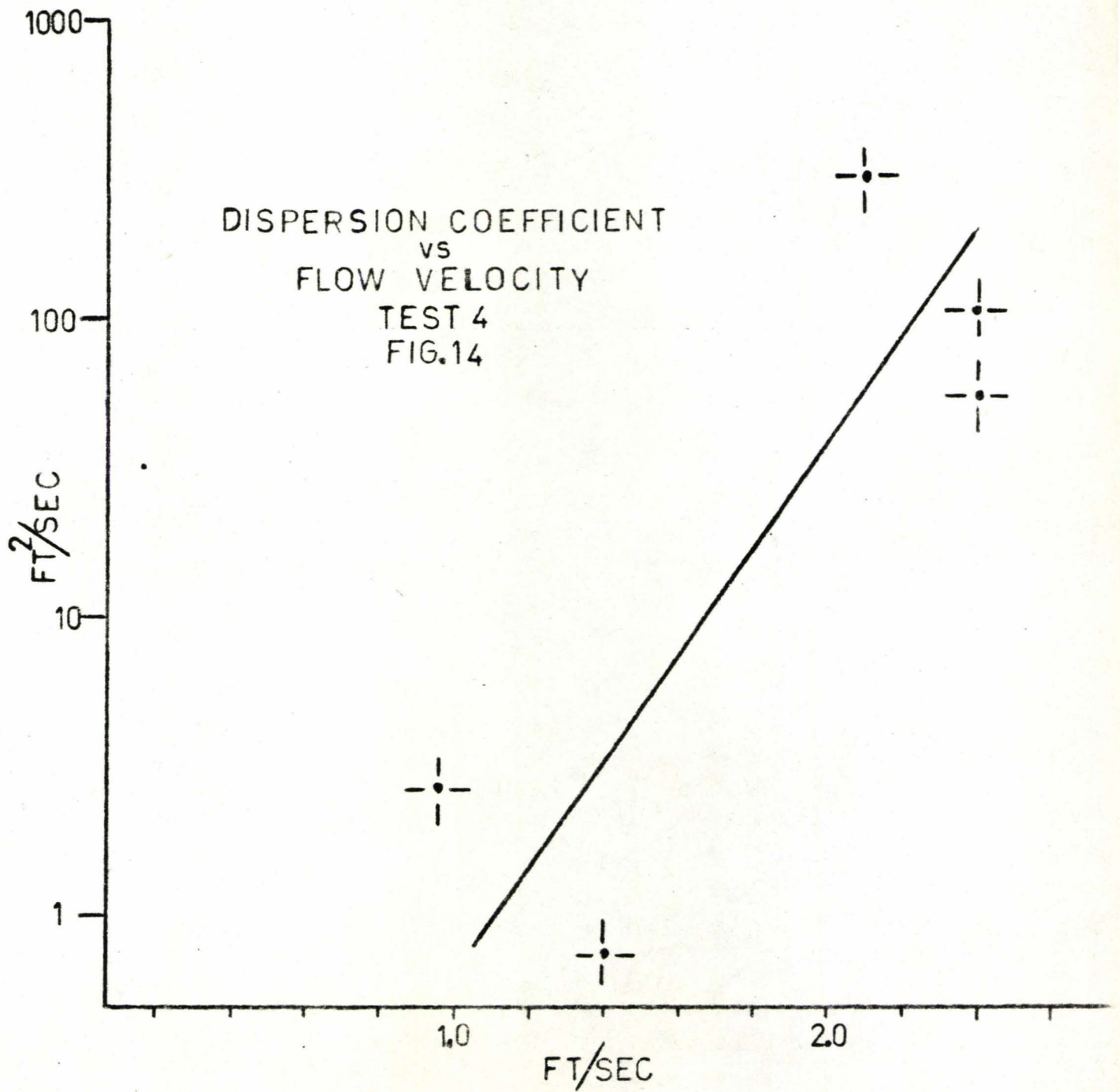
During the five tests, a wide range of flows were observed varying from very low values of less than 20 cfs to larger values of over 300 cfs. Figure 19 illustrates the effect of flow variation on the dispersion coefficient. Upstream values of D are larger than those downstream. Figure 19 shows that D increases as Q increases.

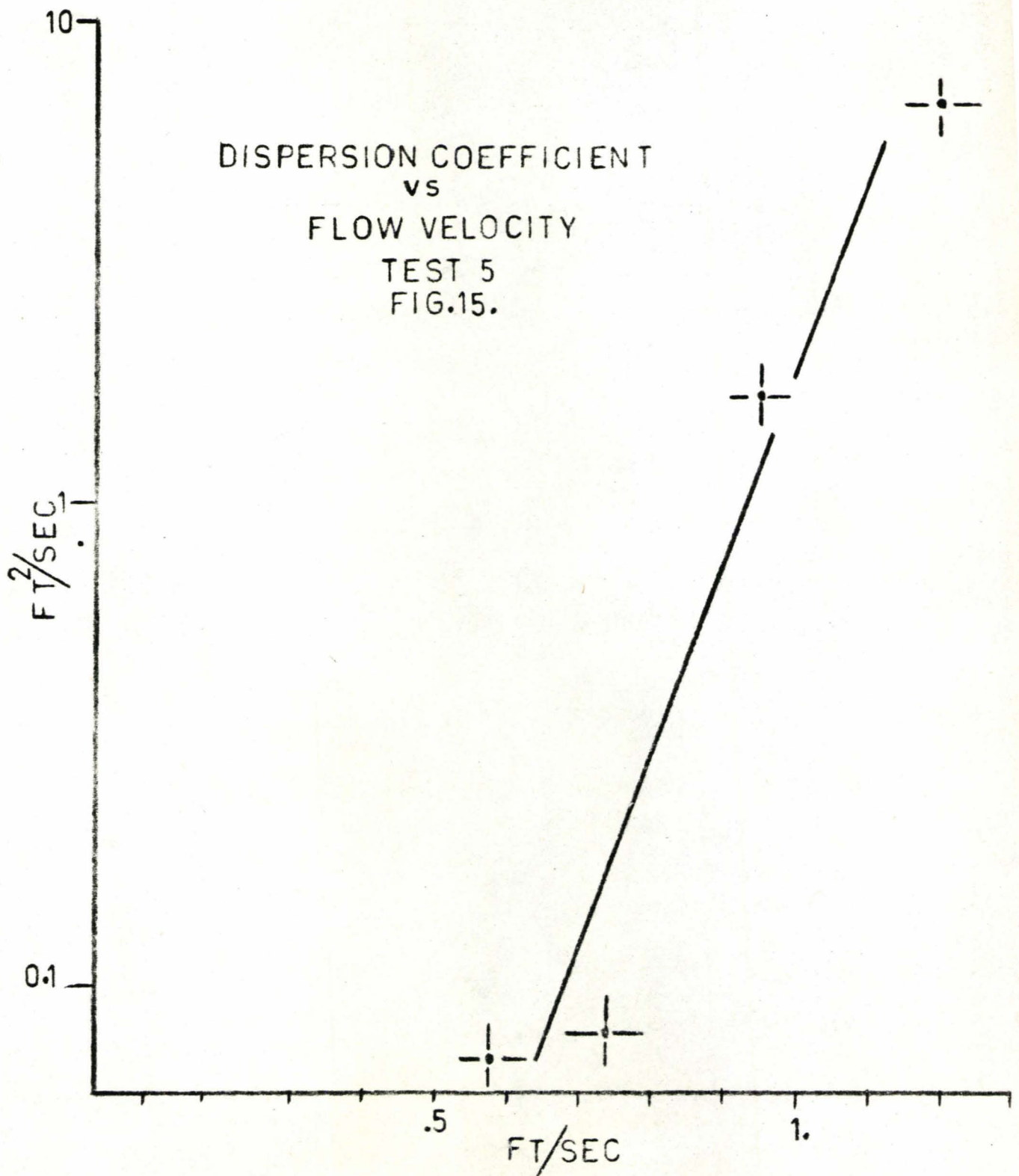
Figure 20 illustrates the division that can be made between upstream (steep) and downstream (flat) sampling stations. Upstream stations tend to have larger values of D than the downstream stations. In all cases, the value of D increases as the flow velocity increases.

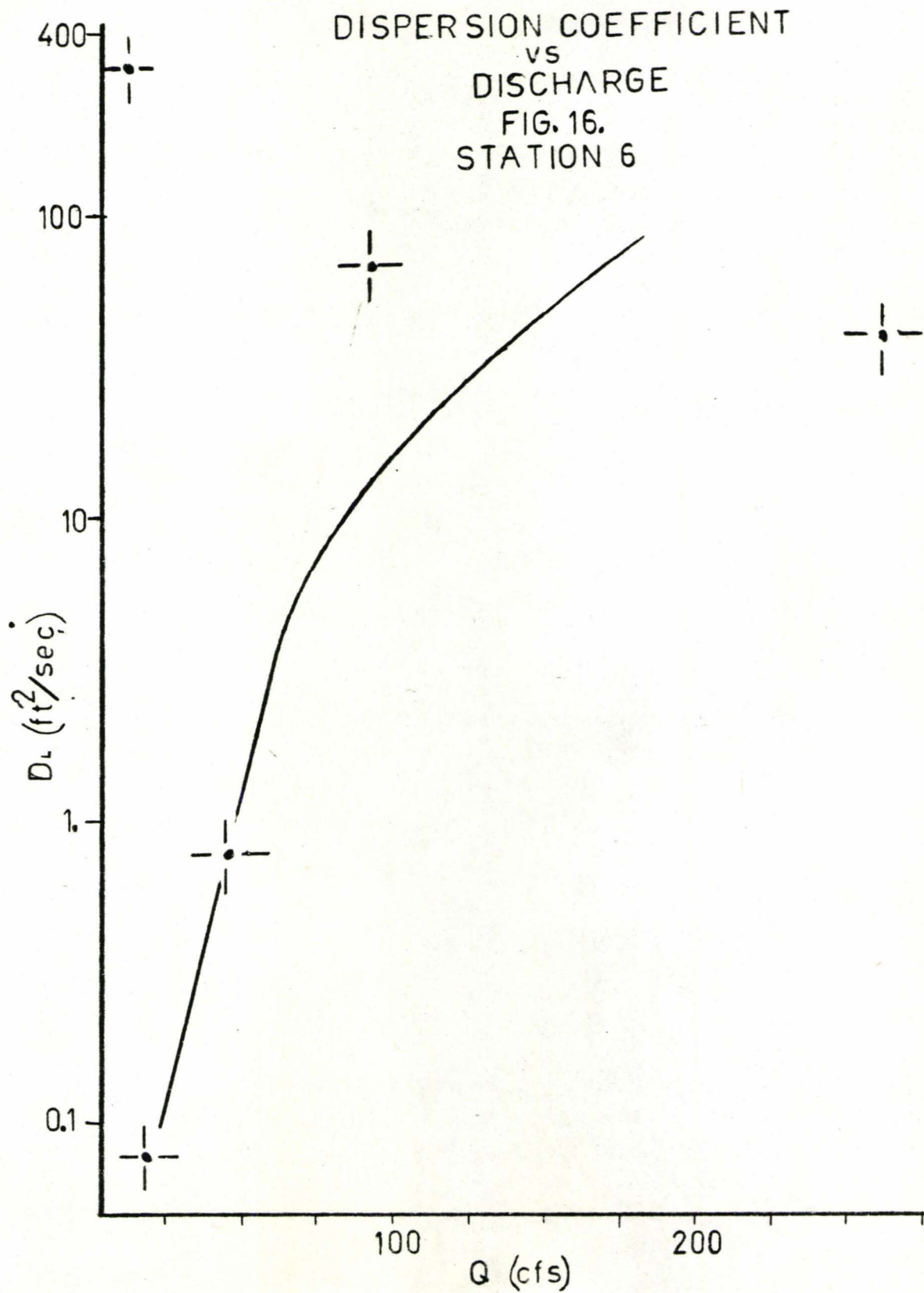
During tests #1 and #5, conditions at sampling station #8 caused an interesting phenomenon. As the dye cloud approached the sampling station it disappeared. In fact, it was found to be moving under the water surface past this sampling station then returning to the surface farther downstream. Figure 21 shows the physical characteristics of this section. For both tests samples were taken at various depths at points

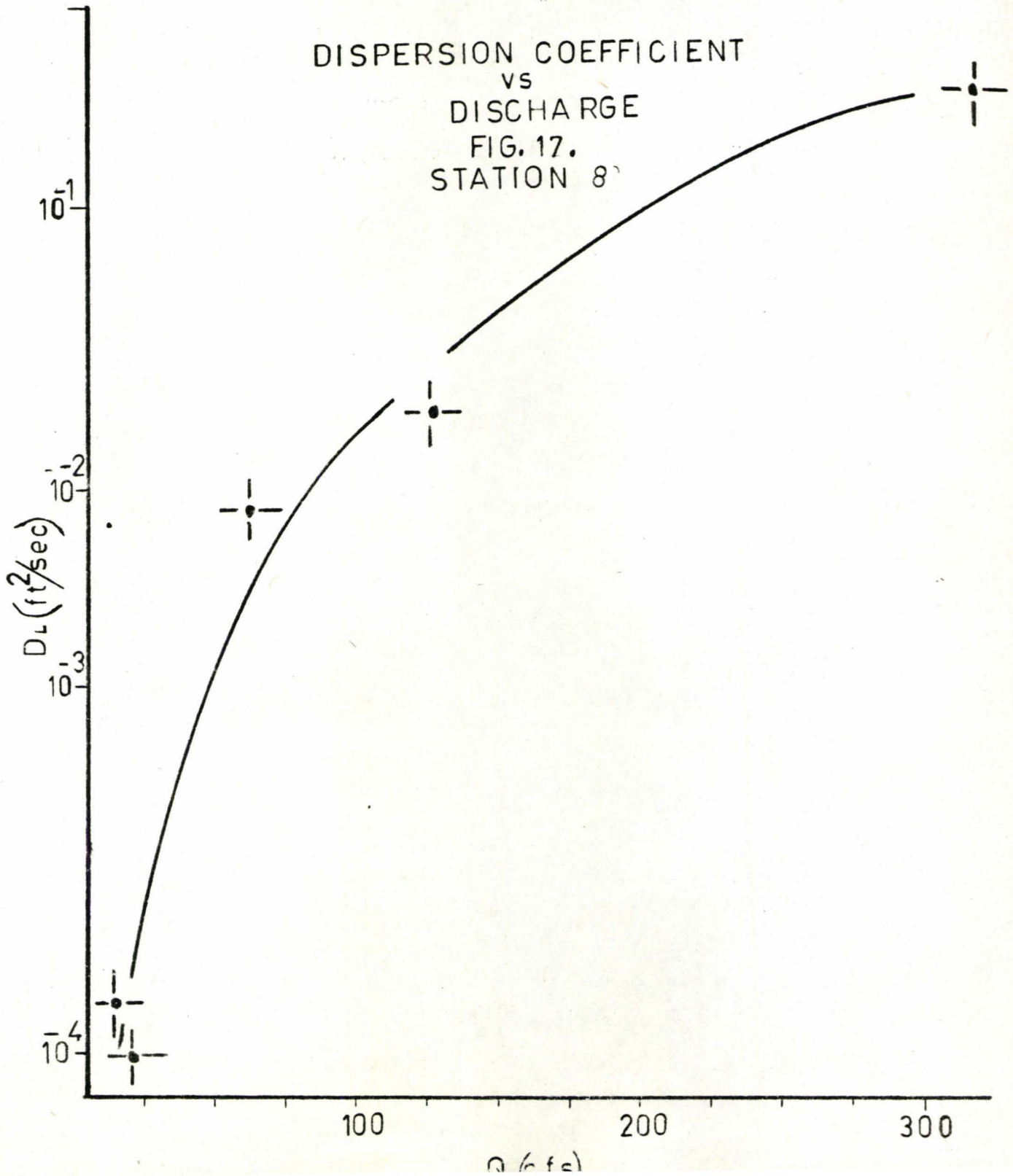


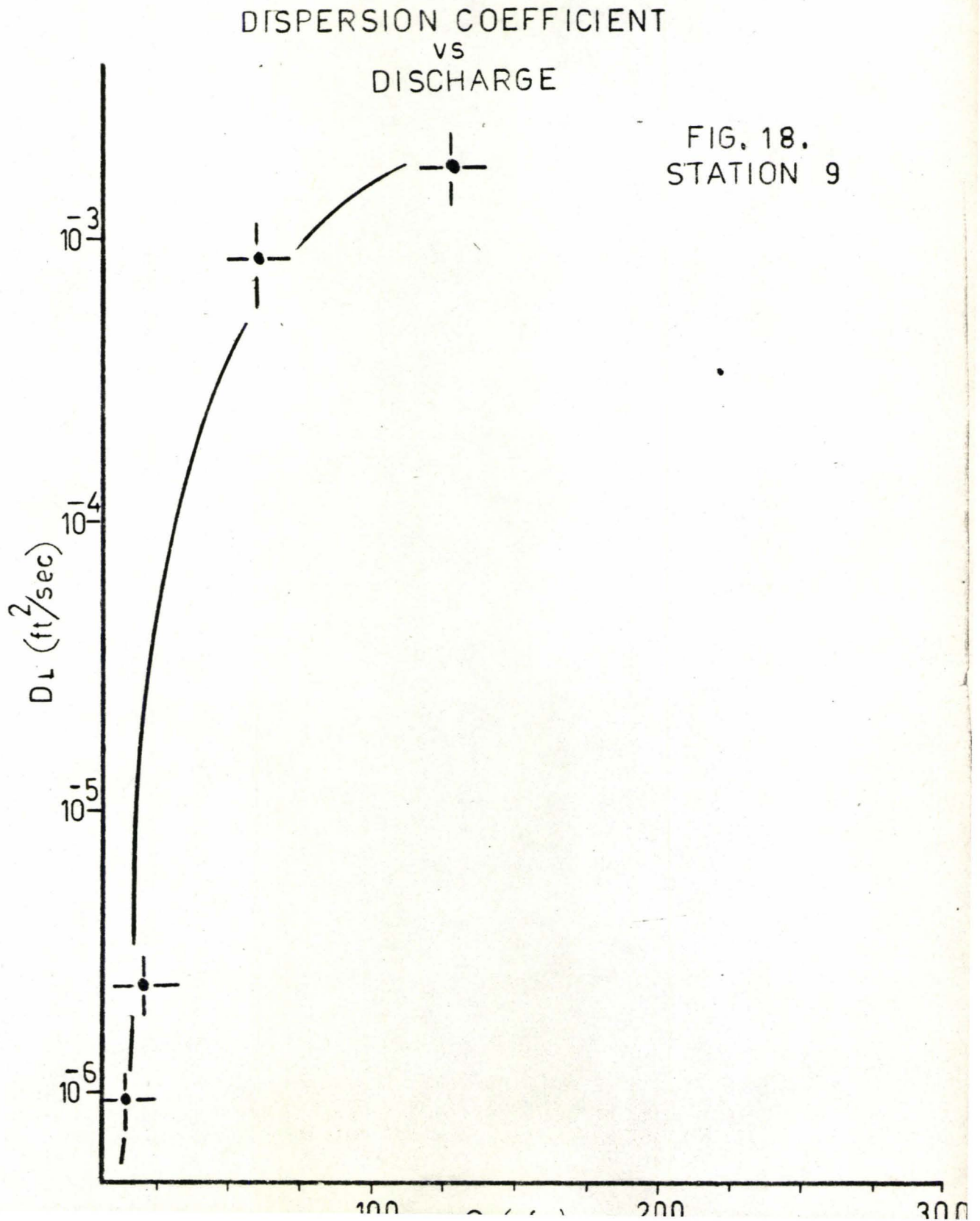












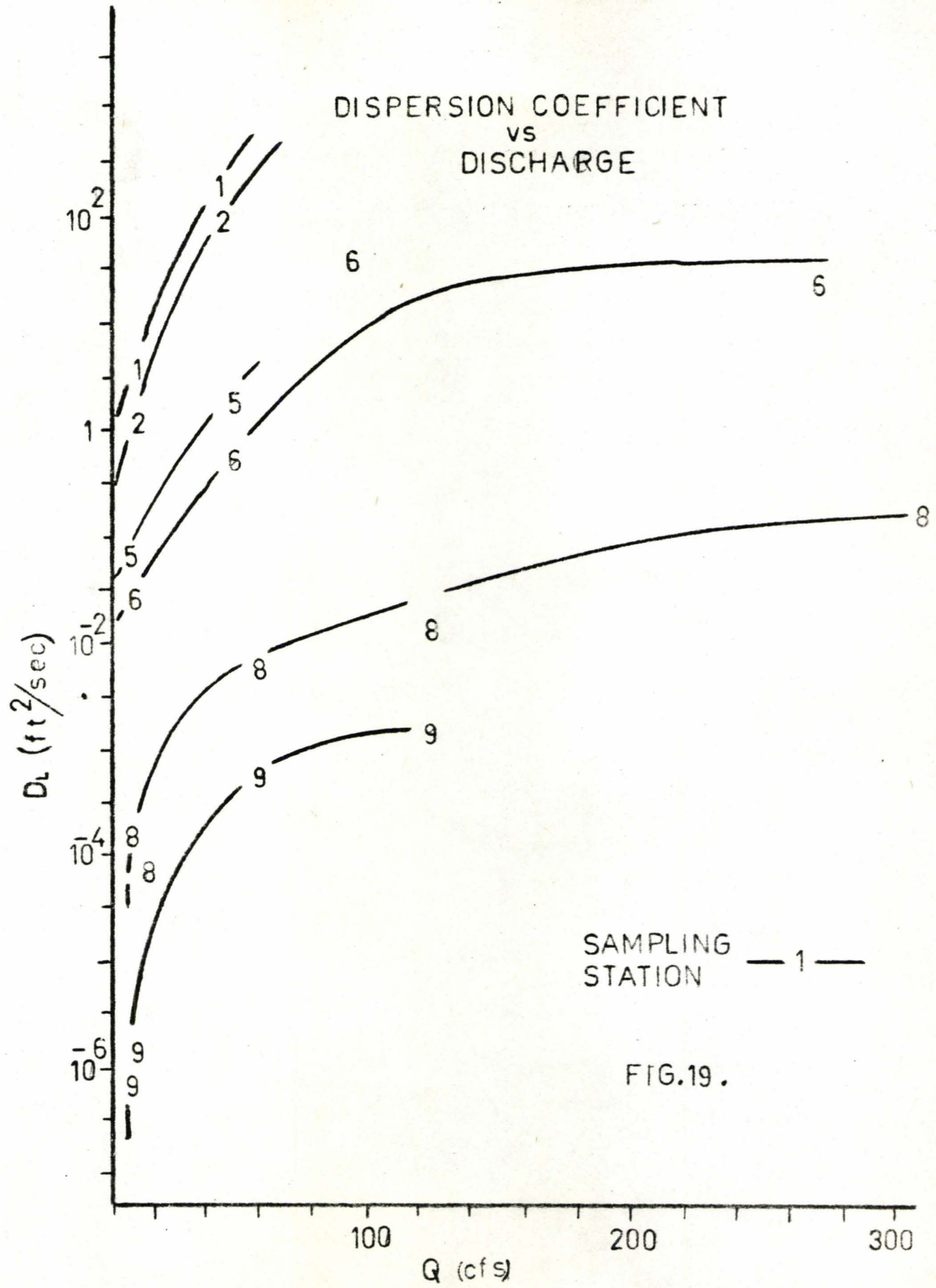


FIG.19.

DISPERSION COEFFICIENT VS FLOW VELOCITY

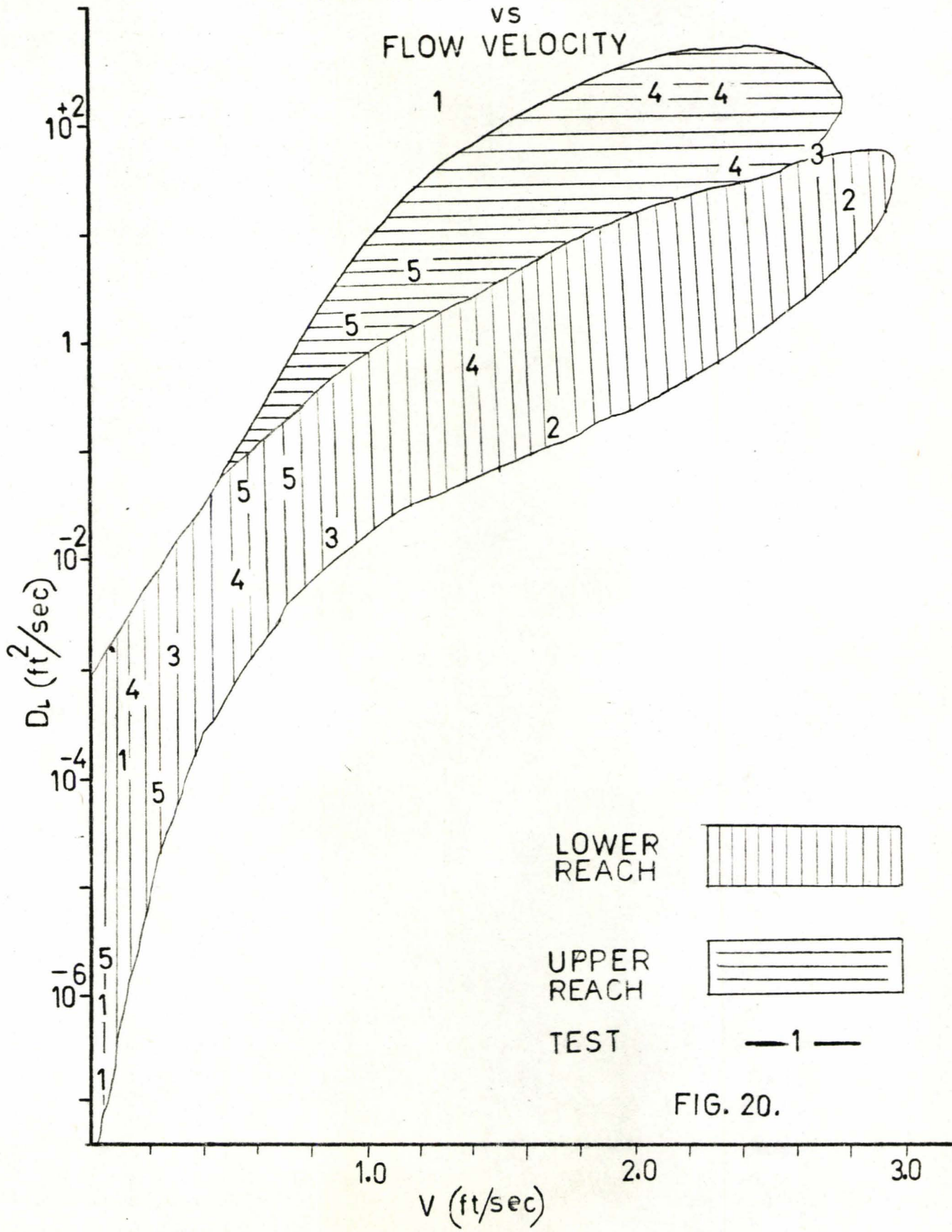
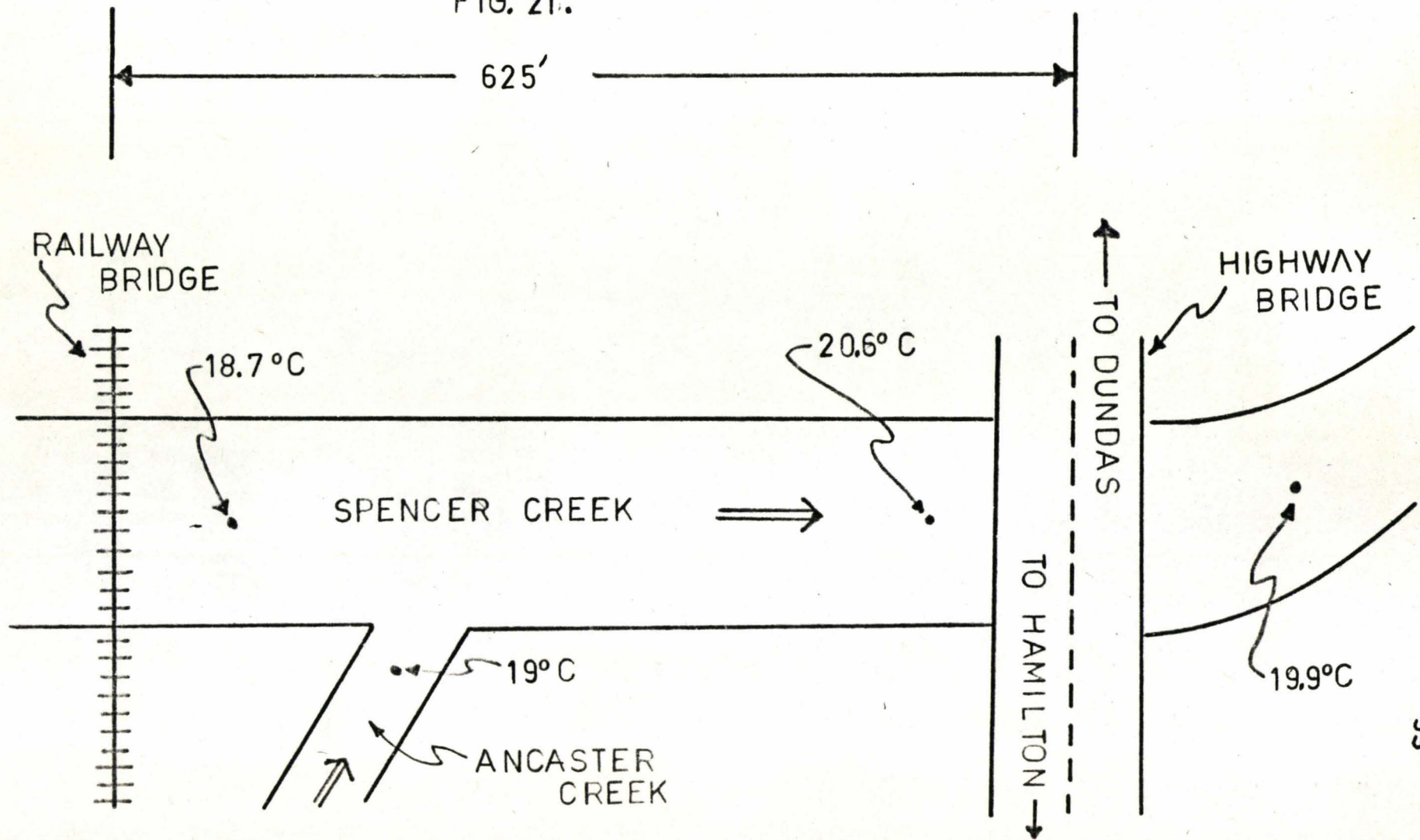


FIG. 20.

SAMPLING STATION
#8

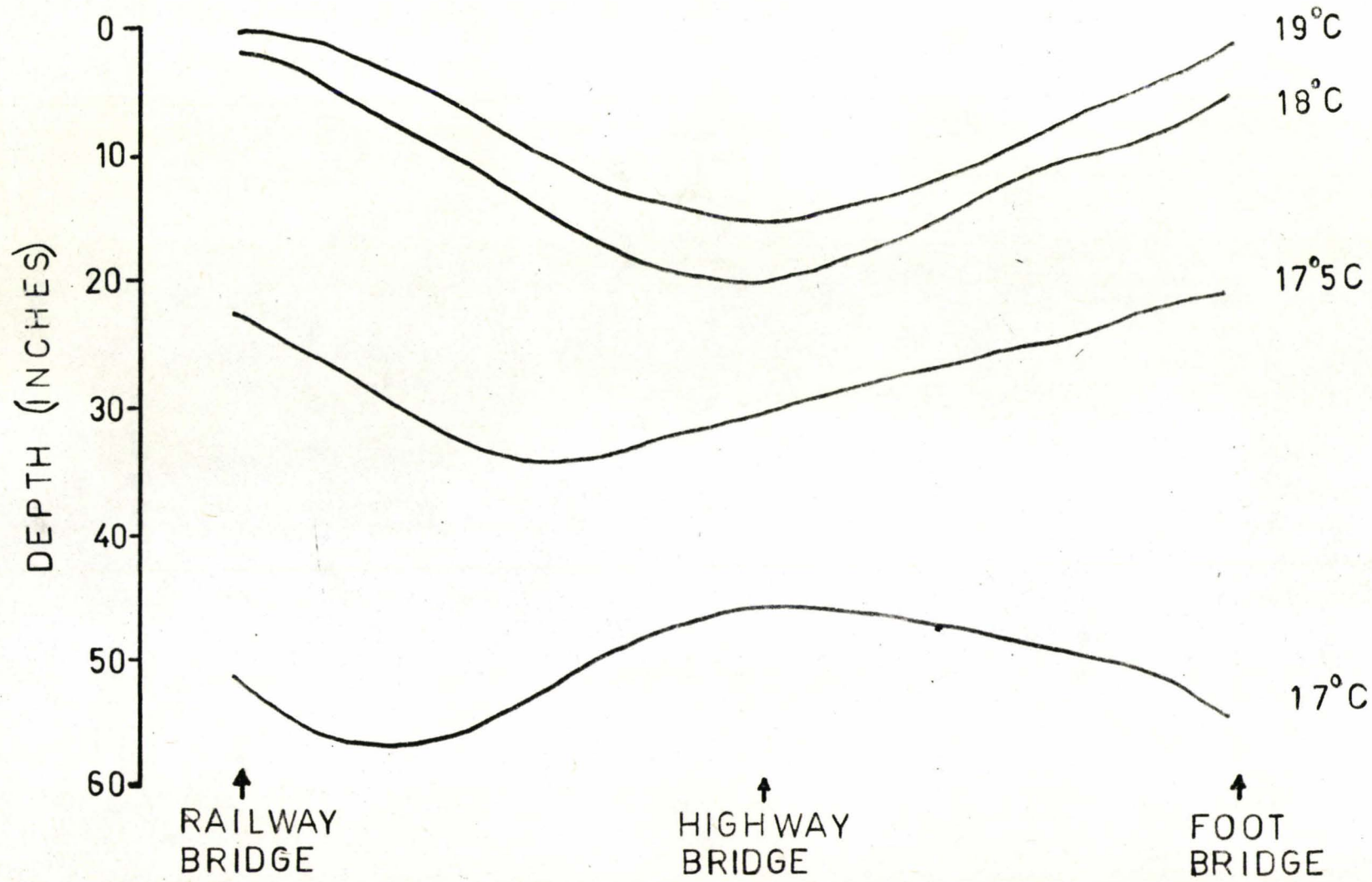
FIG. 21.



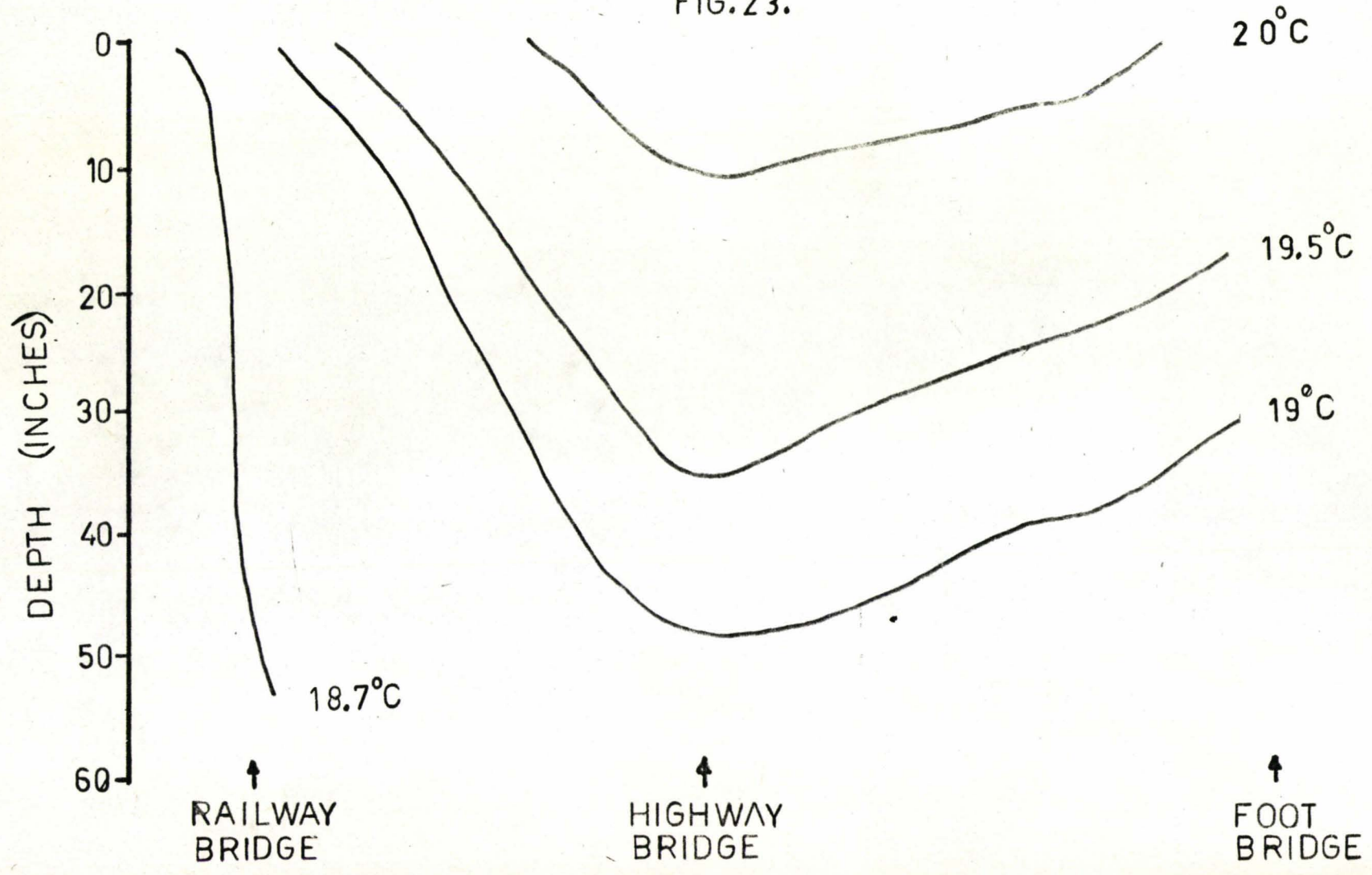
upstream and downstream from sampling station #6, as well as the station itself. Figure 22 and Figure 23 show the thermal stratification which caused the dye to flow in a density current at the upstream temperature. This occurrence has three possible causes. Firstly, this section is open to direct sunlight whereas the upstream sections were well shaded. Secondly, a tributary enters at this point with water slightly higher in temperature. Both of these will tend to increase the temperature of the surface waters causing a "density current" of upstream water to flow under the warmer water. Thirdly, warm water in the shallow parts of Cootes Paradise will be moved upstream whenever the wind changes to a prevalent Easterly. With relaxation of the wind, there is a warm water front upstream at the highway #102 bridge with colder water flow moving downstream. The interface is gradually eroded by eddy diffusion.

The phenomenon was not further investigated in this study.

ISOTHERMAL LINES
TEST 1
FIG. 22.



ISOTHERMAL LINES
TEST 5
FIG.23.



D

NUMERICAL MODEL

D. NUMERICAL MODEL

The numerical model presented in this part of the report was developed to compute concentrations at specific times after injection and at each sampling station in the test reach. Observed values of mean velocity and longitudinal dispersion coefficient are input to the program as well as the concentration distribution observed at station #1. A finite difference solution is computed for the one dimensional dispersion equation:

$$\frac{\partial \bar{c}}{\partial t} = D_L \frac{\partial^2 \bar{c}}{\partial x^2} - \bar{u} \frac{\partial \bar{c}}{\partial x}$$

where \bar{c} is the cross-sectional mean concentration; \bar{u} is the mean lagrangian velocity; t is the time after injection; x is the distance in the direction of flow; and D_L is the longitudinal dispersion coefficient.

The program used is still being developed by Dr. James as part of a graduate course, and is not yet fully tested. In fact the solution still becomes numerically unstable with decreasing amplitude after the concentration recession passes each station. Nevertheless it is felt that the results indicate that values of the dispersion coefficient computed in Chapter 3 are of the correct magnitude, so far as a prediction model for peak concentration is concerned.

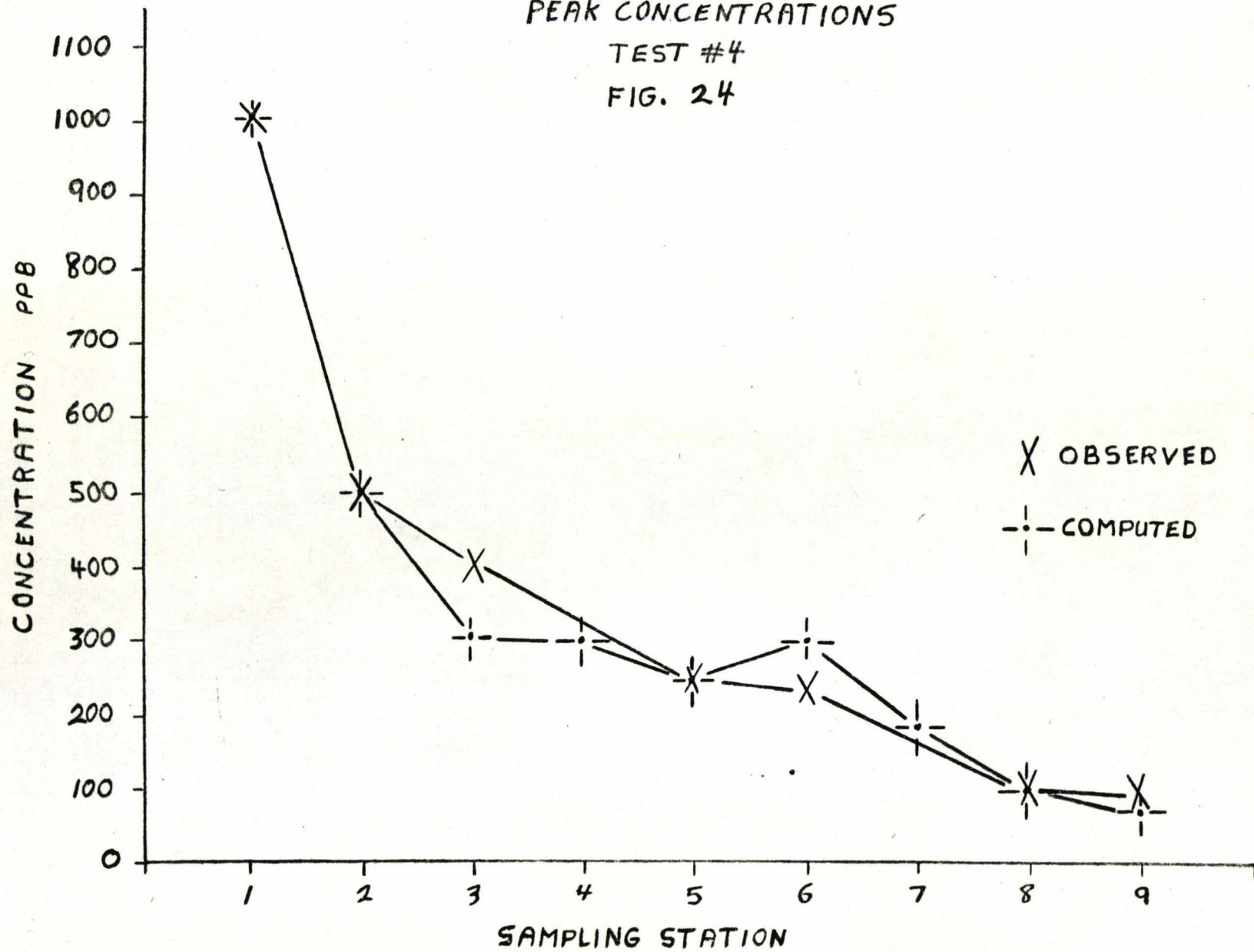
In this chapter are presented trial computer runs for Tests #4. Results are presented in Figures 24 and 25. The results indicate that the peak concentrations are better reproduced than the time of travel. Differences are probably caused by widely differing river reaches, discontinuous lagrangian velocities and

inaccurate dispersion coefficients used in the finite difference schematization.

PEAK CONCENTRATIONS

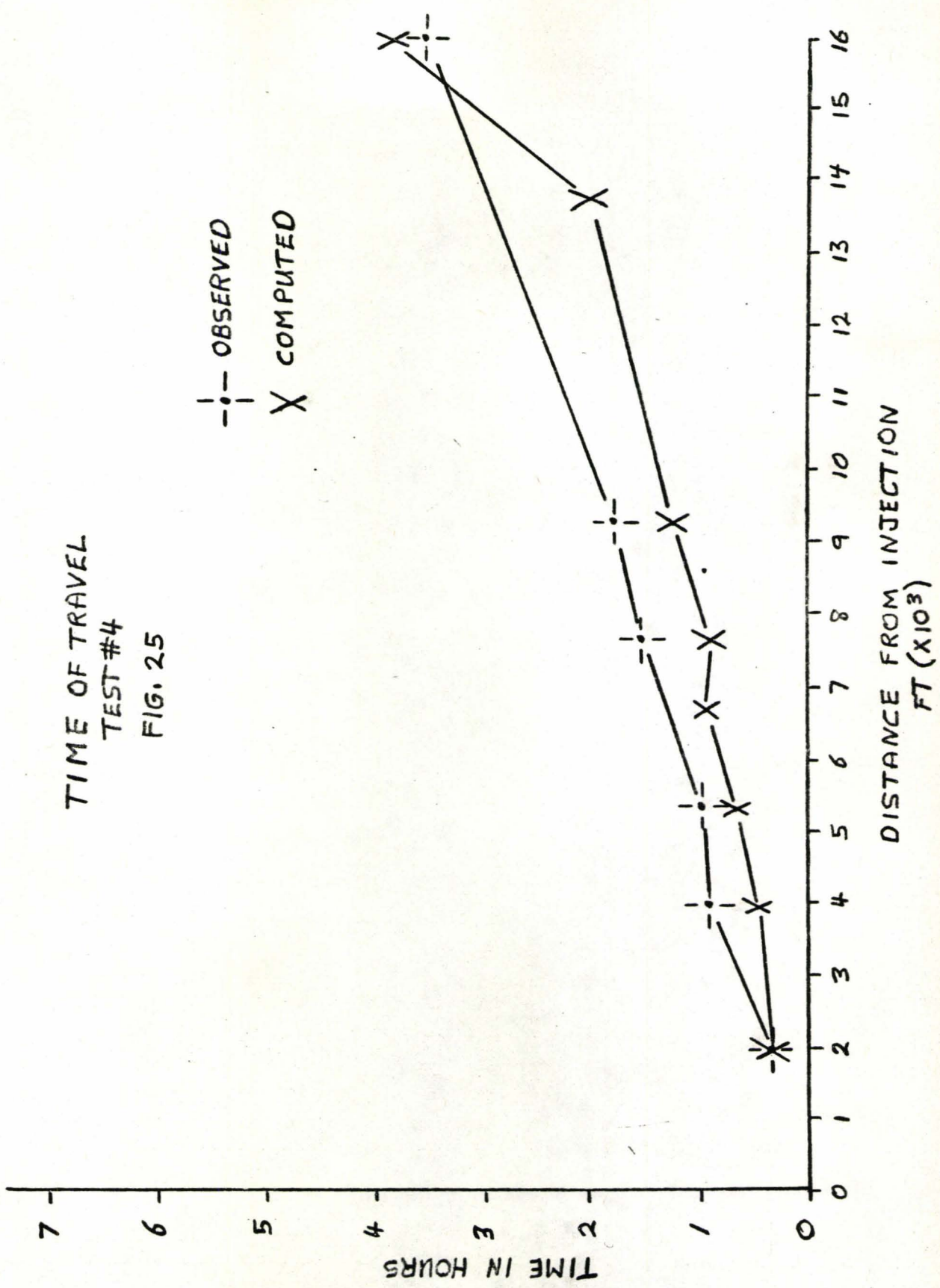
TEST #4

FIG. 24



TIME OF TRAVEL
TEST #4
FIG. 25

--- OBSERVED
X COMPUTED



E

DISCUSSION

Experimental methods for predicting dispersion coefficients in natural streams have been presented in this report.

It has been demonstrated that valuable information can be obtained with a minimum of equipment and personnel. Injection of a predetermined slug of dye and sampling at downstream locations can be reasonably easily carried out by one person, at least on streams not larger than the Spencer Creek. The distance between sampling stations must be long enough so that sampling times do not overlap. Sampling is much easier from permanent structures over the stream. Such sampling conditions do not always occur. Overlapping of sampling times and the need for floating sampling platforms render one-person tests difficult or impossible. The author found that three people could easily handle the most difficult sampling situations.

The use of a tracer that is readily observable as it moves downstream may cause temporary colour problems, but sampling is much easier if the dye cloud can be easily followed and timed. The use of a colourless tracer requires accurate estimations of time-of-travel in order that samples may be taken as the tracer passes a station. The review of various tracer materials available was included in this study since the test reach passed through a heavily populated area and ended in a conservation area. Care was required to ensure that the tracer material was non-toxic at levels used and that it was physically undetectable over prolonged periods of time. After tests #1, #4, and #5 the lower reach was viewed from a small aircraft. The dye cloud was not

detectable as it moved into the conservation area. Rhodamine WT satisfactorily met all requirements, was easily detectable at low concentrations and was stable in the natural environment.

The styrofoam cups used as sample containers were carefully tested for sample adsorption and absorption. Test samples at various concentrations were allowed to remain in the cups for a period much longer than that expected during the tests. It was found that no appreciable change occurred in the sample concentrations over this time period. Handling of the samples when returning to the laboratory was found to require great care. The plastic lids loosen easily and the sample may be lost. If a great number of samples is not required it is recommended that glass containers be used so that they may be sealed properly during transportation.

The Recovery Ratio at each sampling station was computed to approximate the sampling efficiency. Table 3 shows that Recovery Ratios exceeded a value of 1.0 for stations #6 and #8 during tests #2 and #3. In theory, this indicates that more dye was recovered or sampled than the actual amount injected. Of course, this is not possible in practice. The physical characteristics of these sites can offer a possible explanation for these anomalies. Immediately upstream from both sites additional flow is brought into Spencer Creek. Ancaster and Sulphur Creeks enter just above sampling station #7. The quantity of this additional flow could not be accurately accounted for. Following advice from the Spencer Creek Conservation Authority these additional inputs were estimated to

be 5% and 20% for Ancaster Creek and Sulphur Creek respectively. The combination of a poor estimate and incomplete mixing of the flow inputs with Spencer Creek flow can be a possible explanation of the large recovery ratios in these particular instances. Overall, the dye recovered by grab sampling was adequate enough to accurately represent the tracer movement past each sampling station.

Figure 20 shows that as the velocity of flow increases an increase in the longitudinal dispersion coefficient occurs. It should be pointed out that the higher values of D_1 occurred in the upstream sub-reaches. The flow velocity decreases in the downstream direction as a result of increased width and depth. Tests #4 and #5 were started in the upstream sections resulting in the dispersion coefficients being grouped higher than the results of tests #1, #2, and #3 (See Figure 20).

A wide range of flows was made possible because of local heavy rainfalls during the month of August (1972). Figure 19 illustrates the variation of D_1 with flow quantity. The dispersion coefficient tends to become constant during high flow values, e.g. Q greater than 80 cfs.

The initial slug is not plotted in this report, since results for the first test reach are unlikely to be reliable. The dispersion coefficient increases rapidly for a short time after release, i.e. during the "Taylor" or diffusion period. The initial diffusion is not able to keep pace with convection. The initial uniform distribution is quickly destroyed by velocity gradients;

but is re-established by vertical and lateral diffusion after the initial mixing period.

Appendix D presents a series of photographs taken along the study area. These may have some long term value for identifying any local effects, especially in the event of changes by man or nature.

The results of the numerical model are very encouraging. Good agreement between observed and computed peak concentrations has been illustrated. The model is based on a one-dimensional equation. Further work on this model using a better schematization is recommended as a subsequent validation of the field dispersion coefficients.

It has been previously established that non-uniformity of flow caused by widely varying depth, slope, and width, or the presence of bends, islands, sloughs, control structures, or other discontinuities render the use of equations inappropriate. Velocity gradients in the transverse direction and in the vertical direction may tend to produce large dispersion coefficients. Experimental techniques may influence test results, but to a lesser degree, probably, than do convective effects. Further development of the model may produce reliable results. However it is felt that under natural conditions, the mixing coefficient should be measured in situ for the range of discharges under consideration.

F. APPENDICES

APPENDIX A**FLUOROMETER CALIBRATION AND CALIBRATION CURVES**

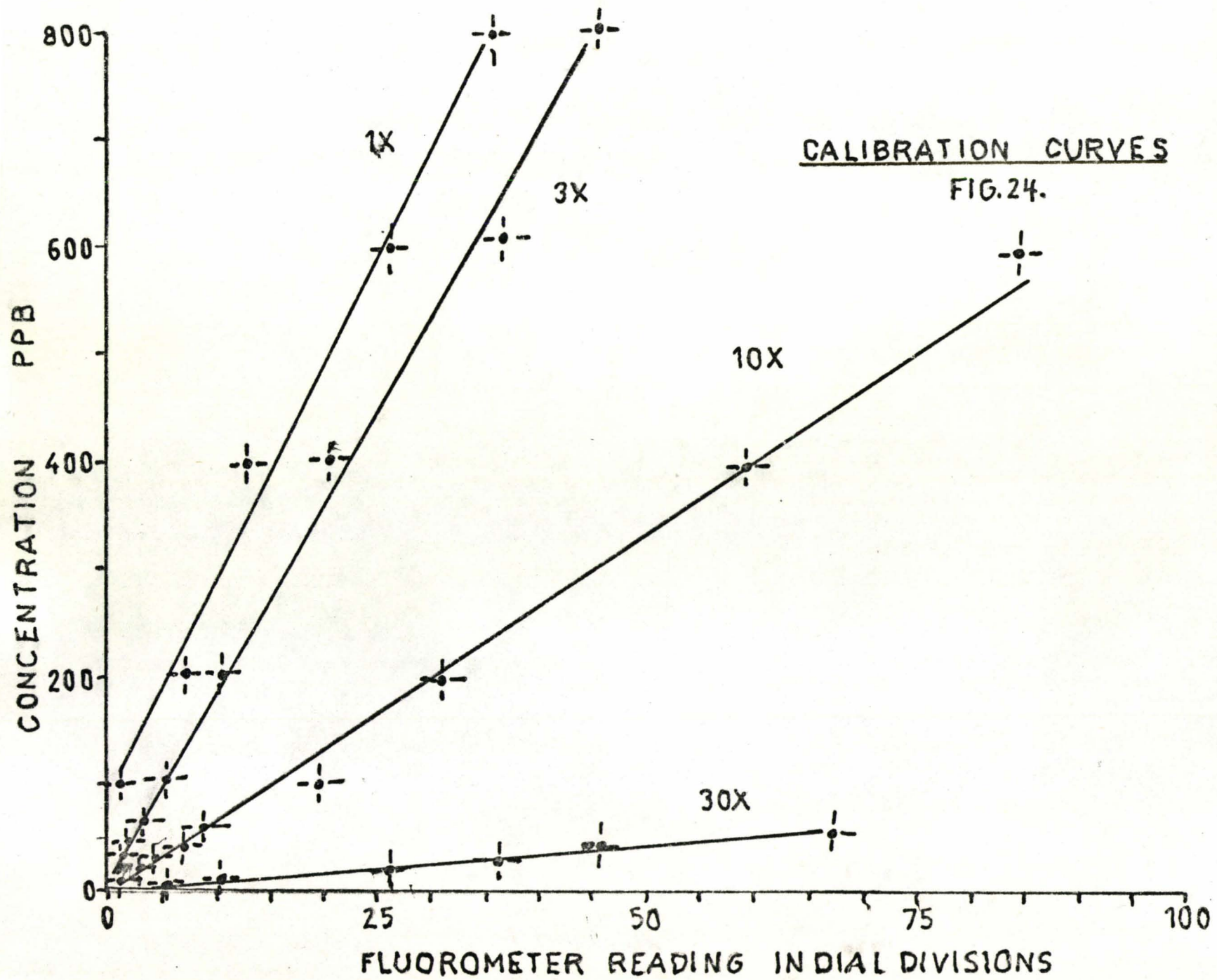
Fluorometer Calibration and Calibration Curves

For accurate calibration of all four fluorometer scales, a wide range of dye concentrations is necessary. Using Rhodamine WT (20% solution) and distilled water, solutions of concentrations varying between 2.4 ppb to 800 ppb were made as follows:

<u>Solution Number</u>	<u>Concentration</u>
I*	2.38×10^8 ppb
II	4.00×10^6 ppb
III	4.00×10^4 ppb
IV	800. ppb
V	600. ppb
VI	400. ppb
VII	200. ppb
VIII	100. ppb
IX	60. ppb
X	40. ppb
XI	30. ppb
XII	20. ppb
XIII	9. ppb
XIV	6. ppb
XV	2.4 ppb

* Initial solution 20% Rhodamine WT, S.G. 1.19
 Initial concentration $1.19 \times .2 = 2.38 \times 10^8$ ppb

The fluorometer was set up and switched on in the laboratory two hours before calibration and normal use. Standard solutions were pumped through the fluorometer and recirculated back into its container. During pumping a scale reading was obtained from each of the four scales. Temperature changes during the test period were insignificant (less than 0.5°C) and did not affect fluorescence. Slight nonlinearity was detected in the calibration curves for scales X30 and XI only, presented in the following plot (Figure 10). Calibration constants are listed in Table 4.



To make up the series of calibration solutions a number of dilutions are necessary. The laboratory equipment required is a range of pipettes and 1,000 ml. volumetric flasks. The following equation was used to calculate the volume of dilutant required for each calibration solution.

$$(V_a + V_i) C_f = C_i V_i$$

where C_i = initial concentration

V_i = initial volume

C_f = desired final concentration

V_a = volume of dilutant

If the initial volume of dye used is 1 ml. and a desired concentration of 10,000 ppb is desired, then the volume of dilutant necessary is

$$\begin{aligned} V_a &= \frac{C_i \times V_i}{C_f} - V_i \\ &= \frac{2.38 \times 10^8 \times 1}{10,000} - 1 \\ &= 2.38 \times 10^4 \text{ ml} \\ &= 23.8 \text{ l} \end{aligned}$$

Table 5 presents the calibration procedure for the 10X fluorometer scale.

Table 4 shows that 10 trials were made then averaged arithmetically to produce a calibration constant. This constant was used to convert the fluorometer reading to a concentration in parts per billion for each sample analysed.

Table 4

CALIBRATION CONSTANTS

d/c	1X	3X	10X	30X
1	22.5	17.6	7.15	0.89
2	23.1	16.2	6.8	0.88
3	32.0	20.0	6.9	0.84
4	28.6	20.0	5.2	0.77
5	25.0	20.0	6.7	0.82
6	24.0	21.8	5.7	0.80
7	-	20.0	6.7	0.60
8	-	20.0	9.0	-
9	-	20.0	8.0	-
10	-	18.0	-	-
Total	155.2	193.6	62.2	5.60
d/c	25.8	19.4	6.9	0.80

where c is the concentration of the test solution in ppb
d is the fluorometer dial reading

TABLE 5

Calibration of Fluorometer 10X Scale

Concentration of Test Solution in ppb	Fluorometer Dial Reading	c/d
2.4	off scale	-
6	off scale	-
9	1	9
20	3	6.8
30	4	7.5
40	6	6.7
60	9	6.7
100	14	7.1
200	28	7.1
400	58	6.9
600	83	7.2
800	off scale	-

where c is the test solution concentration in ppb
d is the fluorometer dial reading

APPENDIX B

FIELD EXPERIMENT COUNTDOWN AND FLOWCHART

Field Experiment Countdown and Flowchart

The purpose of this countdown is to aid any conservation group to carry out similar tests.

STUDY PROCEDURE

- I Hydrographic Data Collection
- II Tracer Preparation
- III Sampling
- IV Laboratory Analysis

Hydrographic Data Collection

1. Obtain maps and air photos of study area
2. Carry out reconnaissance of the study area
3. Determine sampling points
4. Obtain sounding rod and tape for cross section measurements
5. Select cross sections
6. Sound average depths in study area
7. Determine average discharge during tests
8. Calculate velocity of flow
9. Calculate approximate volume of water in the study area

Tracer Preparation

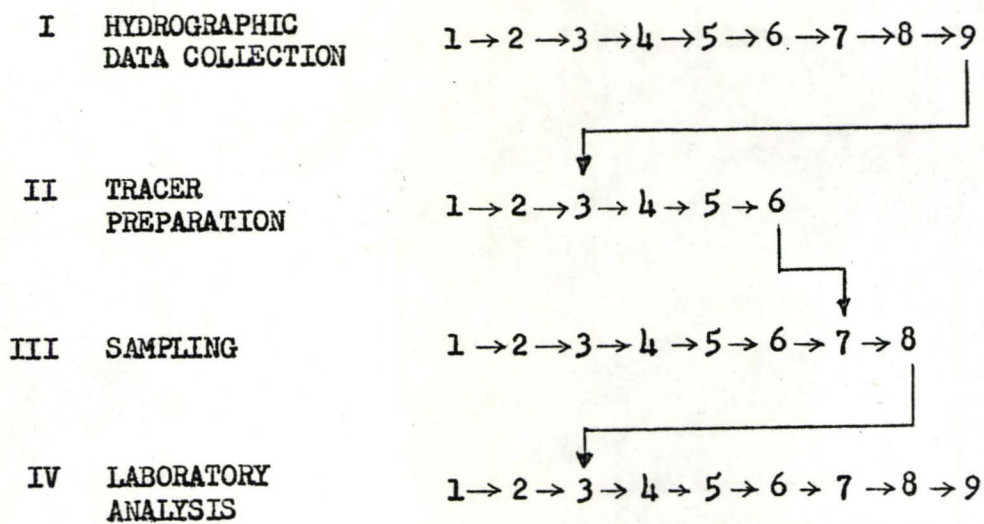
1. Review literature on tracer materials
2. Select tracer material
3. Determine quantity of tracer required
4. Obtain tracer
5. Proportion and mix tracer with water
6. Inject tracer into study area stream

Sampling

1. Determine size of sample required
2. Obtain containers for sample collection
3. Prepare containers for sample collection
4. Obtain boat and sampling equipment
5. Transport sample containers and tracer to the field
6. Label sample containers
7. Collect samples
8. Return samples to the laboratory

Laboratory Analysis

1. Obtain tracer analysis equipment
2. Set up and test analysis equipment
3. Analyse samples from field test
4. Clean or dispose of the sample containers
5. Tabulate results of test
6. Plot time-concentration curves
7. Calculate longitudinal dispersion coefficient
8. Plot D vs. Q for all tests
9. Discuss the value and meaning of the results

STUDY FLOWCHART

APPENDIX C

FLUORESCENCE

Fluorescence

Fluorescence is essentially an instantaneous emission of light from an atom or a molecule of a chemical compound which has been exposed to a high-energy radiation or light of short wavelength from an external source. Upon irradiation, there is a transition of electron energy to higher energy levels and the atom or the molecule is said to be transformed into an "excited state". After a short interval of time (about 10^{-7} to 10^{-8} second) the electrons return to the normal levels or the "ground state" emitting a light of a longer wavelength. It is this emission or radiation of light that constitutes the phenomenon of fluorescence.

Dyes are coloured because they have the properties of selectivity absorbing light of certain wavelengths in the visible region of the spectrum. Therefore, a dye which absorbs blue light will appear yellow-orange because this is the portion of the light which remains to reach the eye: another dye absorbing both blue and green will appear red and so on. Fluorescent dyes are substances which have the properties of converting a high percentage of absorbed energy into emitted (fluorescent) light upon irradiation with ultraviolet or sunlight. The emitted light nearly always has a longer wavelength and lower frequency than the absorbed light because some energy is lost in the process. Thus, each fluorescent dye has two characteristic spectra: the excitation spectrum to cause fluorescence, and the emission spectrum to emit light.

It is this unique property of fluorescence which enables the detection of fluorescent dyes at extremely low concentrations and makes them

valuable as a tracer material.

C.1. Precautions

- (1) The use of dye tracers in heavy concentrations should be avoided where the public may have contact with it and where it is likely to remain long after its application.
- (2) The dyes should be prevented from entering any potable water supplies. Some dyes (notably those of the rhodamine family) have phenol components which, when combined with chlorine, may cause adverse tastes.
- (3) If it is necessary to apply a tracer dye where its entry to the potable water supply cannot be avoided, the use of sodium fluorescein, because of its low toxicity, should be considered. However, the public must be protected from any heavy concentration of the dye solution. The water supply should be diluted, flushed or chlorinated to the point where the dye colour is no longer visible.
- (4) The permissible limit of Rhodamine B in drinking waters should not exceed 370 ppb (policy statement by the U.S. Public Health Services as general guidelines for the use of Rhodamine B in studies of rivers, lakes and underground waters), based on a tolerance of 0.75 mg. per day Rhodamine B on a continuing basis with an expected daily water consumption of $2\frac{1}{2}$ qt. by the individual.
- (5) Certain dyes (especially sodium fluorescein) are susceptible to rapid deterioration. Water samples containing the dye should be analyzed as soon as possible after they have been collected. The samples should be held in dark, light-proof bottles and kept in a dark place and refrigerated.
- (6) Extreme care should be taken when handling dyes. Some dyes (those

of the rhodamine family) are liable to stain clothing and hands. The stains are very difficult to remove. In the event of accidents, rhodamine stains can be removed by spot cleaning with methanol, followed by soaking in a weak solution of household bleach.

C.2. Factors Affecting

The intensity of fluorescence is affected in varying degrees by such physical and chemical factors as solvent, concentration, temperature, pH, effects of bright sunlight and fluorescent quenching.

(1) Solvent

This aspect is unimportant in tracer studies where the main solvent is water.

(2) Concentration

Fluorescence varies linearly with dye concentration in dilute solutions (several hundred parts per billion). At higher concentrations, some reduction occurs in the rate of increase in the intensity of fluorescence due to increasing optical density.

(3) Temperature

Fluorescence increases as temperature decreases.

(4) pH

With some dyes (such as Rhodamine B) there is no effect on the intensity of fluorescence between pH 5 and 10, while with others (such as fluorescein) acid pH may cause some reduction.

(5) Photochemical Decay

Bright sunlight can cause a permanent reduction in fluorescence by photochemical decay or photodecomposition.

(6) Quenching

This is an interaction between the dye molecules and other chemicals in the water which result in the reduction of fluorescence. A quenching agent may do any or all of the following:

- (a) absorb exciting light
- (b) absorb light emitted by the dye and/or
- (c) degrade the excited-state energy
- (d) chemically react and change the nature of the dye molecule (chlorine is an example here)

APPENDIX D

FLUVIOLOGY OF LOWER SPENCER CREEK

Fluviology of Lower Spencer Creek

Spencer Creek enters the town of Dundas immediately below Webster's Falls. The flow is contained in a raceway which causes the creek to turn 90° twice within 500 feet after entering the town. Photos #1 and #2 show the above sections. The flow regime initiated here is characteristic of the following reach of approximately two miles; shallow depth and rapid flow (depth less than one foot, and velocities greater than 1 fps but less than 3 fps). Photo #3 shows that the flow falls twice, each approximately one foot in height. Immediately following the completion of the second curve mentioned above, the creek enters a section of natural river-bed. The bed is composed of various sizes of gravel which extends to either side to form small banks. Photo #4 shows that the banks are covered heavily with willow trees and other small bushes, making travel along the bank very difficult. The flow in this section is rapid with sections of "white water" periodically interrupted by debris that has become lodged near the bank. The right side of photo #5 and the foreground of photo #6 show typical blockages and small "dead zones" that exist immediately behind each blockage. Photo #7 depicts sampling station #1 (Mill Street Bridge) just upstream from a bridge pier. Note the wooden frame jammed against a rock in the center. As the creek flows under the Mill Street bridge the bed widens, causing a drop in flow speed. A bend precedes a section that is very straight. Photo #8 shows the beginning of the first bend. Photo #9 shows the straight section approaching sampling station #2. At Market Street the flow is constricted

under the bridge (sampling station #2) just before falling over two drops. Photo #11 shows the first drop of approximately 7 feet. Photo #12 shows the lower drop of approximately 3 feet. Immediately below the double falls "dead zones" are present on both sides. Photo #13 shows the right side pool while photo #14 shows the left side pool. Downstream another 1000 feet an artificial falls has been created by the dumping of large chunks of reinforced concrete, shown in photo #15. This appears to have been "constructed" to dam up water for an intake to the municipal arena. An effluent outlet can also be seen in this ponded area, photo #16. The creek continues to be rapid and shallow, with a noticeably increased amount of refuse and junk collected along the river bed and bank. Photo #17 shows a typical section just before the creek turns by about 70°. Sampling station #3 (McMurray Street bridge) is shown in photo #19. As the creek continues through the town it passes along many industrial buildings. The developed side is maintained by concrete retaining walls as shown in photo #20. Just upstream from sampling station #4, there is a small drop of about two feet and an accompanying "dead zone", shown in photo #21. Photo #22 shows sampling station #4 at Ogilvie Street. Approaching sampling station #5 the creek still remains shallow and rapid, although less rapid than the top reach, photo #23. Sampling station #5 is shown in photo #24, along with a drop of about 5 feet just downstream from the Main Street bridge. This section marks the end of the rapid steep reach and the gradual transition to the following slow, relatively deep reach. Photo #25 indicates the gradual transition. The lower reach becomes very slow (speeds less than .5 fps) along with a change in bed from stone to silt and muck. Many trees block

the stream collecting floating debris, as shown in photos #26 and #27. Photo #28 shows the T. H. & B. railway crossing just upstream from sampling station #8. As Spencer Creek enters Cootes Paradise, the width increases to nearly 50 feet with banks lined with large willow trees. A final curve exists as Spencer Creek joins the disused Desjardin Canal and empties into the Cootes Paradise Pond to continue into Hamilton Harbour, then out into Lake Ontario (photo #29).

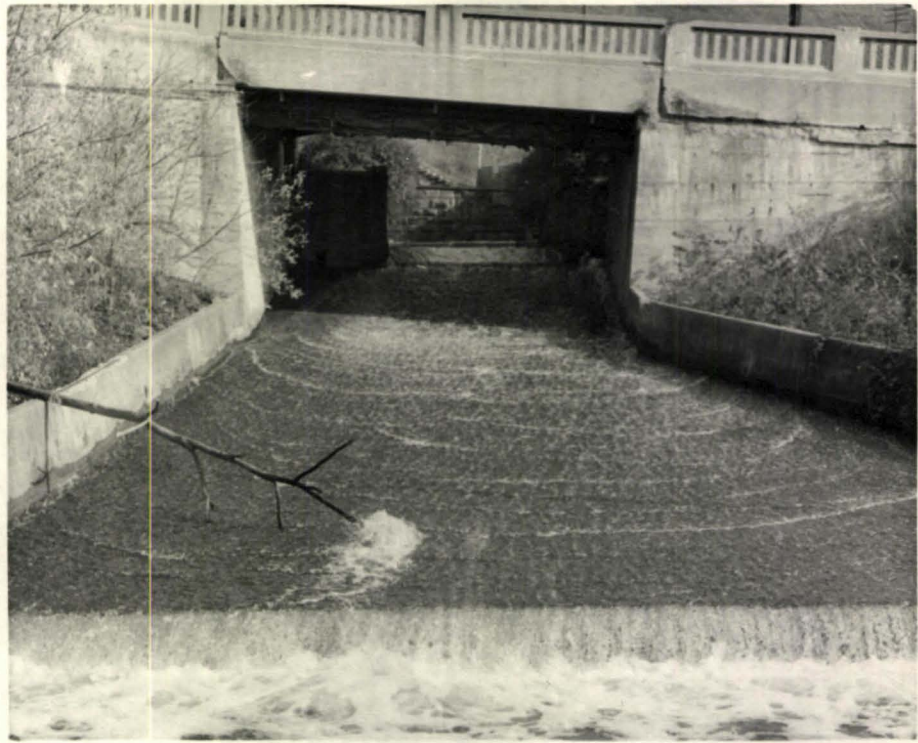


PHOTO #1

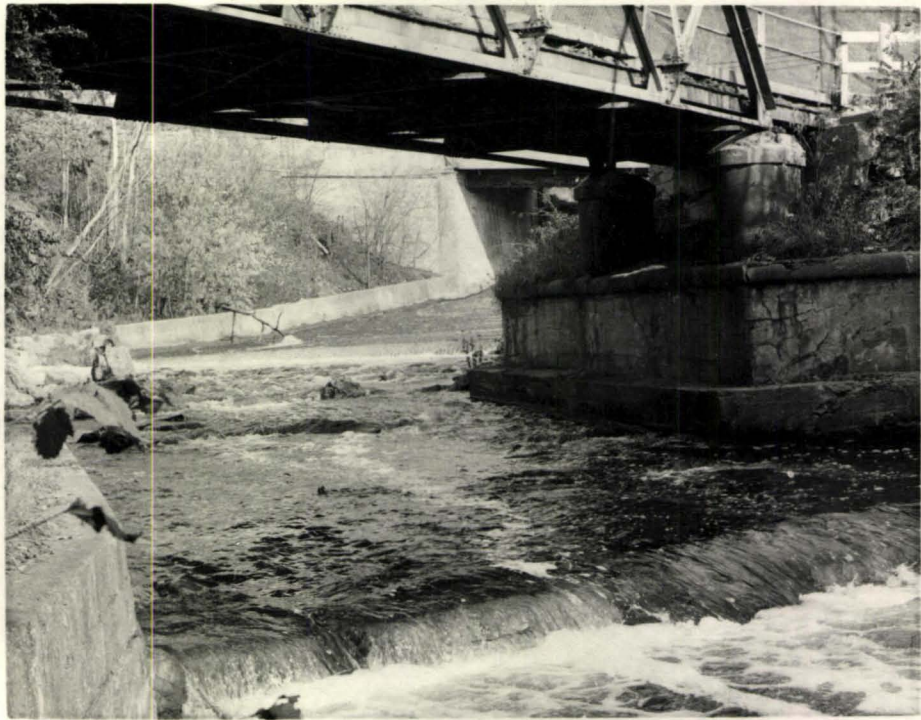


PHOTO #2

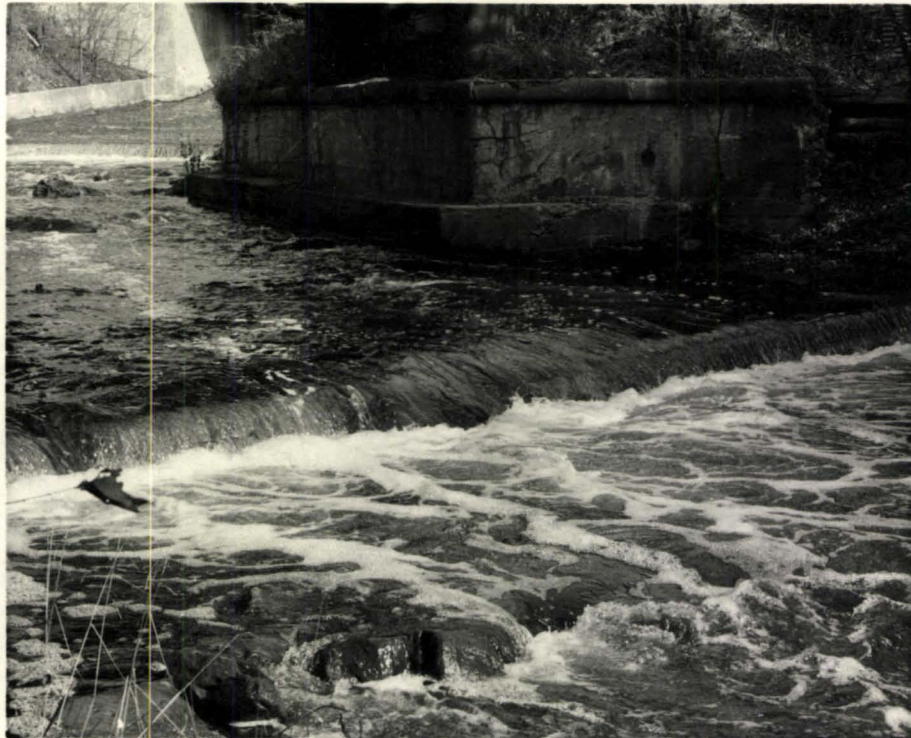


PHOTO #3



PHOTO #4



PHOTO #5



PHOTO #6

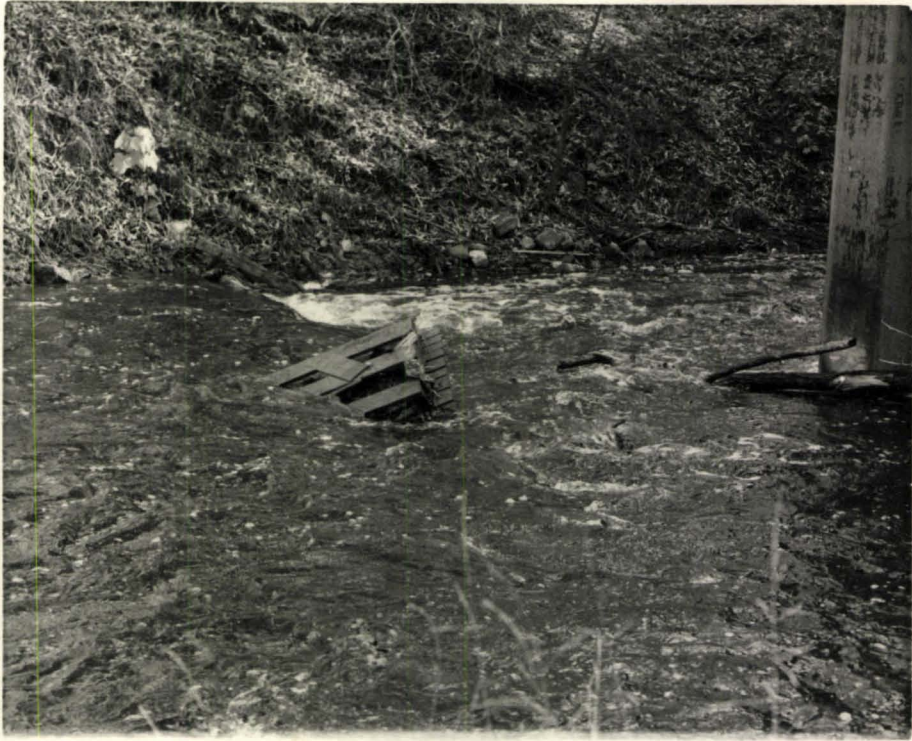


PHOTO #7



PHOTO #8



PHOTO #9



PHOTO #10



PHOTO #11



PHOTO #12



PHOTO #13



PHOTO #14



PHOTO #15



PHOTO #16



PHOTO #17



PHOTO #18



PHOTO #19



PHOTO #20



PHOTO #21



PHOTO #22



PHOTO #23



PHOTO #24



PHOTO #25



PHOTO #26



PHOTO #27



PHOTO #28

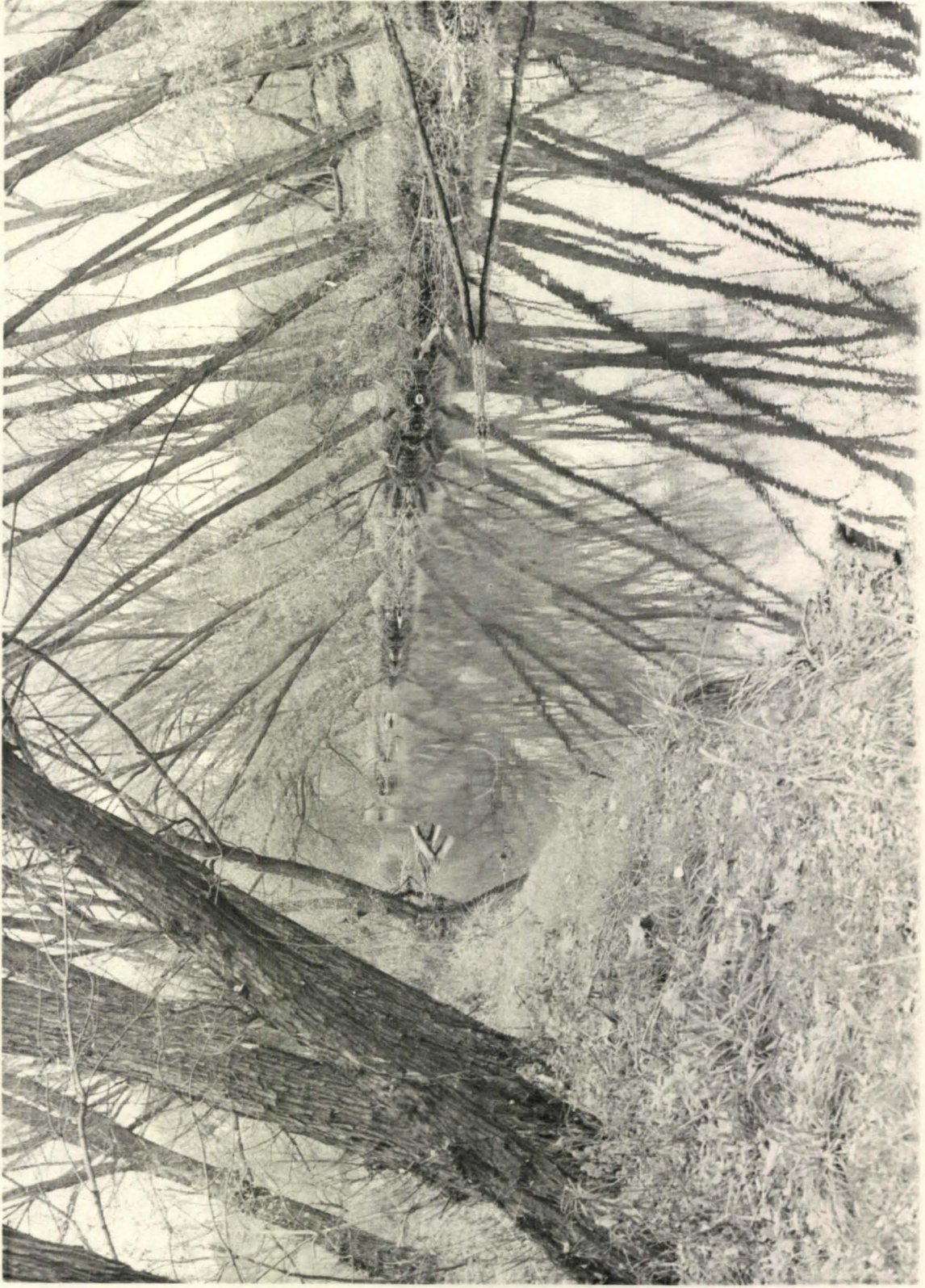


PHOTO #29

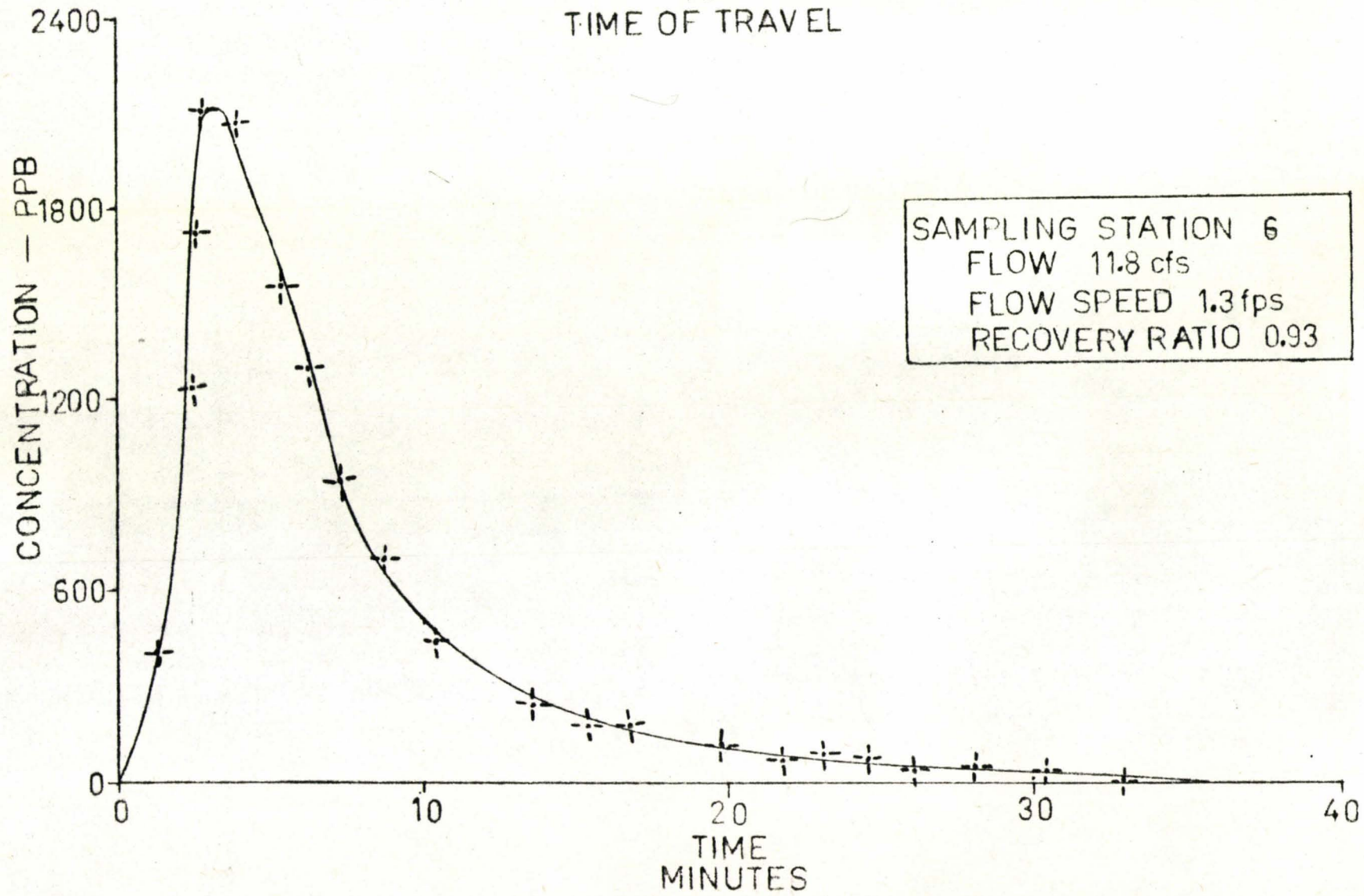
APPENDIX E

CONCENTRATION OBSERVATIONS

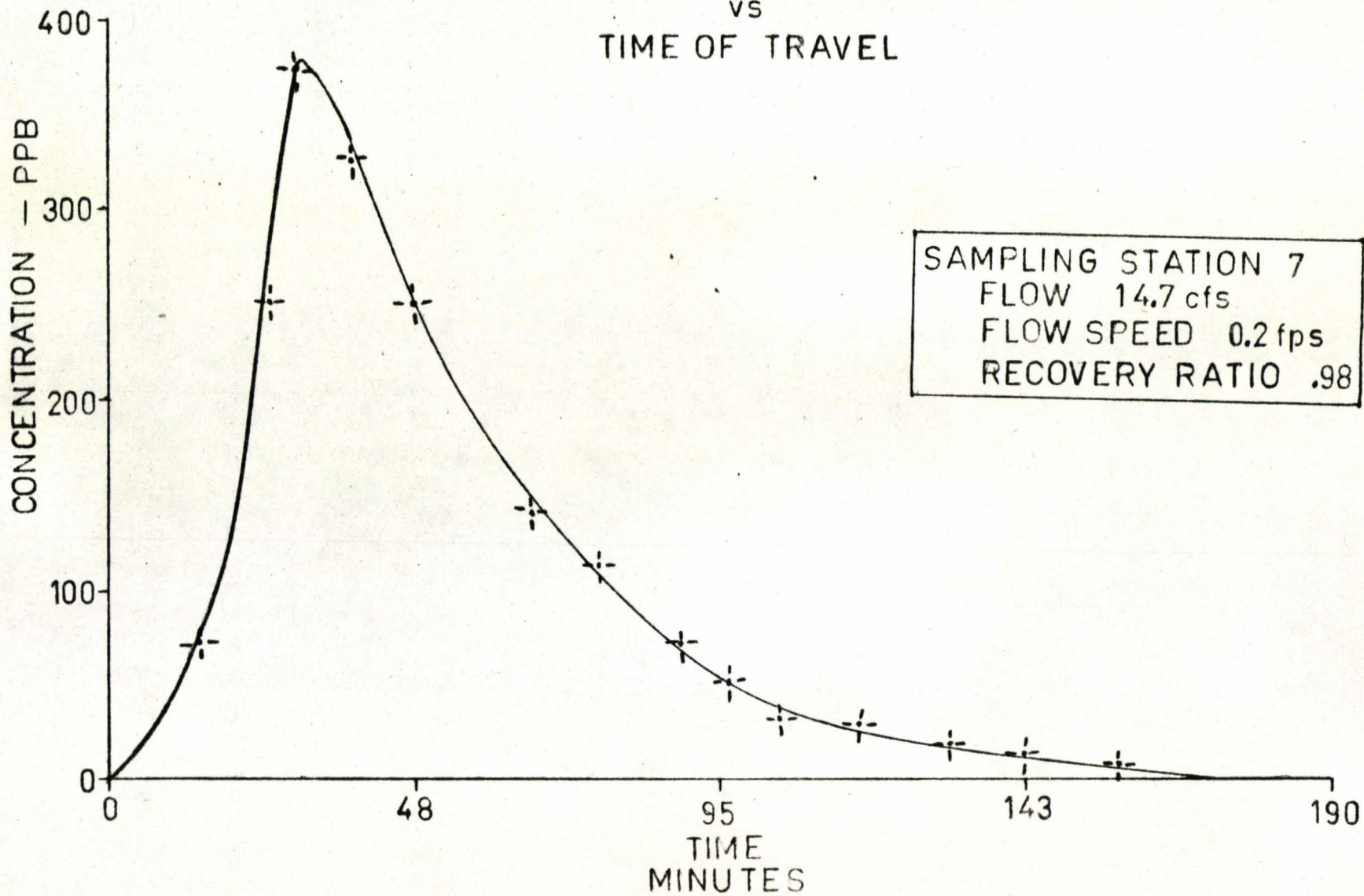
TEST #1

June 19, 1972 - June 20, 1972

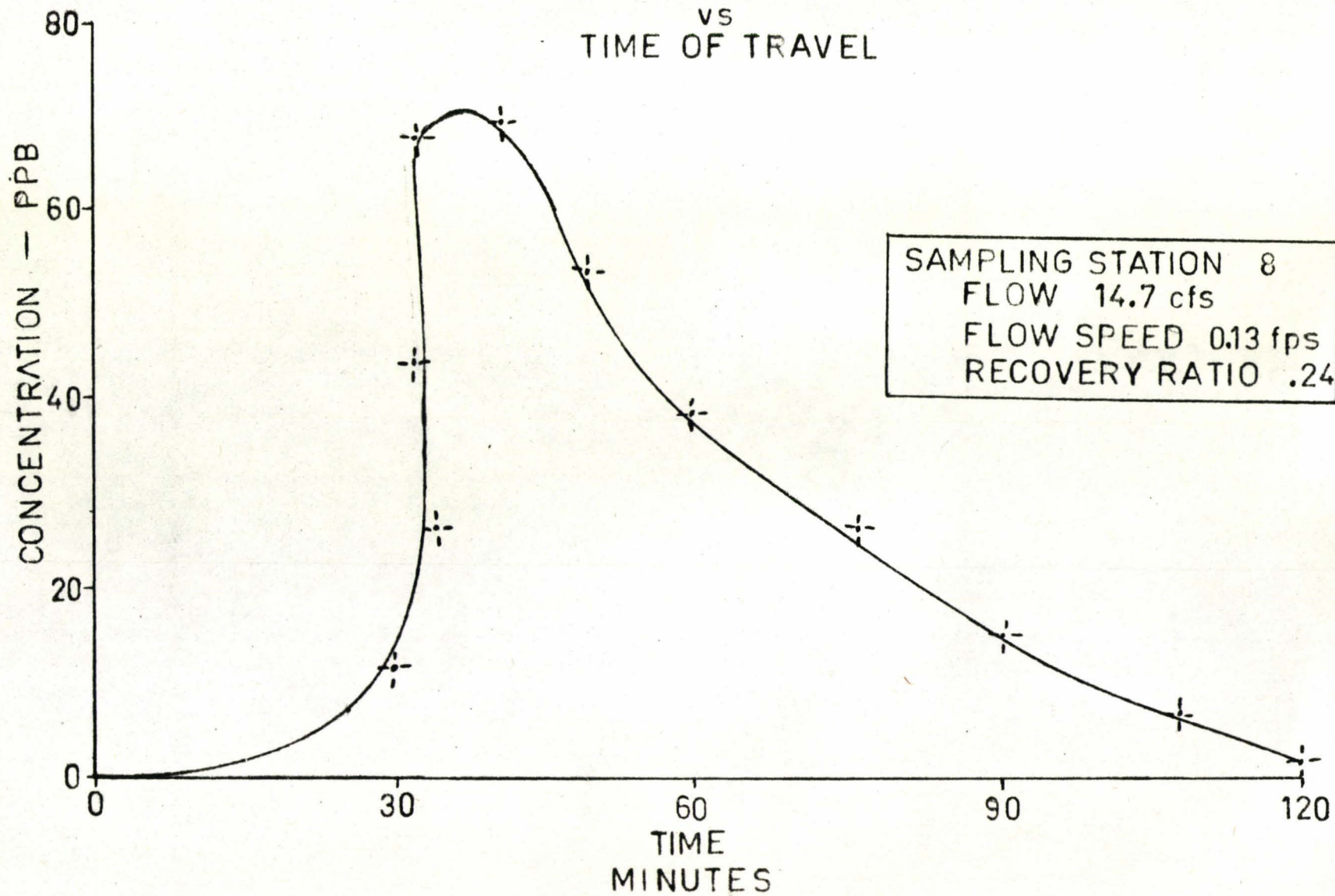
DYE CONCENTRATION
VS
TIME OF TRAVEL



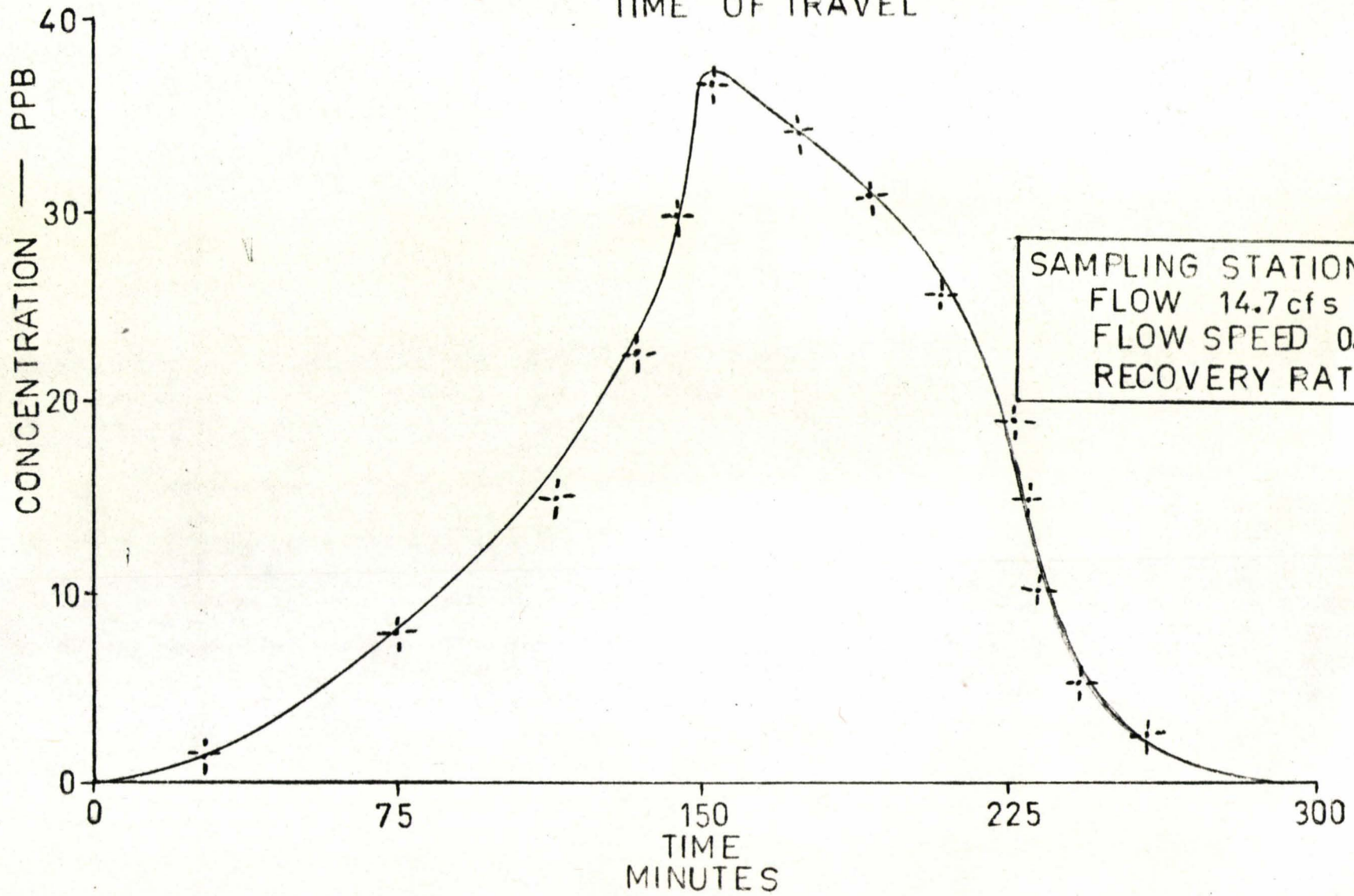
DYE CONCENTRATION
VS
TIME OF TRAVEL



DYE CONCENTRATION
VS
TIME OF TRAVEL

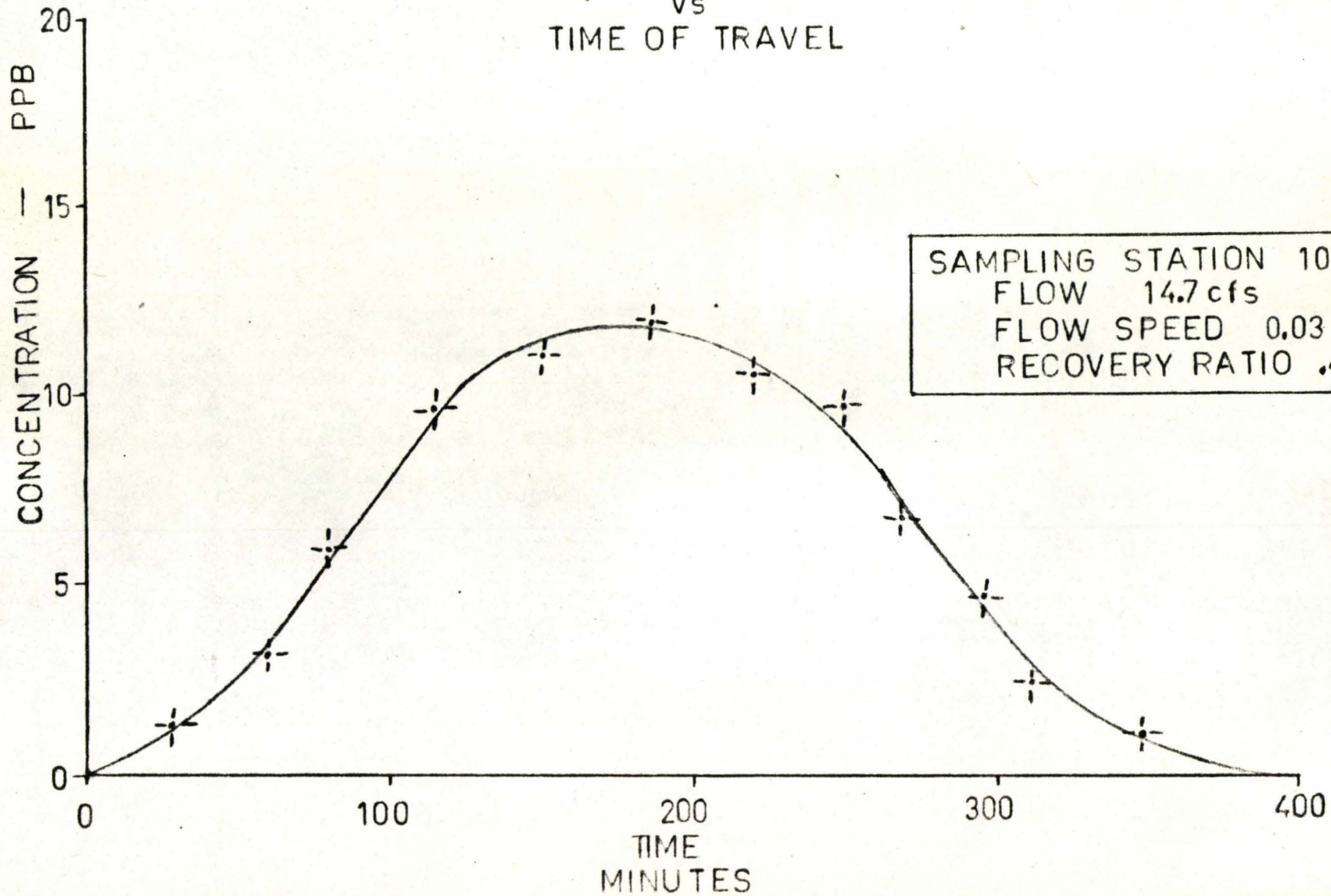


DYE CONCENTRATION
VS
TIME OF TRAVEL



SAMPLING STATION 9
FLOW 14.7 cfs
FLOW SPEED 0.05 fps
RECOVERY RATIO .32

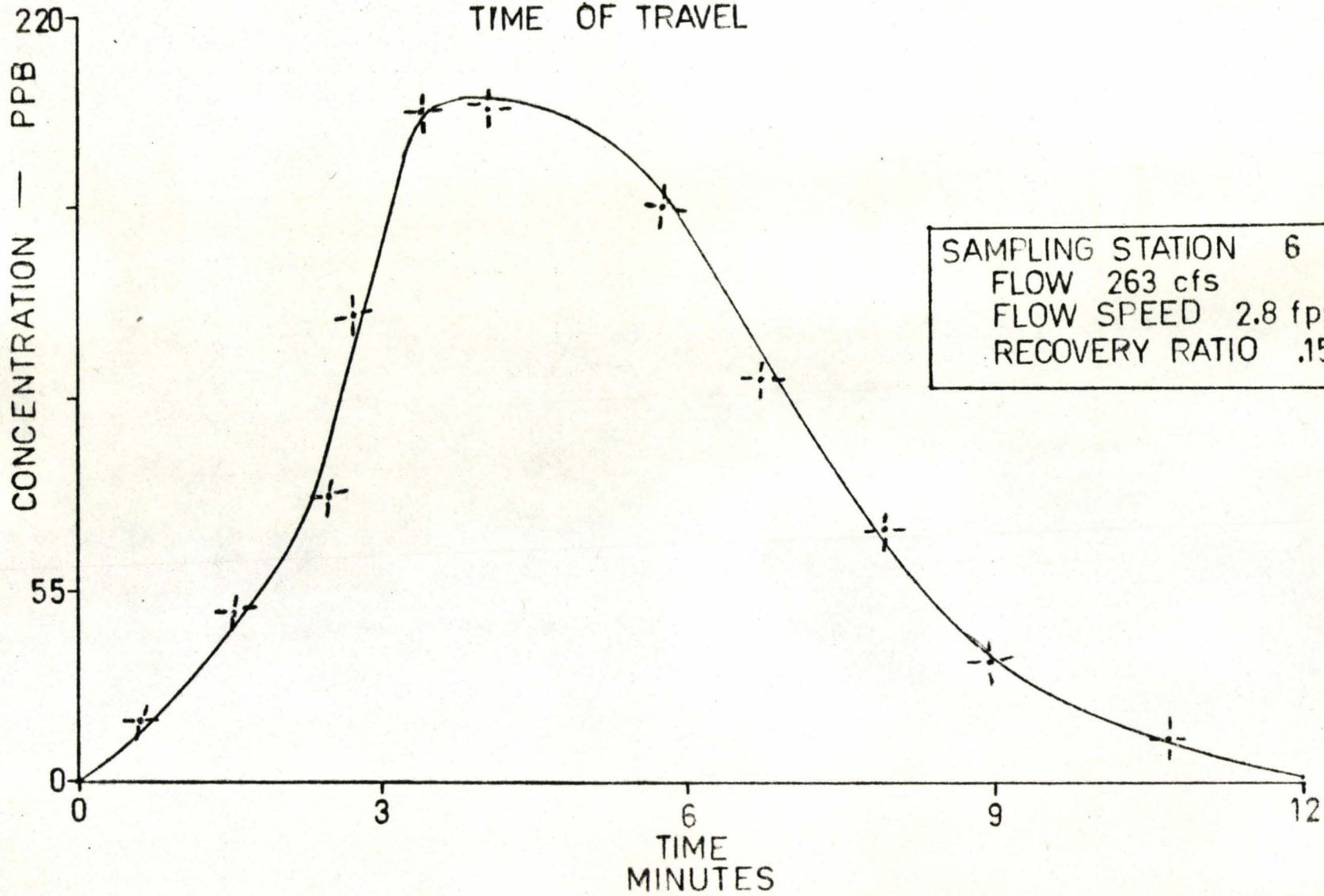
DYE CONCENTRATION
vs
TIME OF TRAVEL



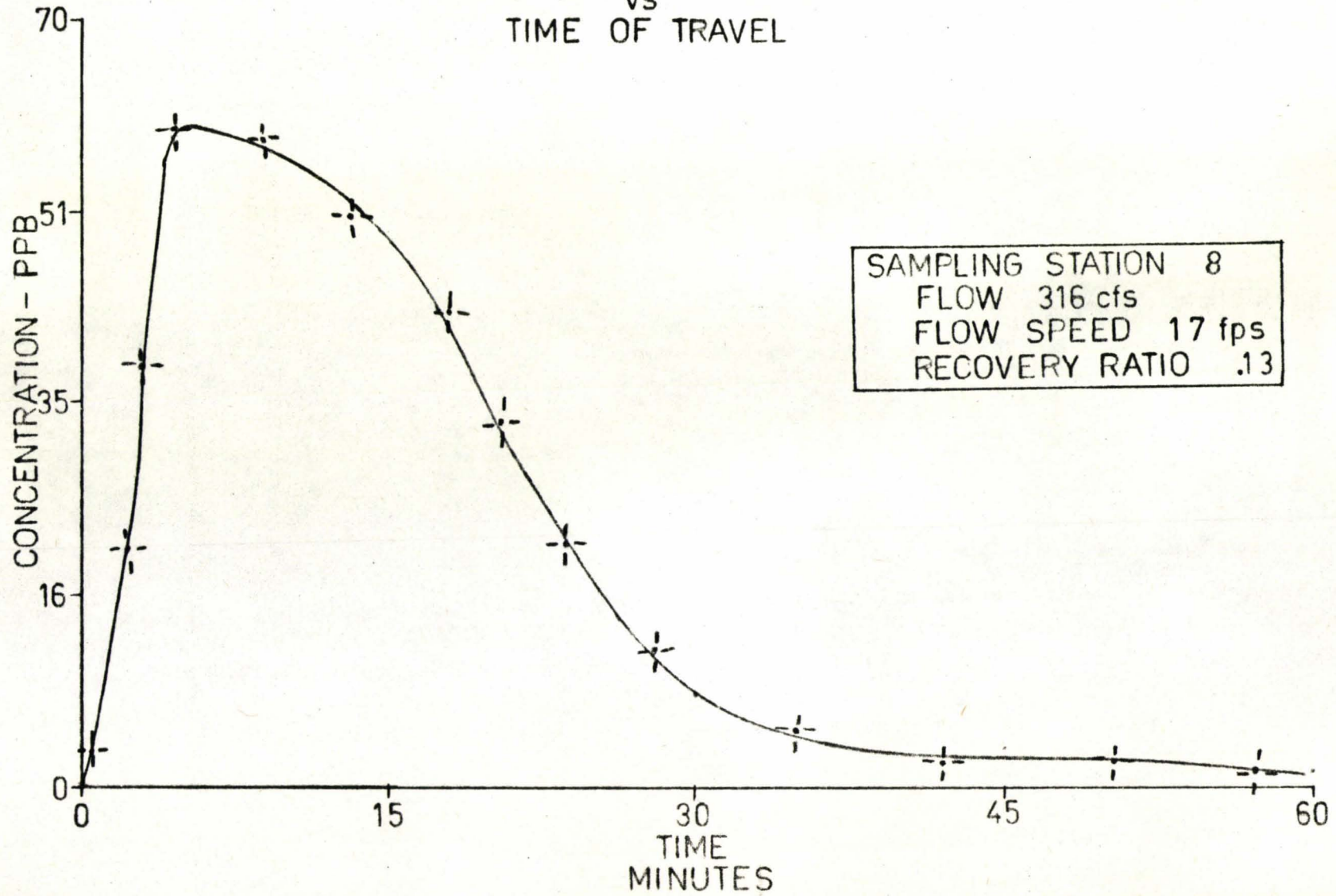
TEST #2

August 9, 1972

DYE CONCENTRATION
VS
TIME OF TRAVEL



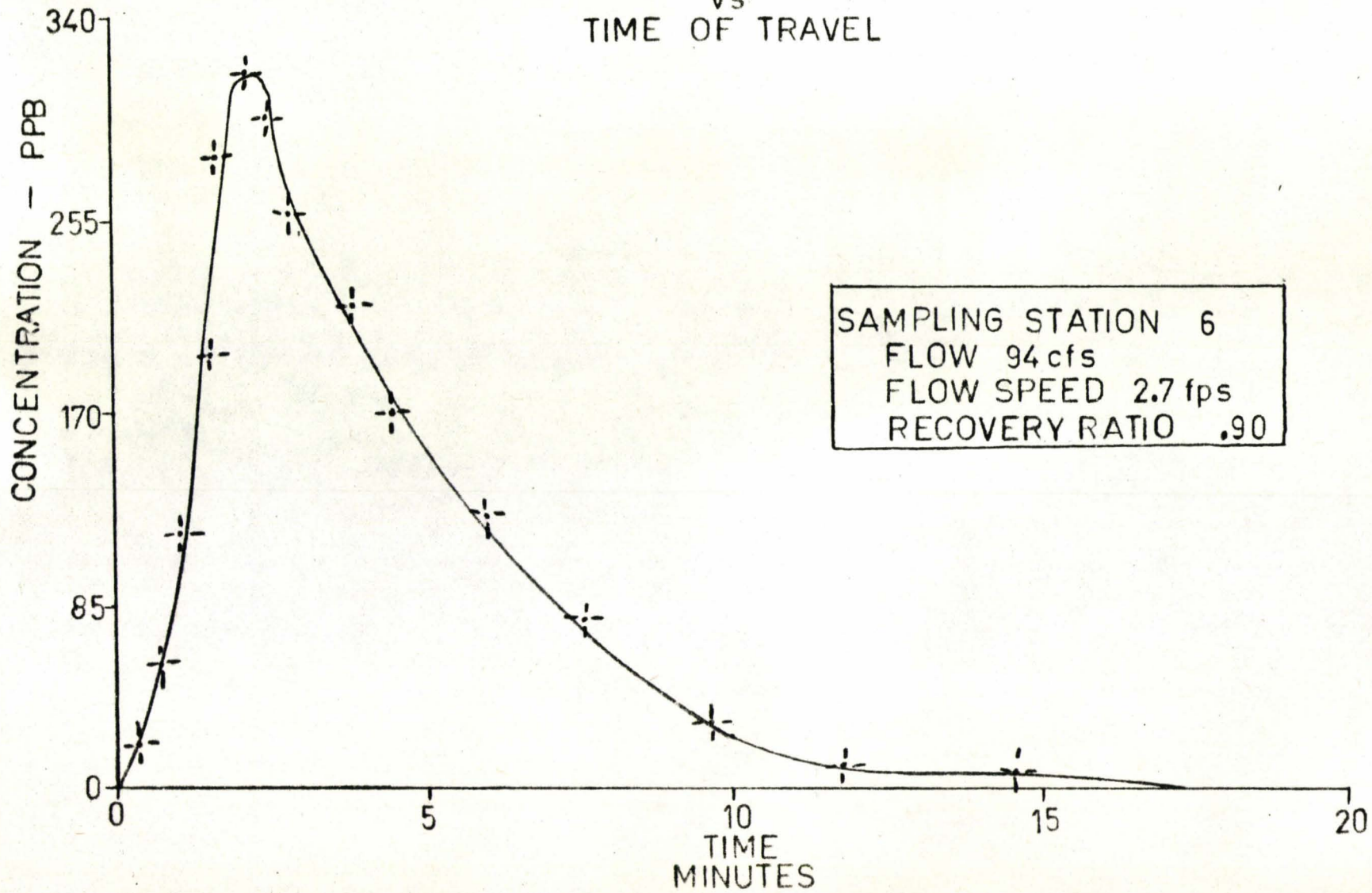
DYE CONCENTRATION
VS
TIME OF TRAVEL



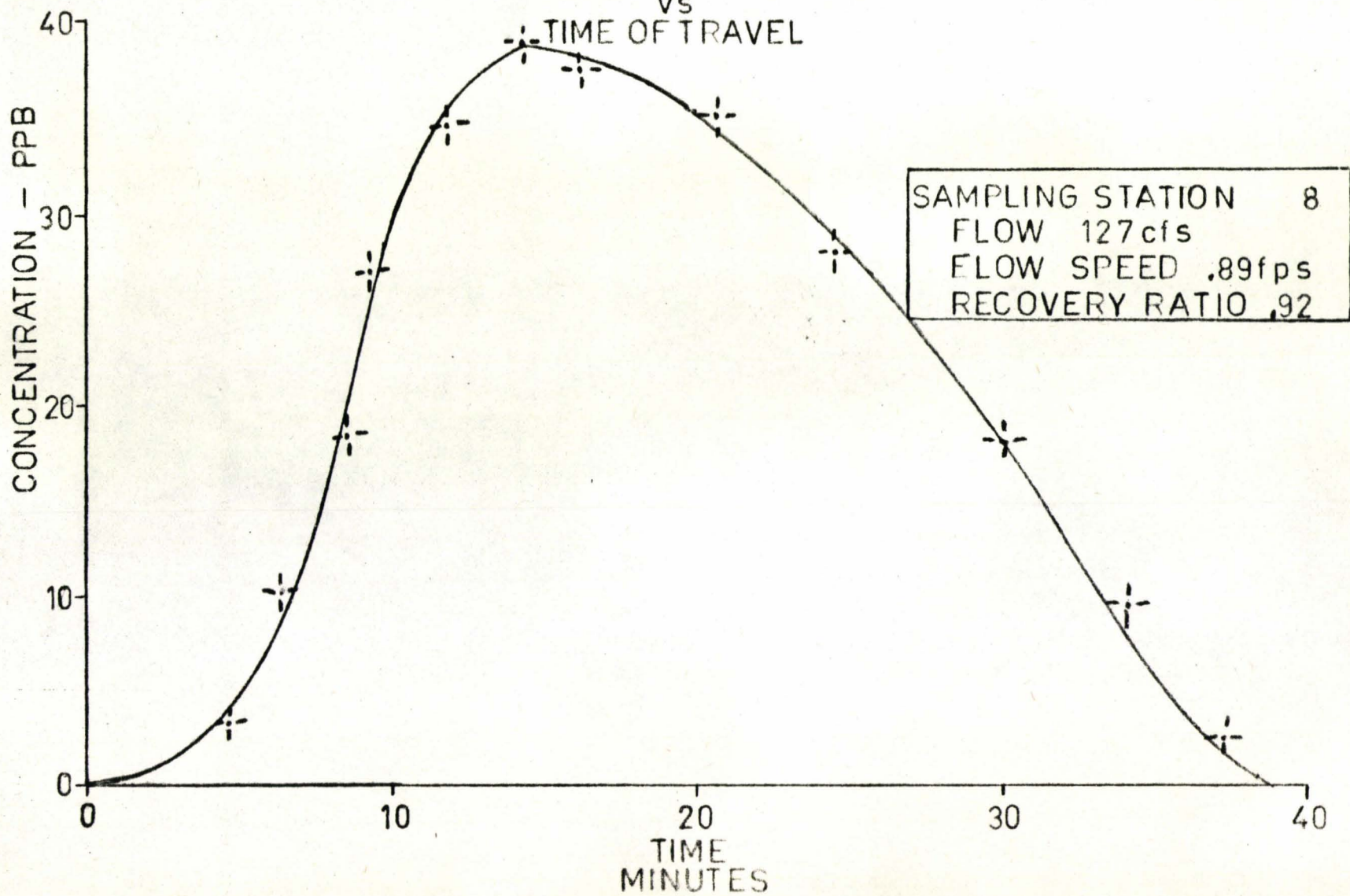
TEST #3

August 15, 1972

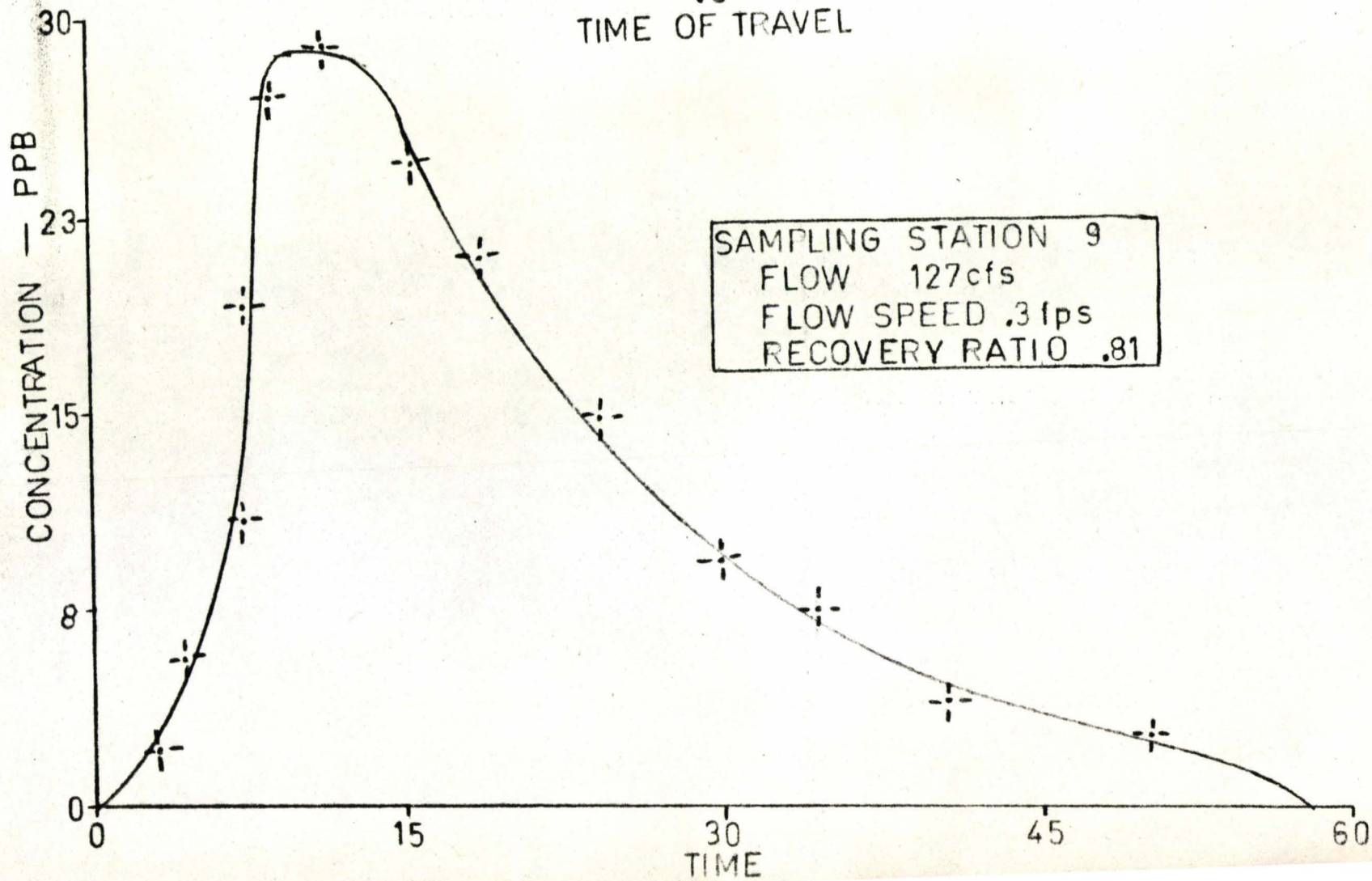
DYE CONCENTRATION
vs
TIME OF TRAVEL



DYE CONCENTRATION
VS
TIME OF TRAVEL



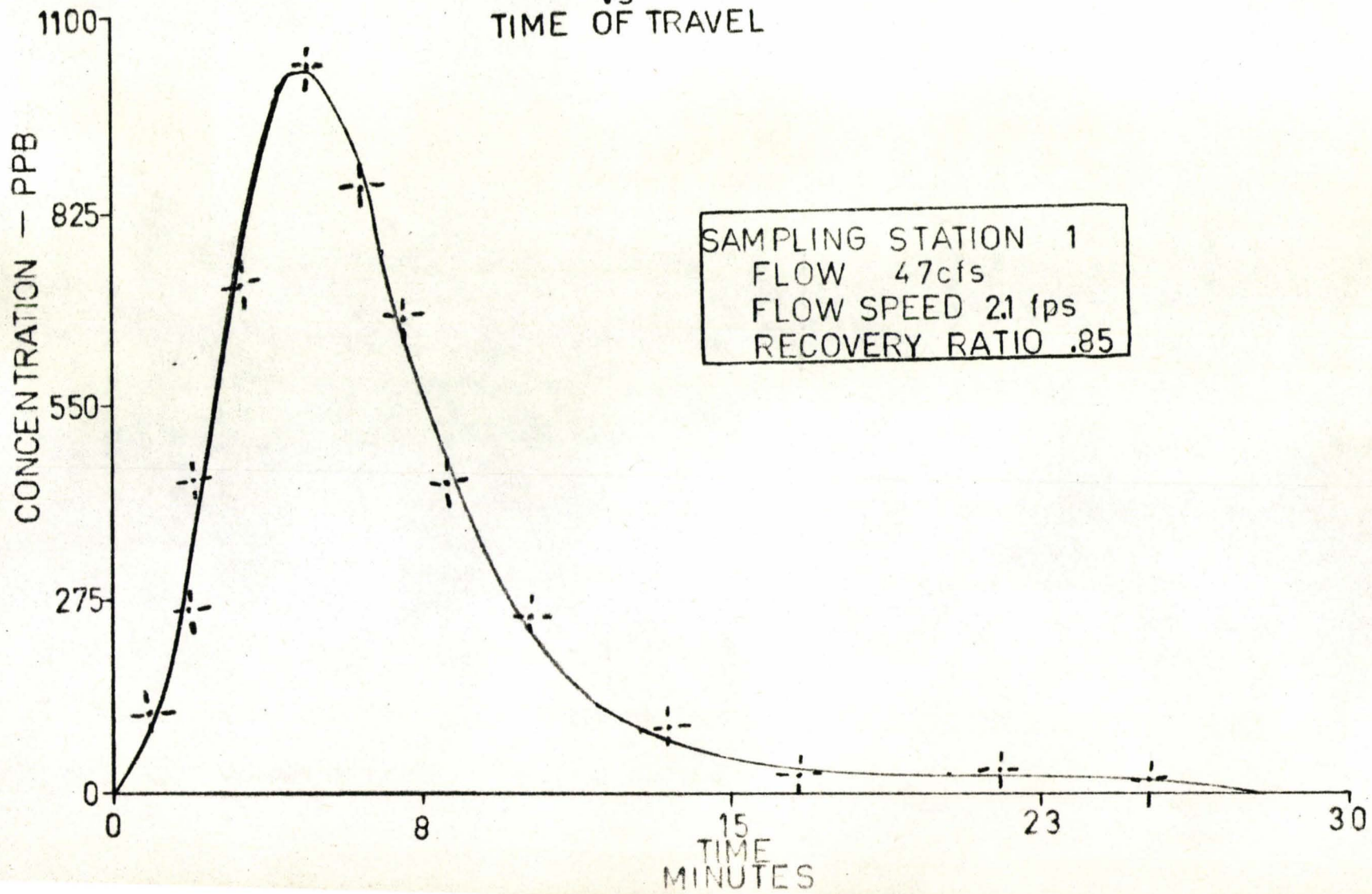
DYE CONCENTRATION
VS
TIME OF TRAVEL



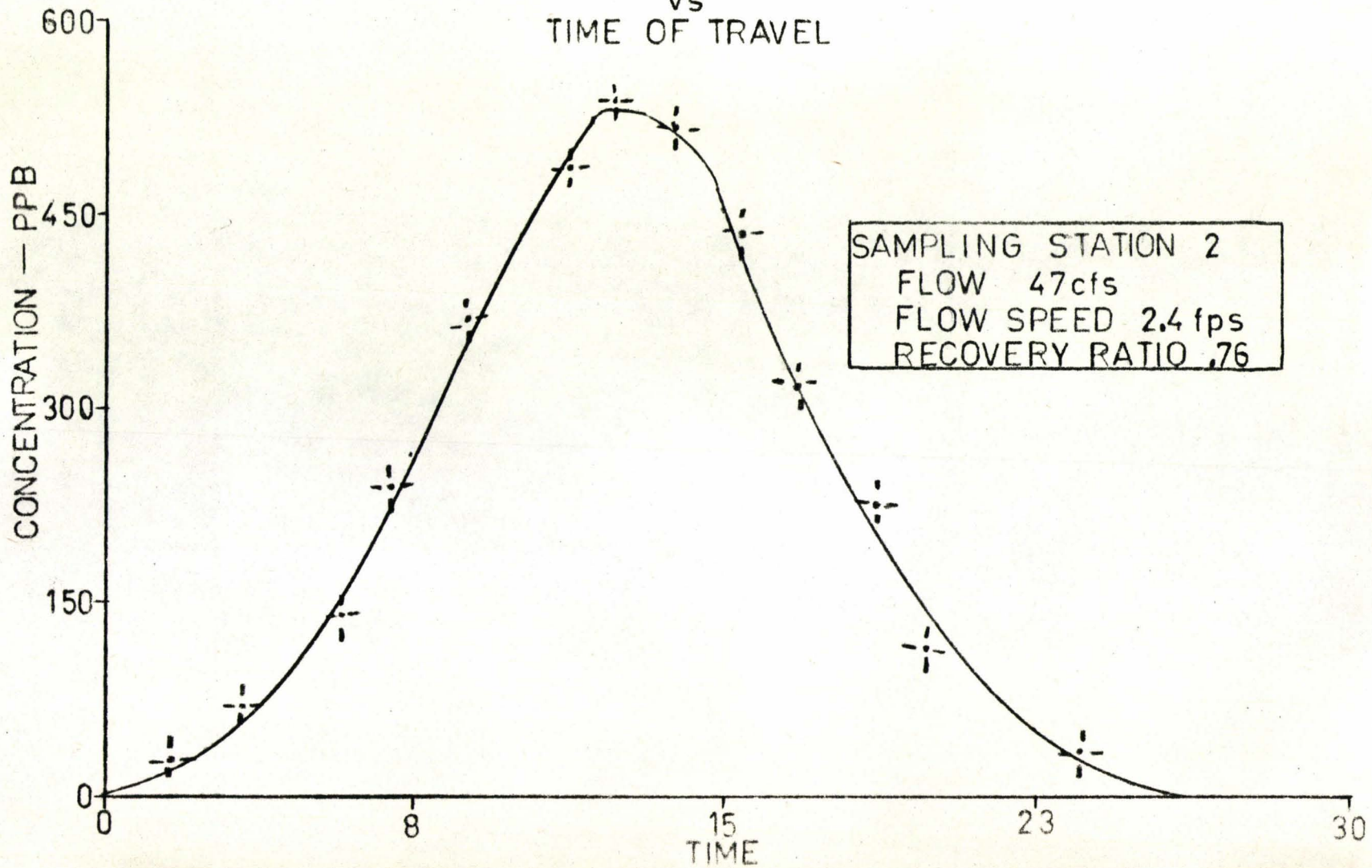
TEST #4

August 18, 1972

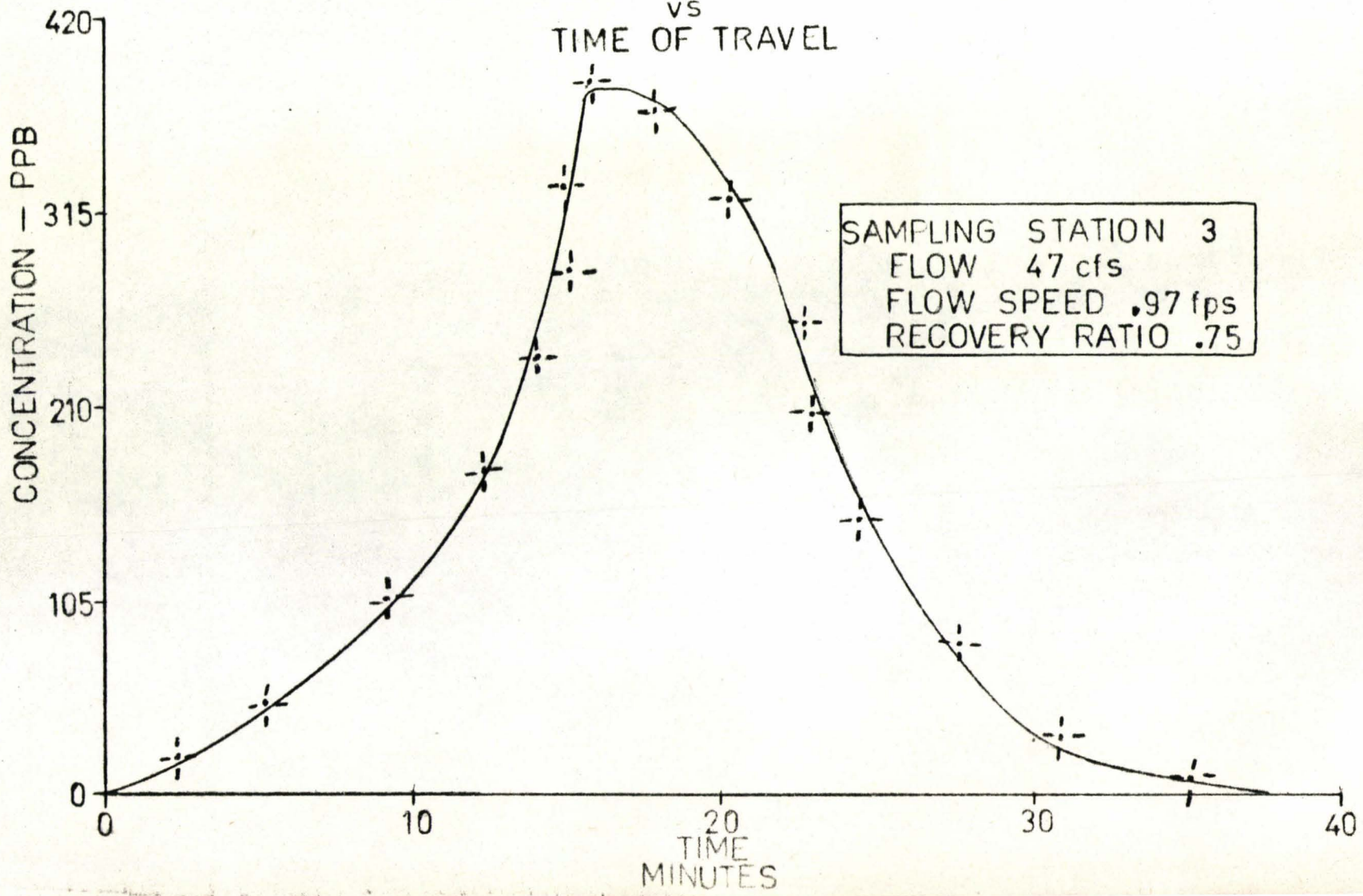
DYE CONCENTRATION
vs
TIME OF TRAVEL



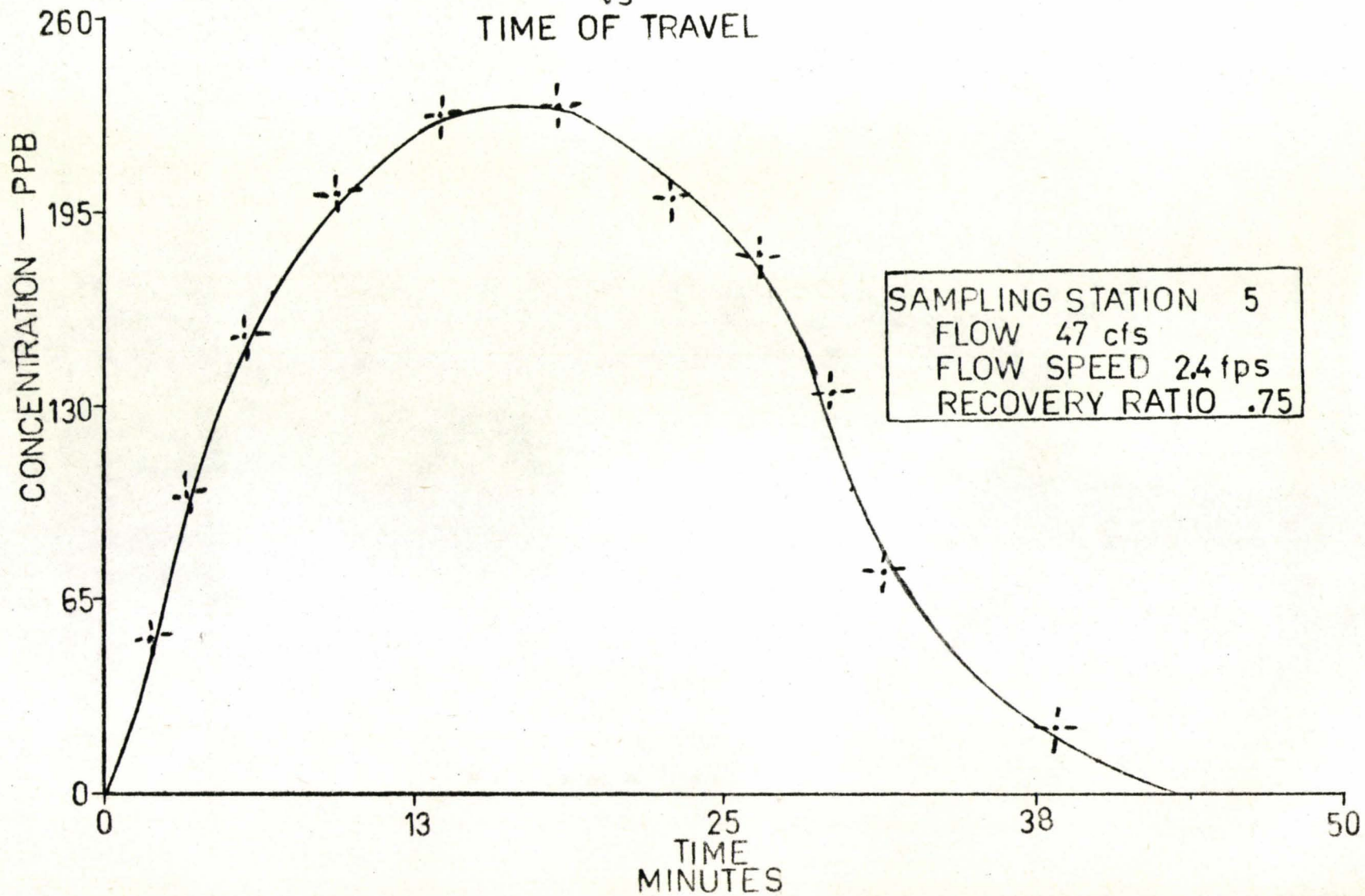
DYE CONCENTRATION
vs
TIME OF TRAVEL



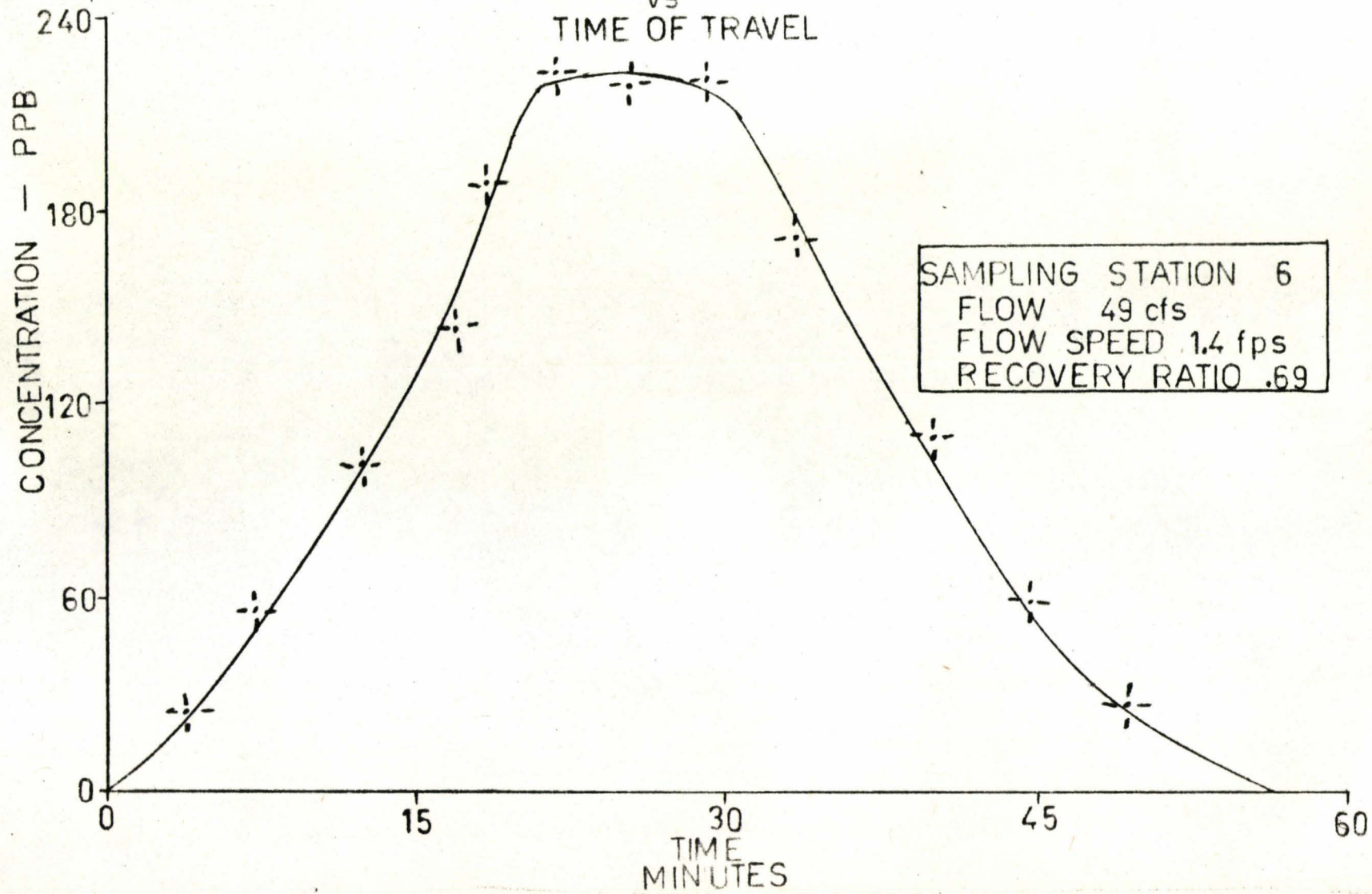
DYE CONCENTRATION
vs
TIME OF TRAVEL



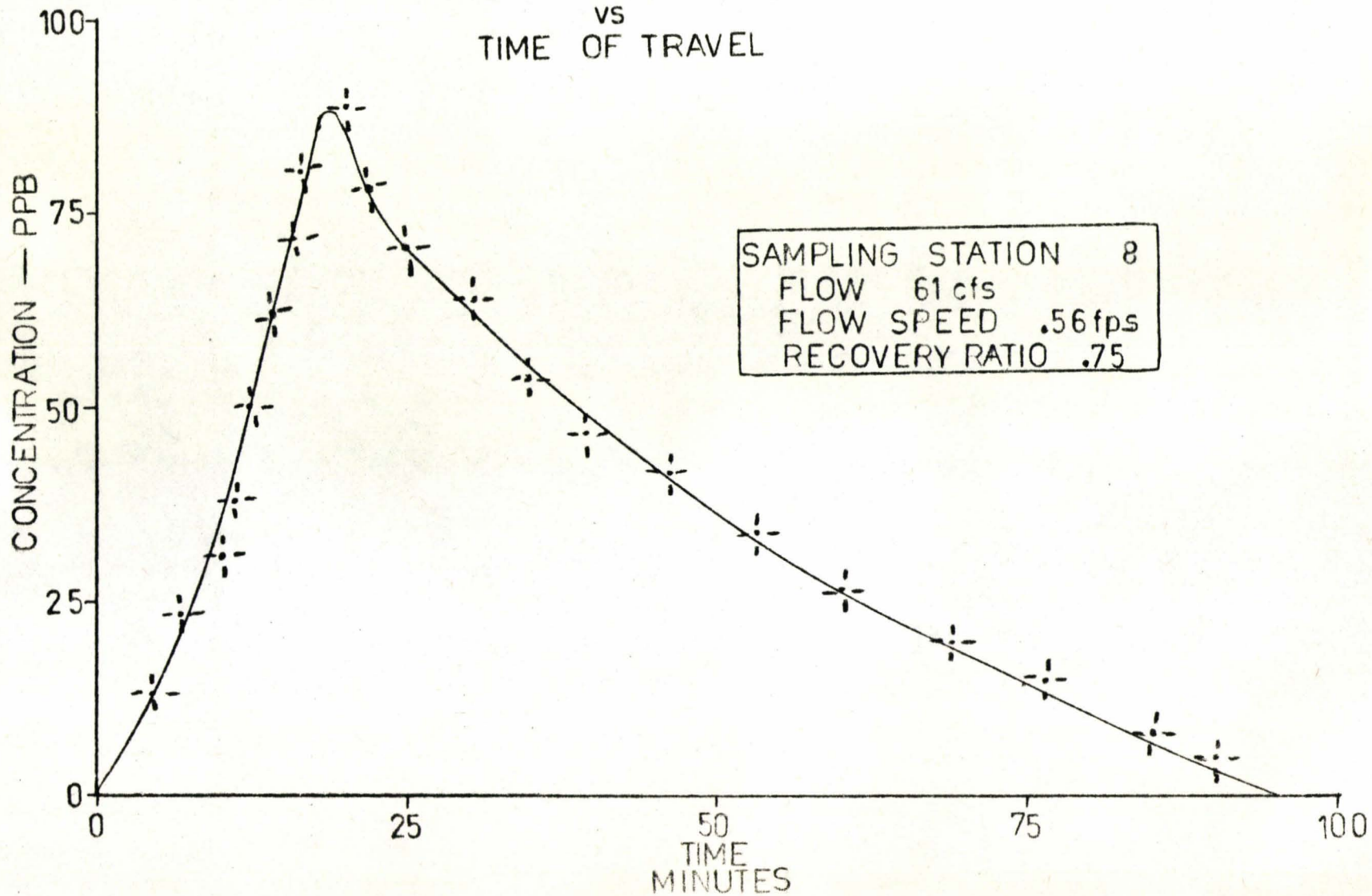
DYE CONCENTRATION
vs
TIME OF TRAVEL



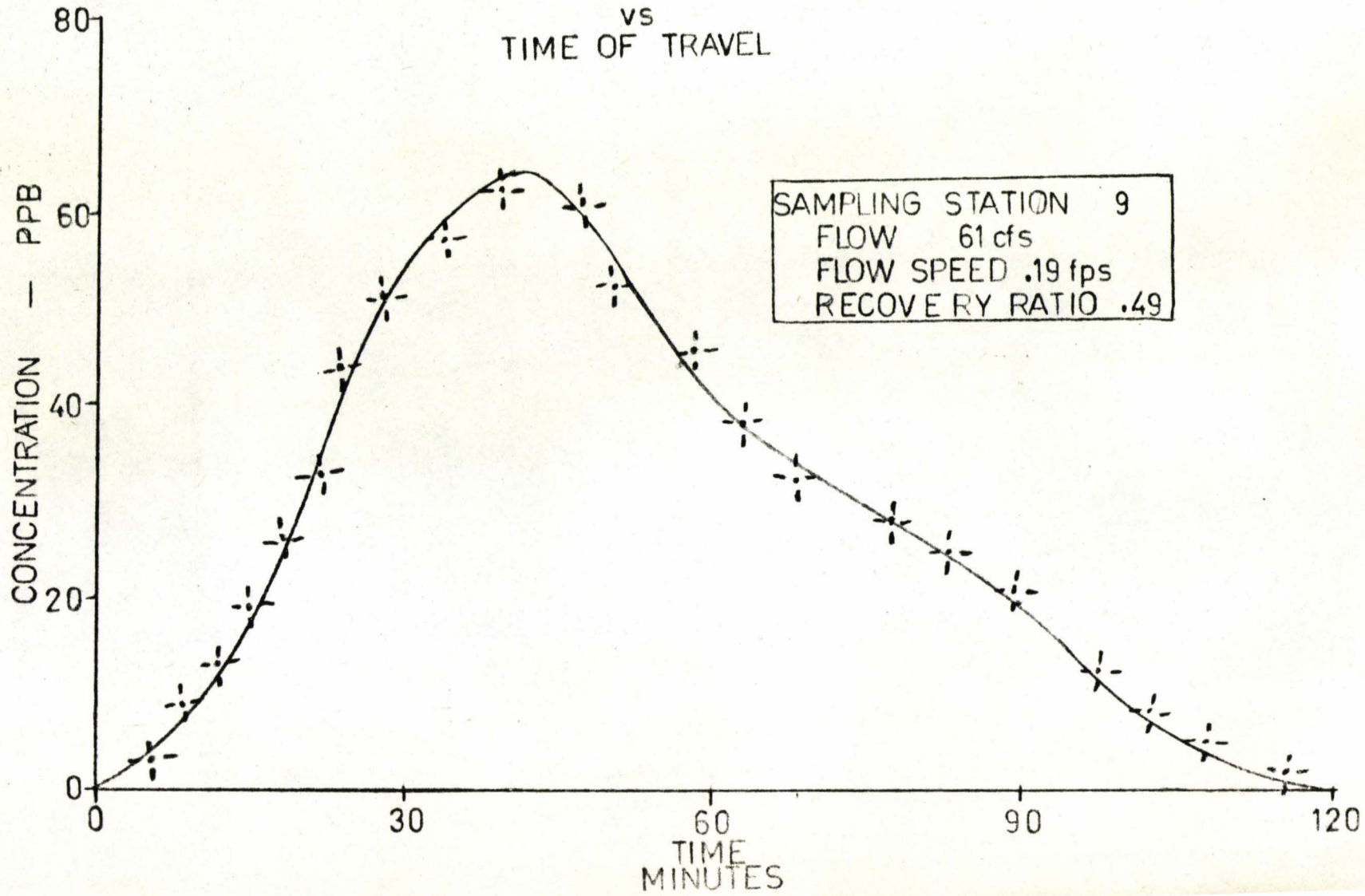
DYE CONCENTRATION
VS
TIME OF TRAVEL



DYE CONCENTRATION
VS
TIME OF TRAVEL



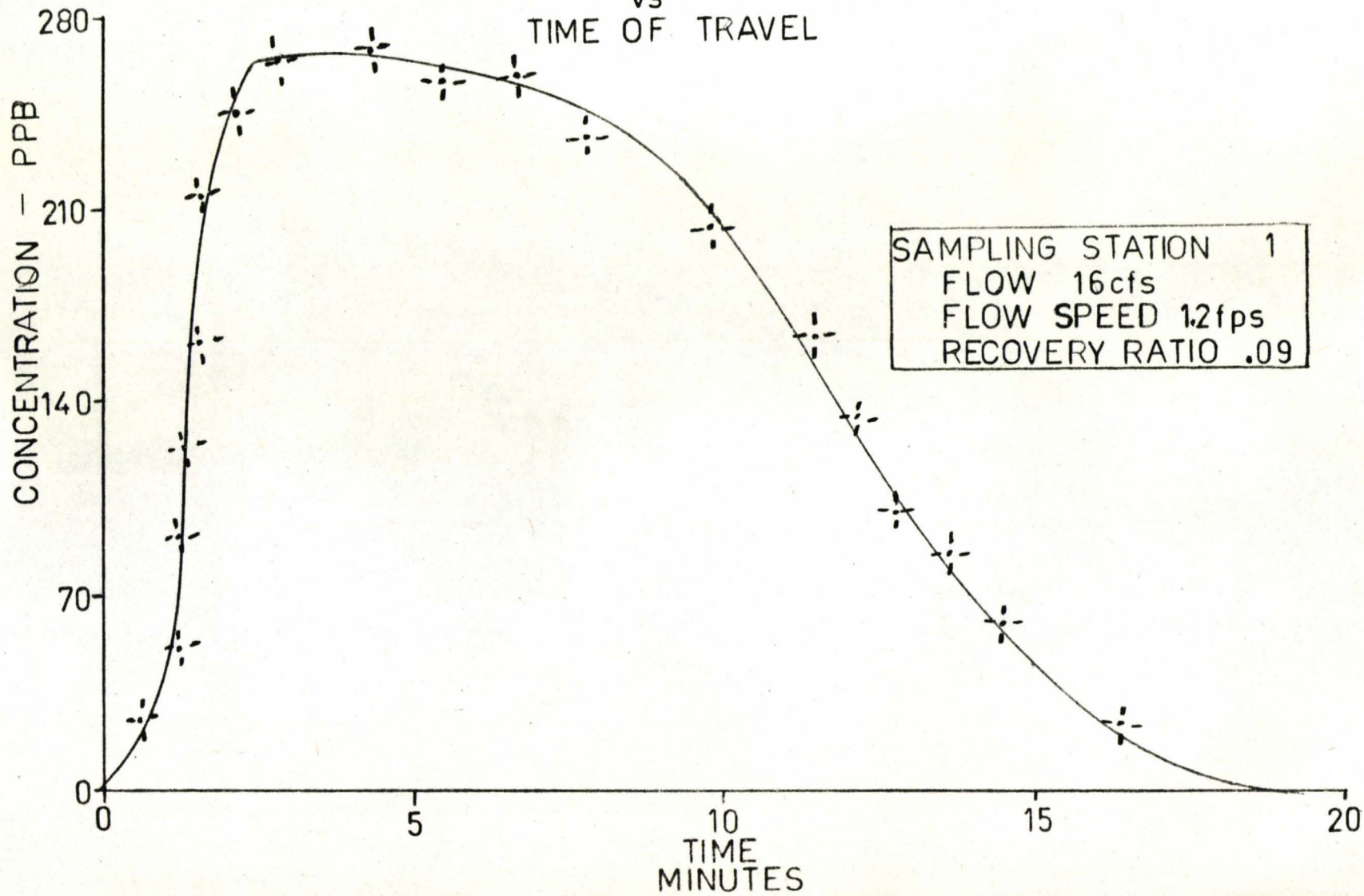
DYE CONCENTRATION
vs
TIME OF TRAVEL



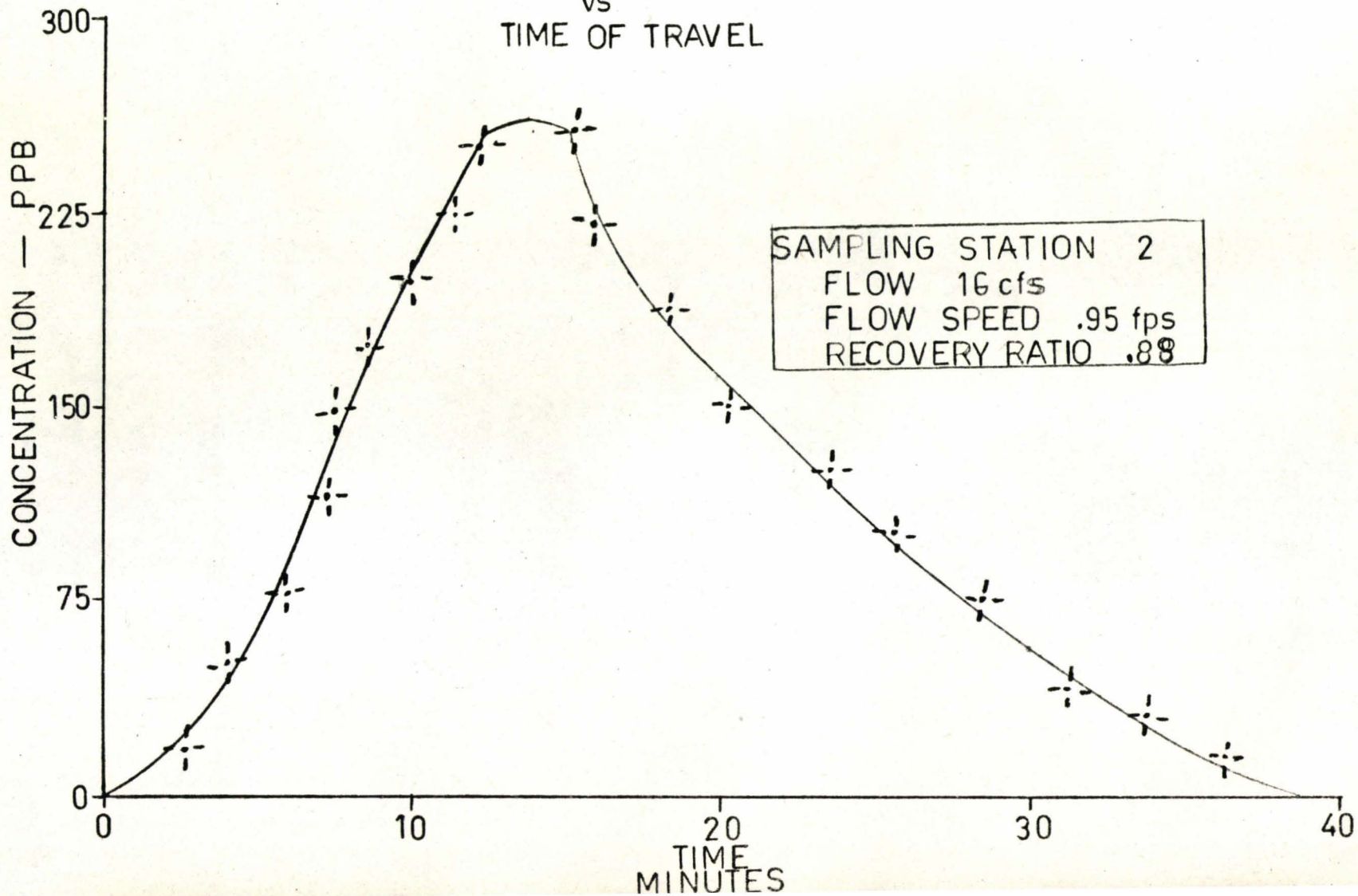
TEST #5

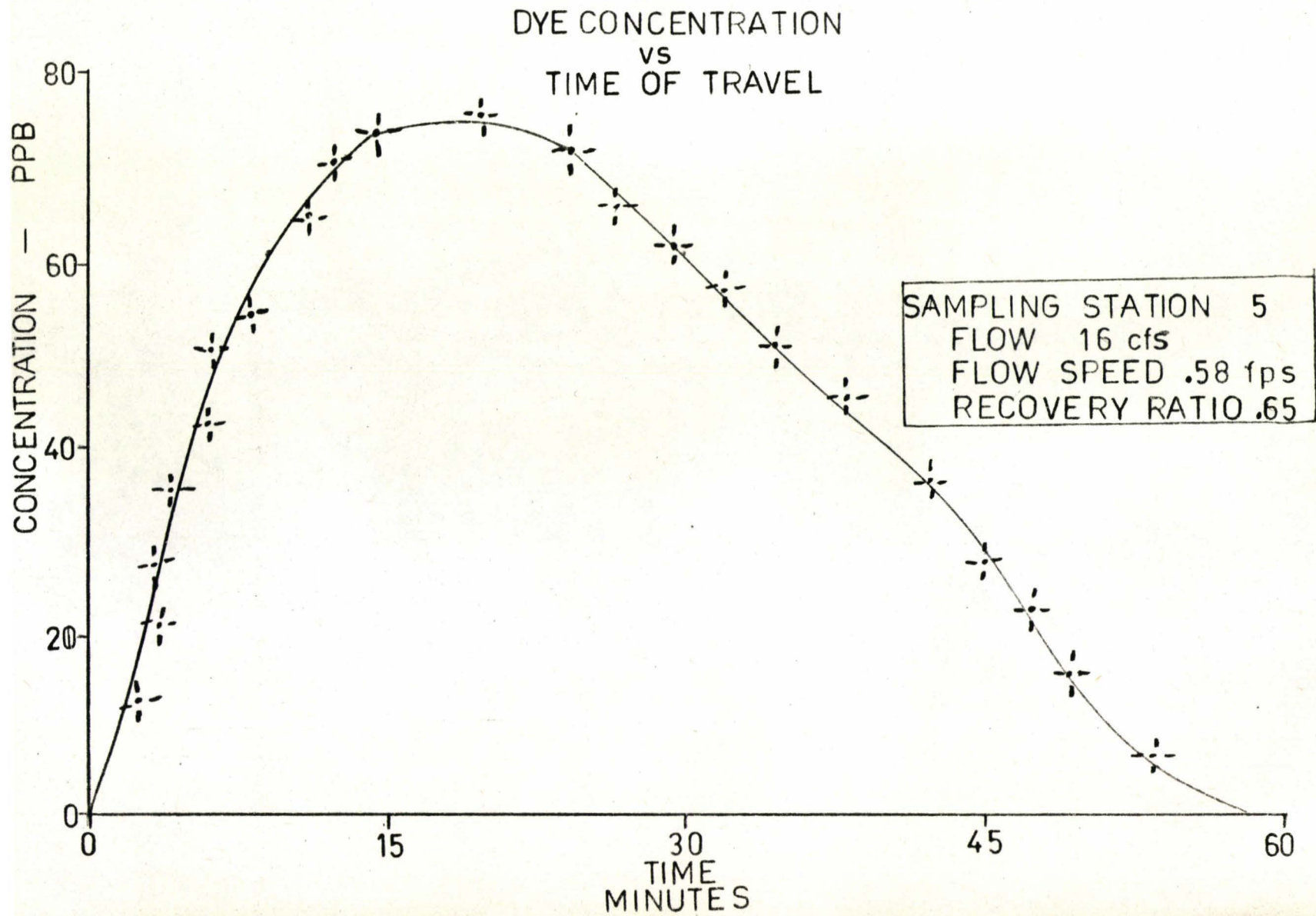
August 31, 1972

DYE CONCENTRATION
VS
TIME OF TRAVEL

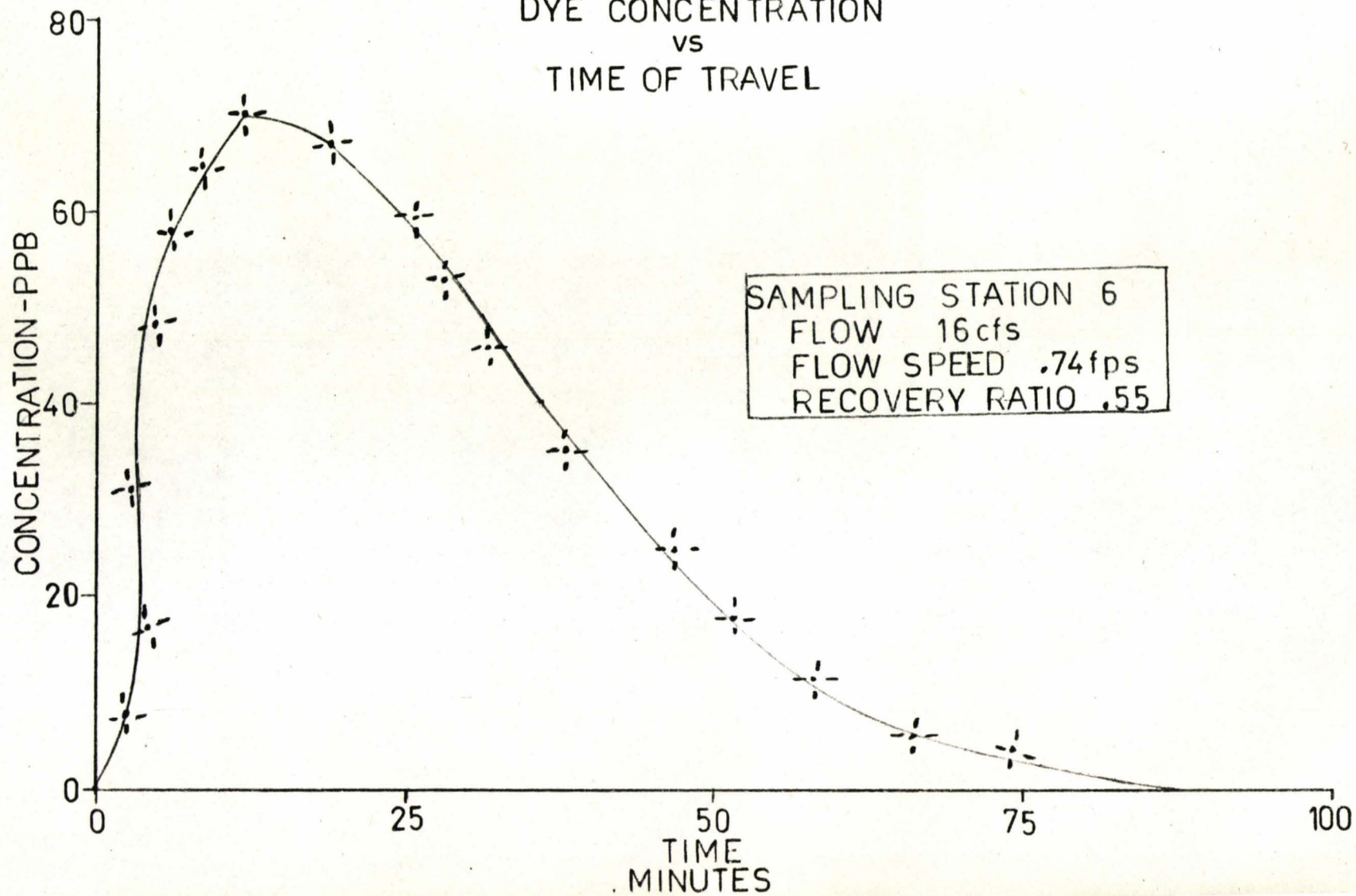


DYE CONCENTRATION
VS
TIME OF TRAVEL

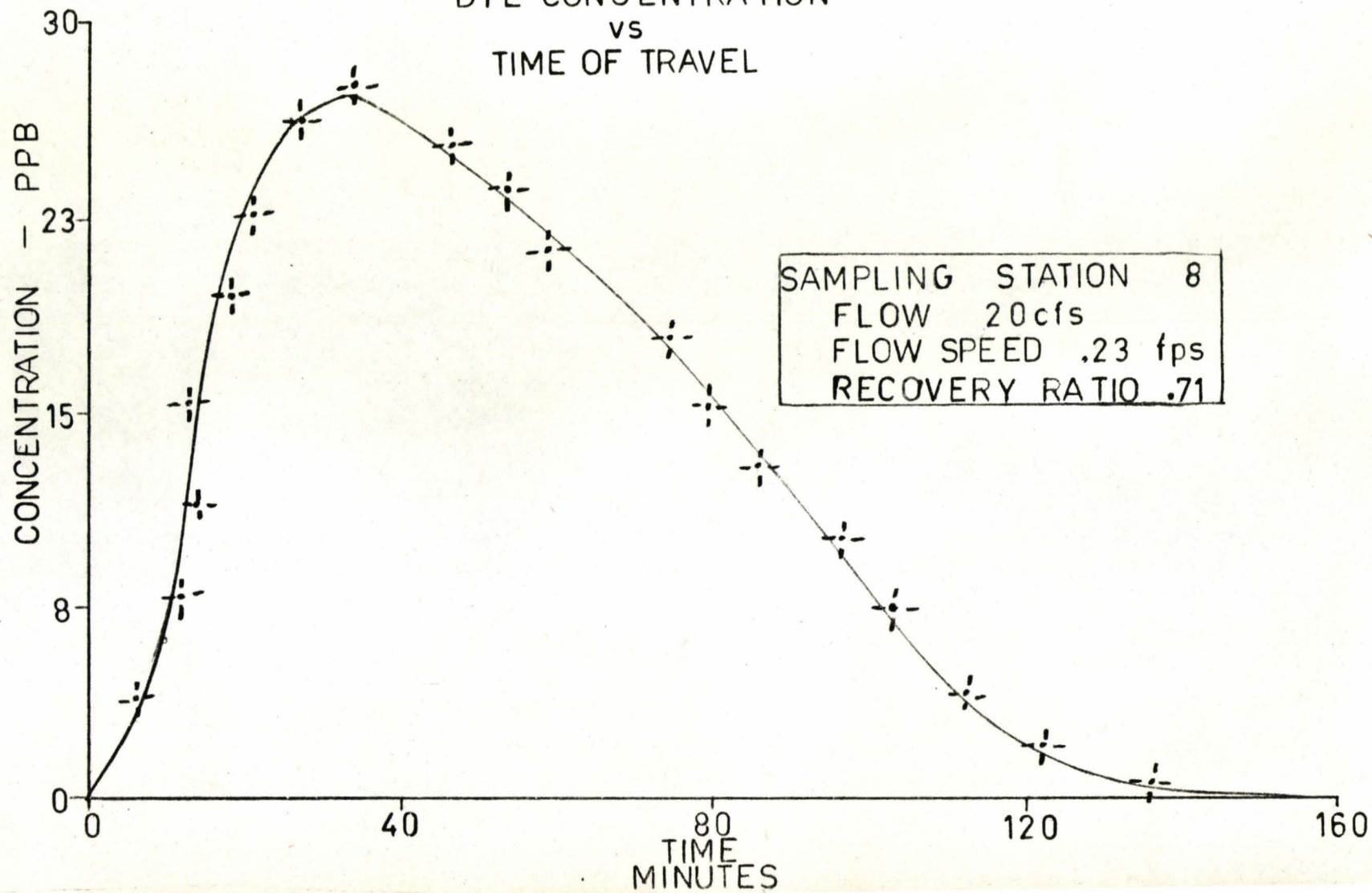




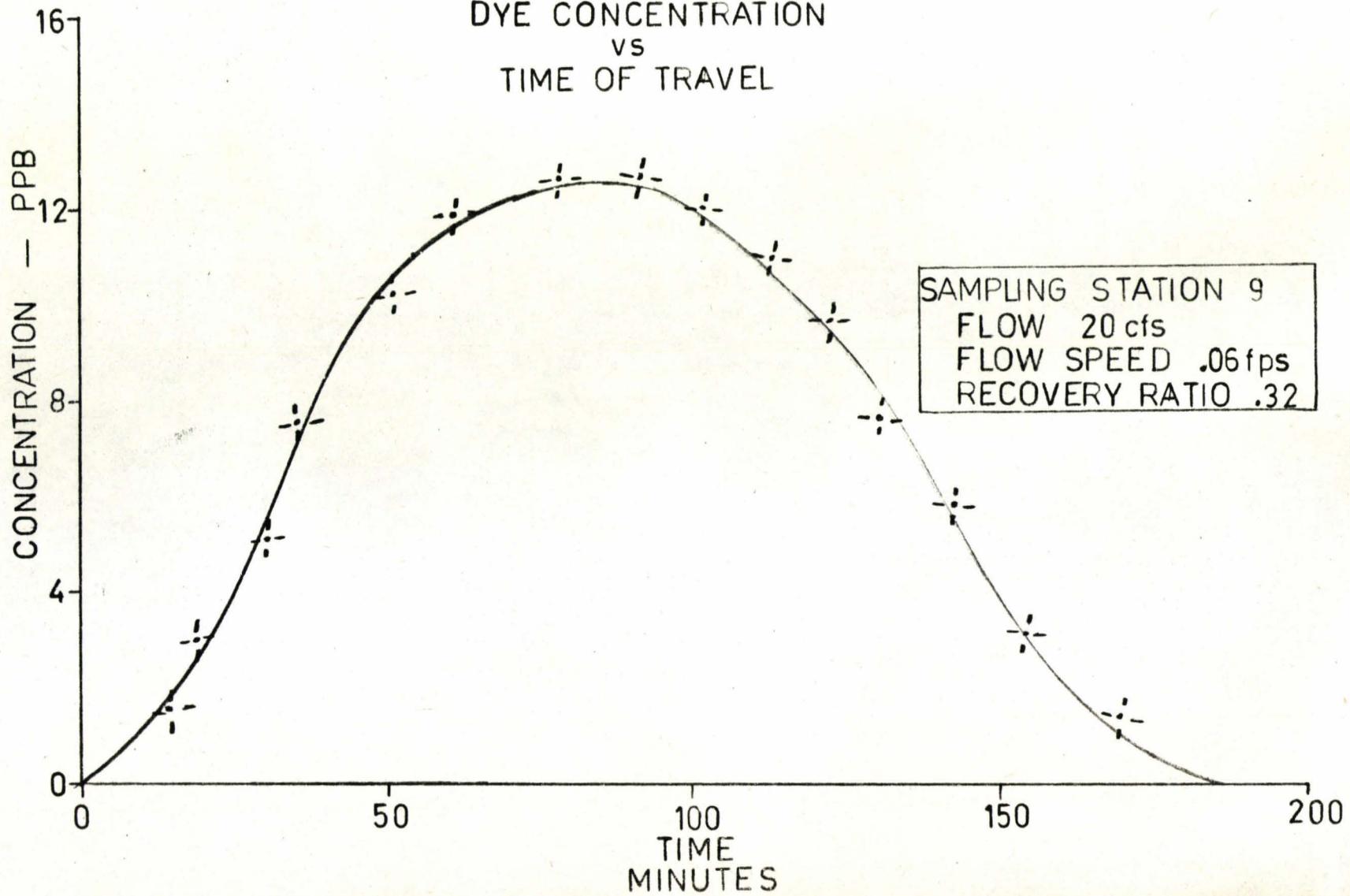
DYE CONCENTRATION
VS
TIME OF TRAVEL



DYE CONCENTRATION
vs
TIME OF TRAVEL



DYE CONCENTRATION
VS
TIME OF TRAVEL



APPENDIX F

NOTATION

The symbols used in this dissertation have the following meaning:

c	concentration	ML^{-3}
u	velocity in the x direction (longitudinal) at any point y, z	LT^{-1}
K_x	eddy diffusion coefficient (x direction)	L^2T^{-1}
K_y	eddy diffusion coefficient (y direction)	L^2T^{-1}
K_z	eddy diffusion coefficient (z direction)	L^2T^{-1}
t	time	T
D_L	coefficient of diffusion	L^2T^{-1}
h	depth	L
u^*	friction velocity	
\bar{u}	average cross sectional velocity	LT^{-1}
C_a	concentration in the main stream	ML^{-3}
D_L''	longitudinal mixing coefficient	L^2T^{-1}
K	dead zone mass transfer coefficient	
a	ratio of the interfacial area between the main stream and dead zone to the main stream volume	
C_d	concentration in the dead zone	ML^{-3}
d	ratio of the interfacial area to the dead zone volume	
A	cross sectional area	L^2
u'	deviation of u from cross sectional mean \bar{u}	LT^{-1}
b	width of channel	L
$q'(z)$	depth integrated velocity at any point z	LT^{-1}
$\xi(z)$	lateral turbulent mixing coefficient	L^2T^{-1}
\bar{c}	cross sectional mean concentration	ML^{-3}
x	distance in the direction of flow	L

D	dispersion coefficient	L^2T^{-1}
k	dispersion coefficient	L^2T^{-1}
$C_{p,c}$	dimensionless coefficient	
$C_{l,t}$	dimensionless coefficient	
R	hydraulic radius	L
W	top width of the stream	L

APPENDIX G

BIBLIOGRAPHY

1. Buchanan, T.J., "Time of Travel of Soluble Contaminants in Streams," Journal of the Sanitary Engineering Division, ASCE, Vol. 90, No. SA3, 1964.
2. Butts, T.A., "Fluorometer Calibration Curves and Nomographs," Journal of the Sanitary Engineering Division, ASCE, Vol. 95, No. SA4, 1969.
3. Csanady, G.T., "Coastal Entrapment in Lake Huron," 5th Annual International Water Pollution Research Conference, 1970.
4. Fischer, H.B., "The Mechanics of Dispersion in Natural Streams," Journal of the Hydraulics Division, ASCE, Vol. 93, No. HY6, Proc. Paper, 1967.
5. Fischer, H.B., "Dispersion Predictions in Natural Streams," Journal of the Sanitary Engineering Division, ASCE, Vol. 94, No. SA5, Proc. Paper, 1968.
6. Fischer, H.B., "Methods for Predicting Dispersion Coefficients in Natural Streams, with Applications to Lower Reaches of the Green and Duwamish Rivers, Washington," U.S. Geological Survey Prof. Paper.
7. Fischer, H.B., "The Effects of Bends on Dispersion in Streams," Water Resources Research, Vol. 5, No. 2, 1969.
8. Fischer, H.B., "A Method for Predicting Pollutant Transport in Tidal Waters," Research Report, Hydraulic Laboratory, University of California, Berkeley, 1970.
9. Fleuerstein, D.L., and R.E. Selleck, "Fluorescent Tracers for Dispersion Measurements," Journal of the Sanitary Engineering Division, ASCE, Vol. 89, No. SA4, 1963.
10. Glover, R.E., "Dispersion of Dissolved or Suspended Materials in Flowing Streams," U.S. Geological Survey Prof. Paper.
11. Godfrey, R.G., and B.J. Frederick, "Stream Dispersion at Selected Sites," U.S. Geological Survey Prof. Paper.
12. Holley, E.R., "Unified View of Dispersion," Journal of the Hydraulics Division, ASCE, Vol. 95, No. HY2, Proc. Paper, 1969.
13. Hudspith, R.L., "The Mathematical Modelling of Mixing in Natural Streams," Masters Thesis, Department of Chemical Engineering, McMaster University, Hamilton, Ontario, 1970.
14. Lau, Y.L., "A Note on the Prediction of BOD Profile Due to a Source of Effluent Discharged in a Uniformly Flowing Stream," Water Research, Vol. 6, 1972.
15. Lawson, D.W., "Improvements in the Finite Difference Solution of Two Dimensional Dispersion Problems," Water Resources Research, Vol. 7, No. 3, 1971.

16. Parkhurst, J.D., and R.D. Pomeroy, "Oxygen Absorption in Streams," Journal of the Sanitary Engineering Division, ASCE, Vol. 98, No. SA1, 1972.
17. Sayre, W.W., H.B. Fischer, and N. Yotsukura, "Measurement of Mixing Characteristics of the Missouri River Between Sioux City, Iowa and Plattsburgh, Nebraska," U.S. Geological Survey Water Supply Paper 1899-G, 1970.
18. Schuster, J.C., "Canal Discharge Measurements with Radioisotopes," Journal of the Hydraulics Division, ASCE, Vol. 91, No. HY2, Proc. Paper, 1965.
19. Scott, T.A., "A Short History of Cootes Paradise," The Gardens' Bulletin, Vol. XXIV, No. 1, 1970.
20. Sooky, A.A., "Longitudinal Dispersion in Open Channels," Journal of the Hydraulics Division, ASCE, Vol. 95, No. HY4, Proc. Paper, 1969.
21. Terzidis, G., "Computational Schemes for the Boussinesq Equation," Journal of the Irrigation and Drainage Division, ASCE, Vol. 96, No. IR4, Proc. Paper, 1968.
22. Thackston, E.L., "Longitudinal Mixing in Natural Streams," Journal of the Sanitary Engineering Division, ASCE, Vol. 93, No. SA5, Proc. Paper, 1967.
23. Thackston, E.L., J.R. Hays, and P.A. Krenkel, "Least Squares Estimation of Mixing Coefficients," Journal of the Sanitary Engineering Division, ASCE, Vol. 93, Proc. Paper, 1967.
24. Thackston, E.L., and K.B. Schnelle, "Predicting Effects of Dead Zones on Stream Mixing," Journal of the Sanitary Engineering Division, ASCE, Vol. 96, No. SA2, 1970.
25. "Use of Fluorescent Dyes as Tracers," Applied Sciences Branch, Division of Research, Ontario Water Resources Commission, 1970.
26. Wen-Hsiung Li, "Effects of Dispersion on DO-sag in Uniform Flow," Journal of the Sanitary Engineering Division, ASCE, Vol. 98, No. SA1, 1972.
27. Wilson, J.F., "Fluorometric Procedures for Dye Tracing," U.S. Geological Survey Techniques of Water Resources Inv., BK3, 1968.
28. Wright, R.R., and M.R. Collings, "Application of Fluorescent Tracing Techniques to Hydrologic Studies," Journal of the American Water Works Association, 1964.
29. Wylie, S.C., "The Measurement of River Sediment Loads," Topics in Civil Engineering Fluid Mechanics, University of Natal, King George V Avenue, Durban, 1969.